

Selected topics in experimental nuclear physics studies at Beihang

孙保华

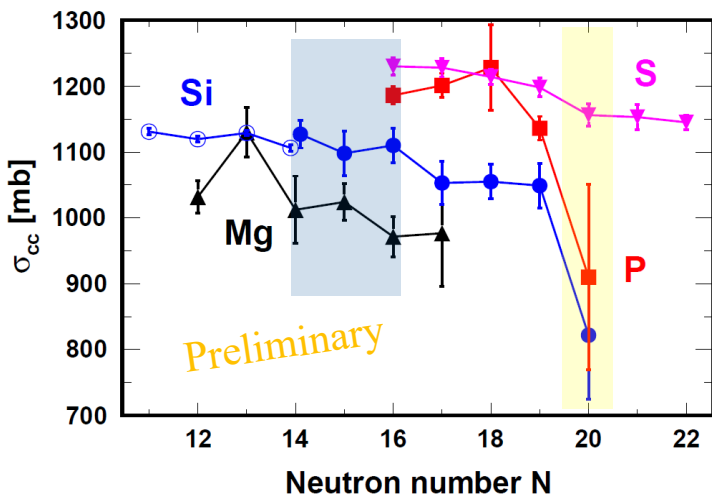
bhsun@buaa.edu.cn

北京航空航天大学

同济大学 • 2022.11.16

Recent focuses

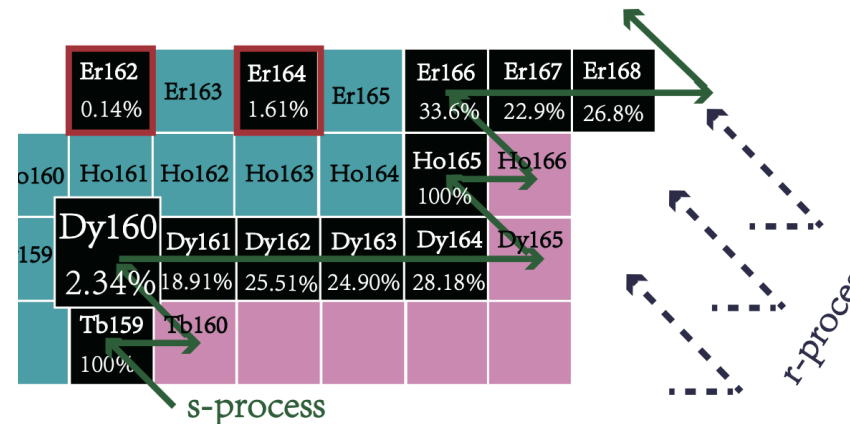
基于HIRFL-RIBLL2的 反应截面测量



sd 壳原子核的电荷改变截面

- 提高实验统计
- $N=20 \rightarrow N=14/16$ 处
- 有望首次提取电荷半径数目 ~ 20 个
- 探究电荷改变截面反应机制

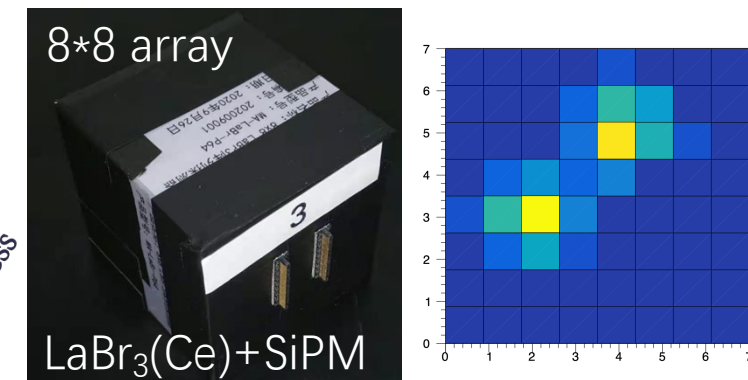
元素起源相关 关键反应与衰变



天体(p, γ)、(γ, n)反应截面

- 系统开展 $A \sim 160$ 稀土区截面测量
- 直接测量 vs. 间接测量
- 活化分析分析 vs. 在束测试
- (p, n), ($d, {}^2He$) 电荷交换反应

探测技术与靶技术

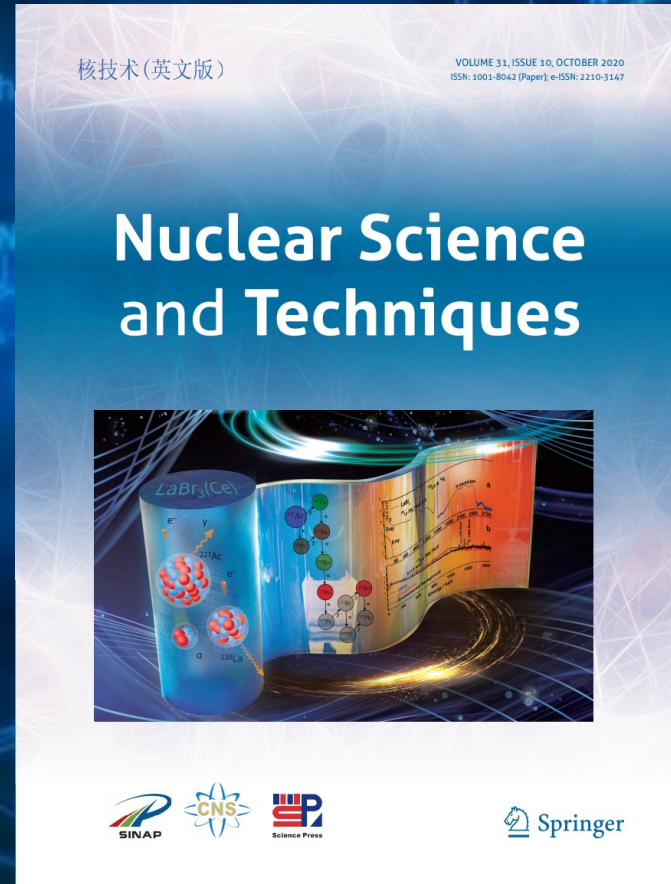


LaBr₃(Ce)像素探测器

- 康普顿相机预研
- 基础、空天、医学
- 固态氢靶研制

溴化镧探测器内辐射本底研究

Nuclear Science and Techniques, 31, 992020(2020)



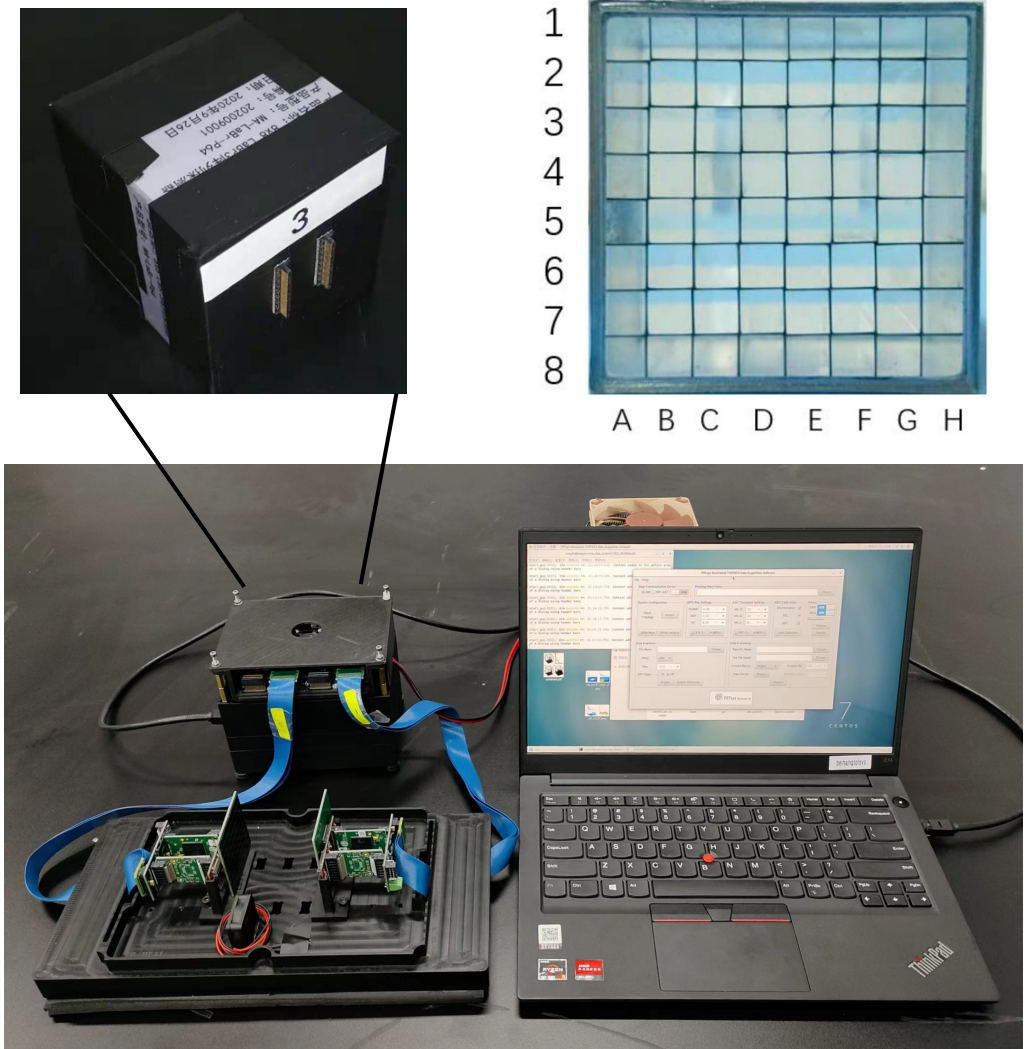
2020.10封面文章



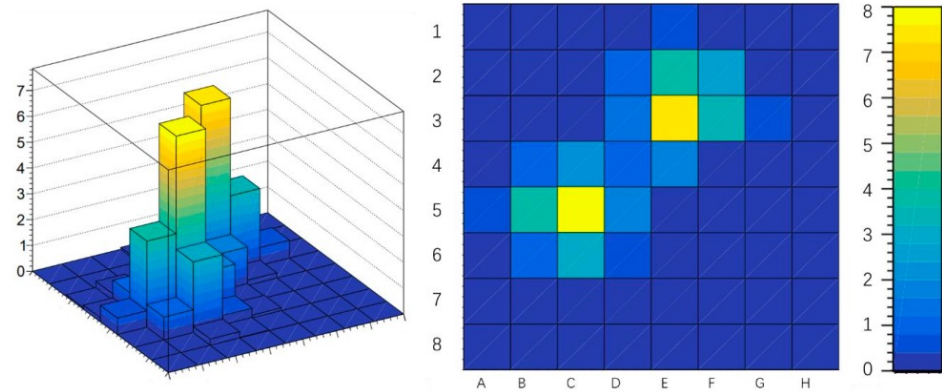
Enhancing the Future of Radiation Technology
by Understanding Scintillator Materials

8X8溴化镧阵列探测器

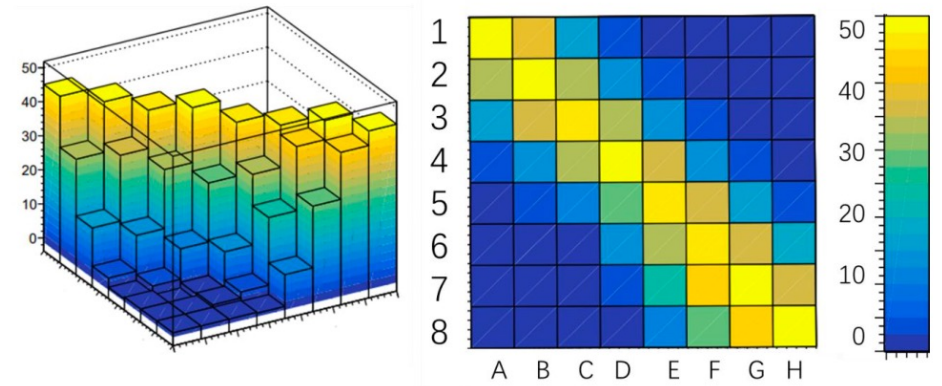
Manuscript in preparation



康普顿事件



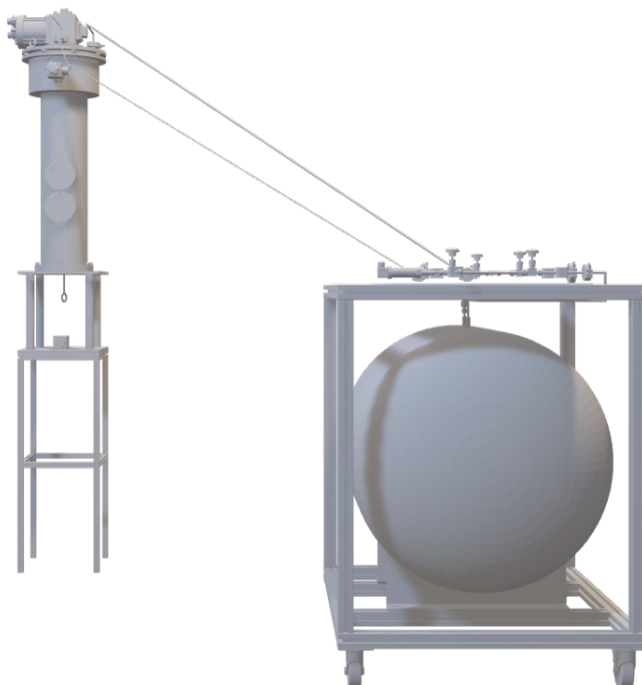
缪子事件



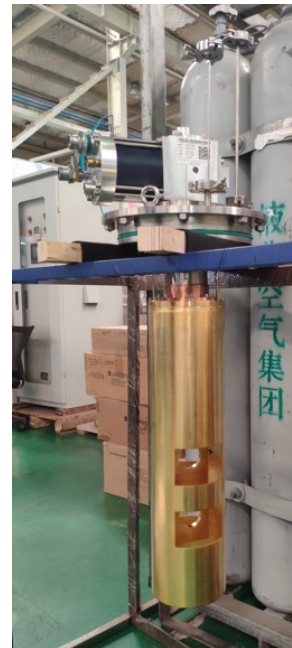
Solid hydrogen target R&D (2019-)

□ 完成了固态氢靶系统的研制：空间占用小、厚度和角度可调

使用 G-M 制冷机作为冷源，通过多屏绝热与真空绝热减少对流和辐射传热。整个设计方案包含供气单元、冷冻单元、靶室单元以及控制单元等部分。



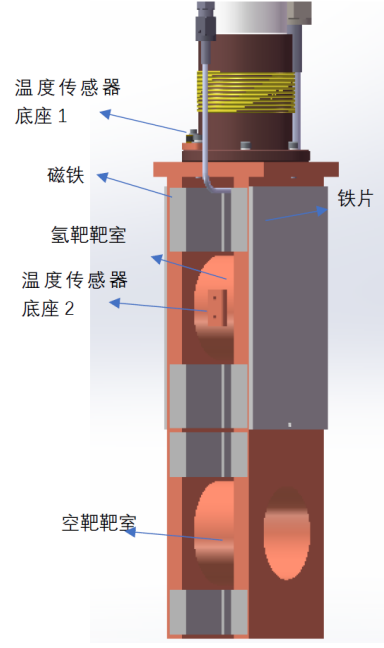
无氧铜冷屏



20mm-target cell

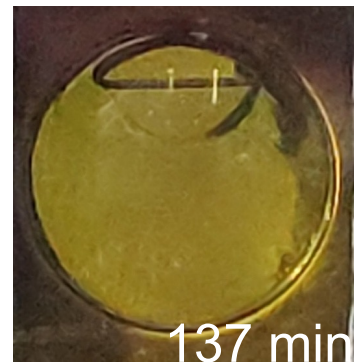
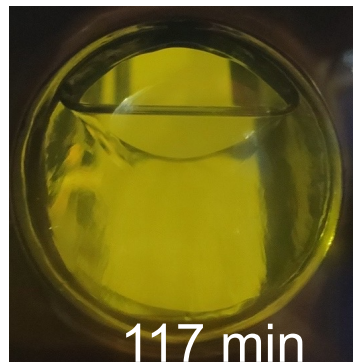
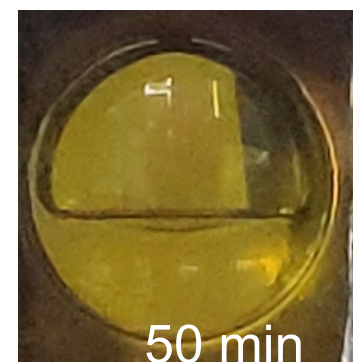
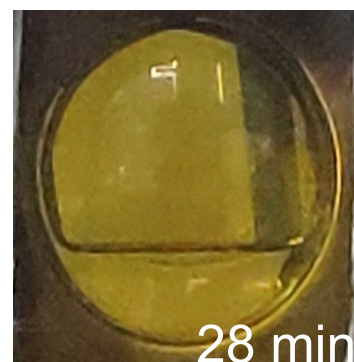
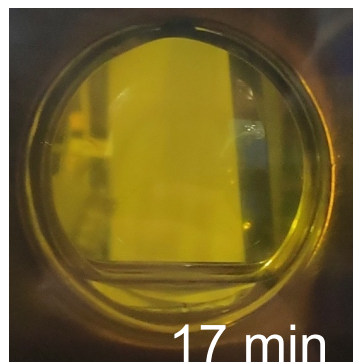
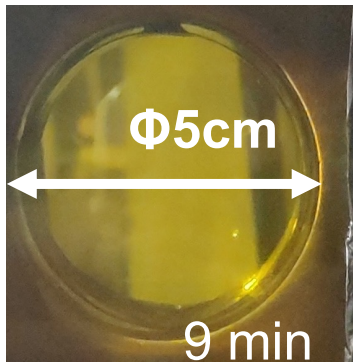


unit



R&D on Solid hydrogen target

Test with nitrogen, 2cm thick x $\Phi 5\text{cm}$



Solid N₂ for test

Test with hydrogen in Progress.

Credit : 王长建、张宇

大纲

- 天体物理相关核反应研究 ($E_p < 10 \text{ MeV/nucleon}$, $E_\gamma < 20 \text{ MeV}$)
统计模型
- 电荷改变反应 ($E \sim 300, 900 \text{ MeV/nucleon}$)
Glauber-type model , fragmentation , IQMD
- 电荷交换反应 ($E \sim 300 \text{ MeV/nucleon}$)
DWBA model

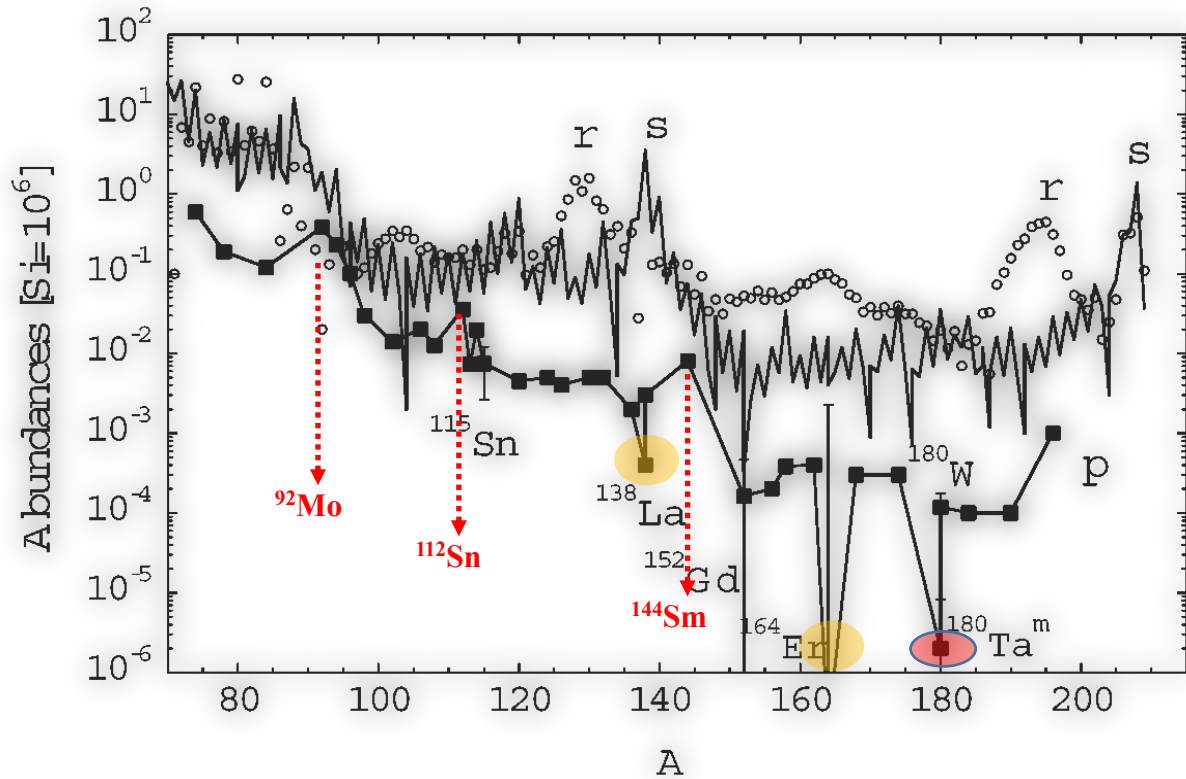
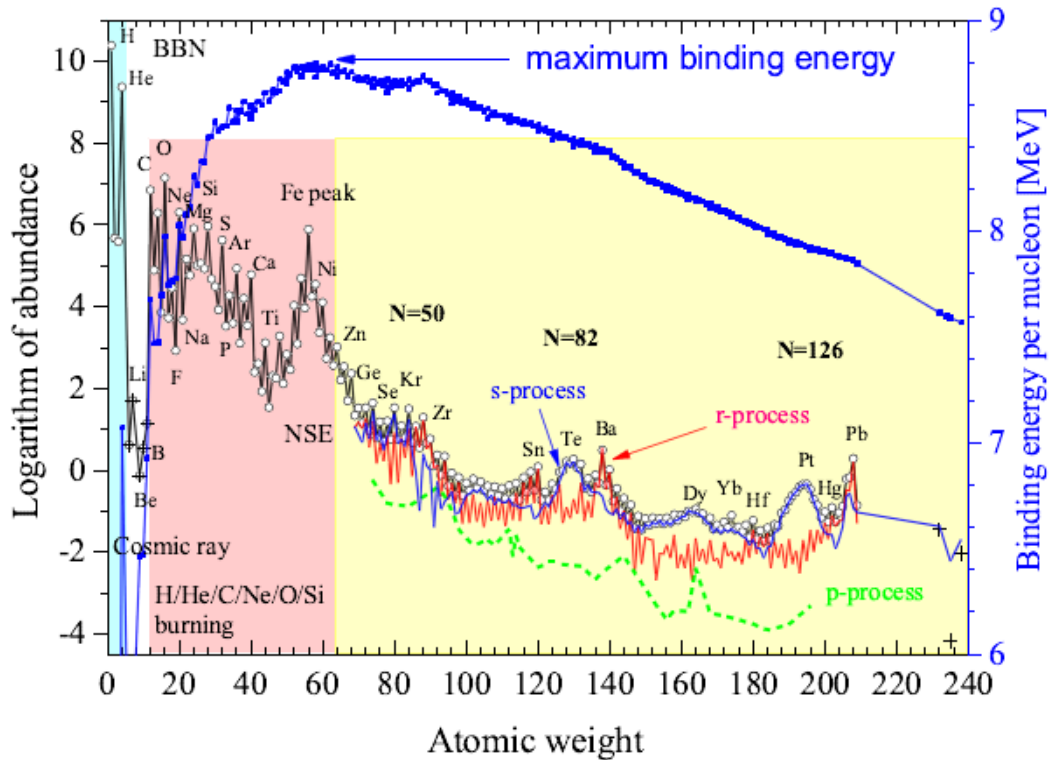
Nucleosynthesis

聚焦在国内大科学装置，发展探测技术，开展实验

- $^{16x}\text{Dy}(\text{p}, \gamma), (\text{p}, \text{n})$ at CIAE
- $^{138,139}\text{La}(\gamma, \text{n})$ at SLEGS
- Stellar lifetime of atomic nuclei

p nuclei and p-process

M. Arnould & S. Goriely, Phys. Rep. 384 (2003) 1



Experimental focuses: origin of Er and La isotopes

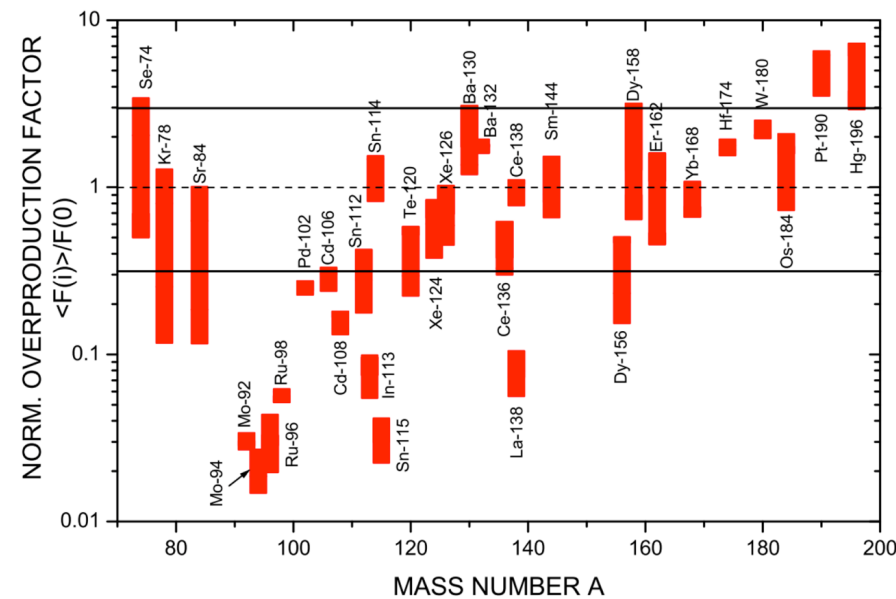
Less is known for “p process”

Arnould and Goriely, Phys. Rep. 384, 1 (2003)

The p-process of stellar nucleosynthesis: astrophysics and nuclear physics status

“The first remarkable feature of this process is the **scarcity of the efforts devoted to its understanding.**

In fact, after about 50 years of nuclear astrophysics research, the number of articles devoted to it still remains inferior to the 35 nuclides traditionally classified as p-nuclides.”

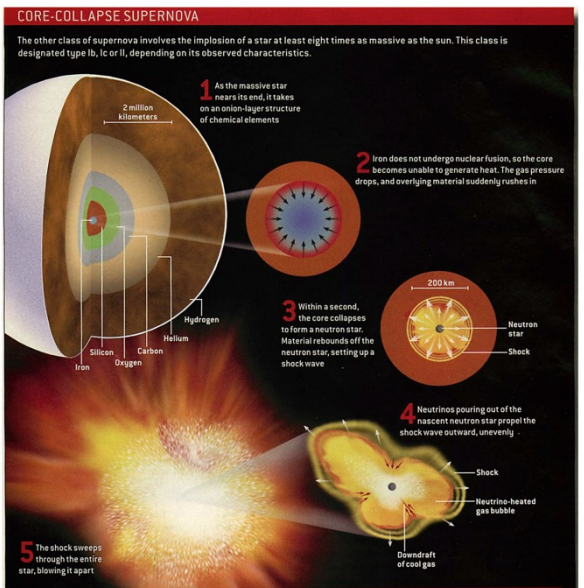


p-process in SN II model ($13-25M_{\odot}$)

p-nuclei production via γ process

γ -process: the most established scenario for the production of the p-nuclei

Core-collapse supernovae



thermonuclear supernovae



The p-nuclei can provide important constrain to the nucleosynthesis in core-collapse and thermonuclear supernovae.

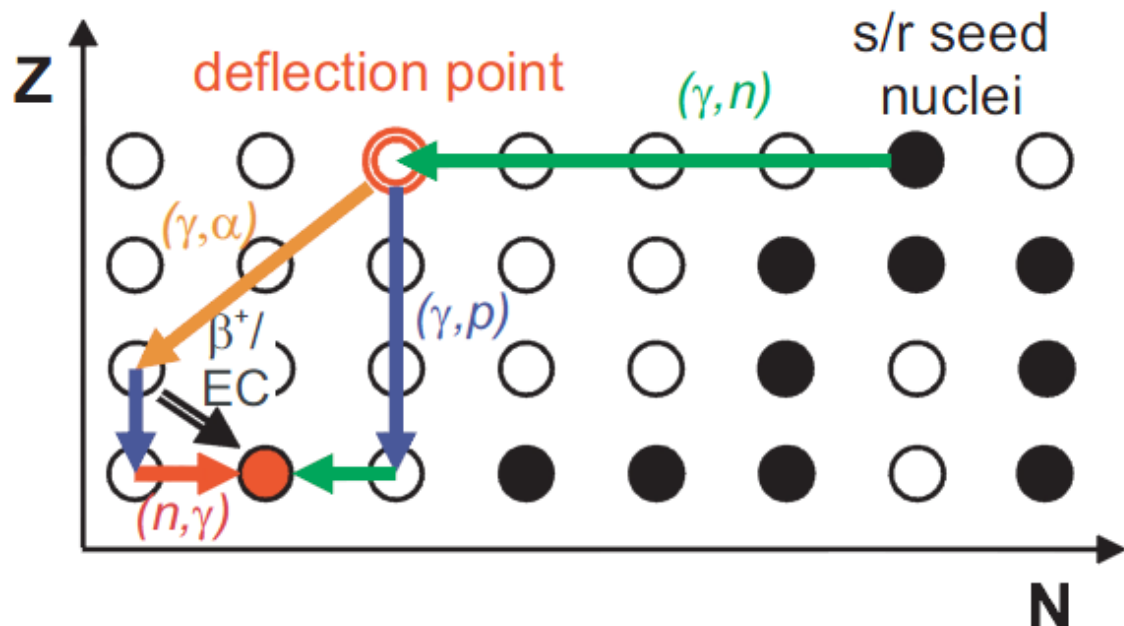
Woosley & Howard ApJS 36,285(1978)

Arnould & Goriely, Phys. Rep. 384, 1(2003)

γ -process

p-nuclei are produced via different photodisintegration paths starting on heavier nuclei.

Typical parameters for the γ -process: $2 \leq T_9 \leq 3$, time scales t in the order of seconds.

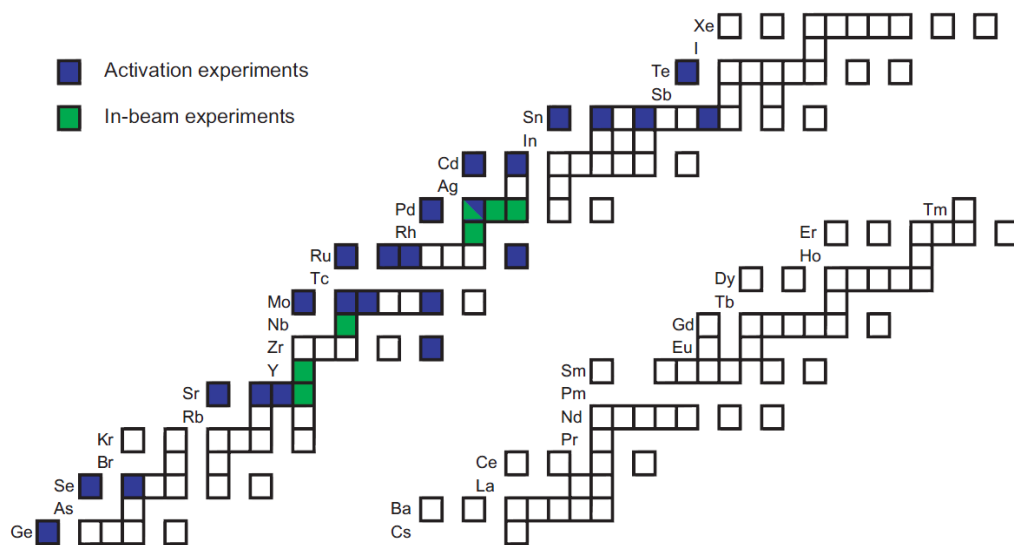


- Seed nuclei from prior strong s/r-process
- $(\gamma, n) \rightarrow$ p-rich nuclides
- Deflection point: $\lambda(\gamma, p) + \lambda(\gamma, \alpha)$ become faster than $\lambda(\gamma, n)$
 - Flow will branch, different isotopic chains
 - With decreasing T , β^+ / EC takeover;
 - At the end, photodisintegration cease;
 β -decay to stable nuclei

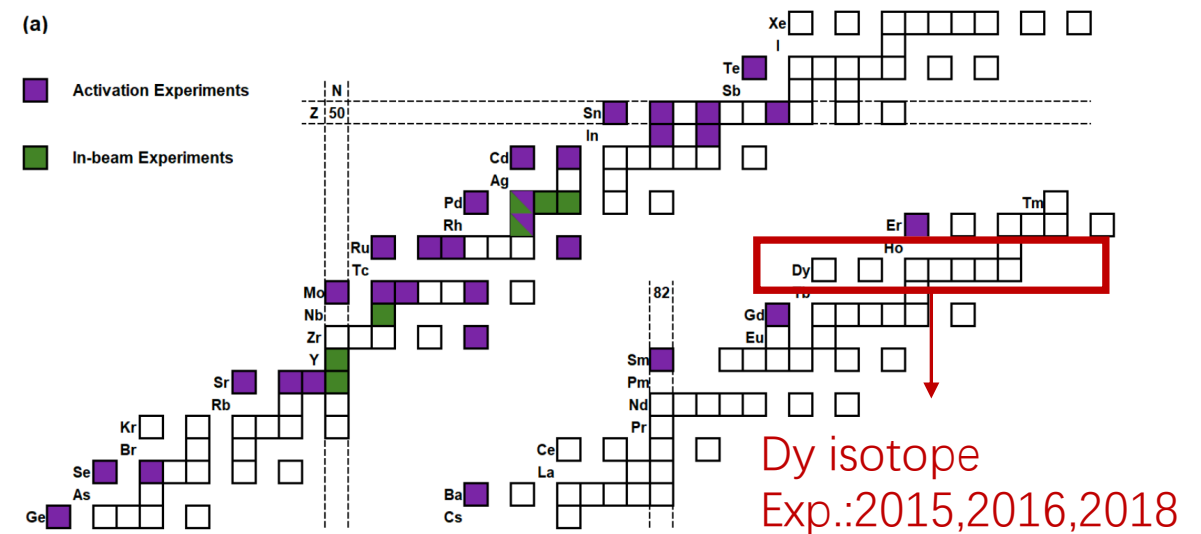
network of ~ 20000 reactions linking about 2000 nuclei (mainly unstable nuclei)

Progress: (p,γ) cross sections

Almost all the reaction rates are based on models, except for some stable medium heavy nuclei using, e.g., (p,γ), (n, γ).



Rauscher et al., 2013

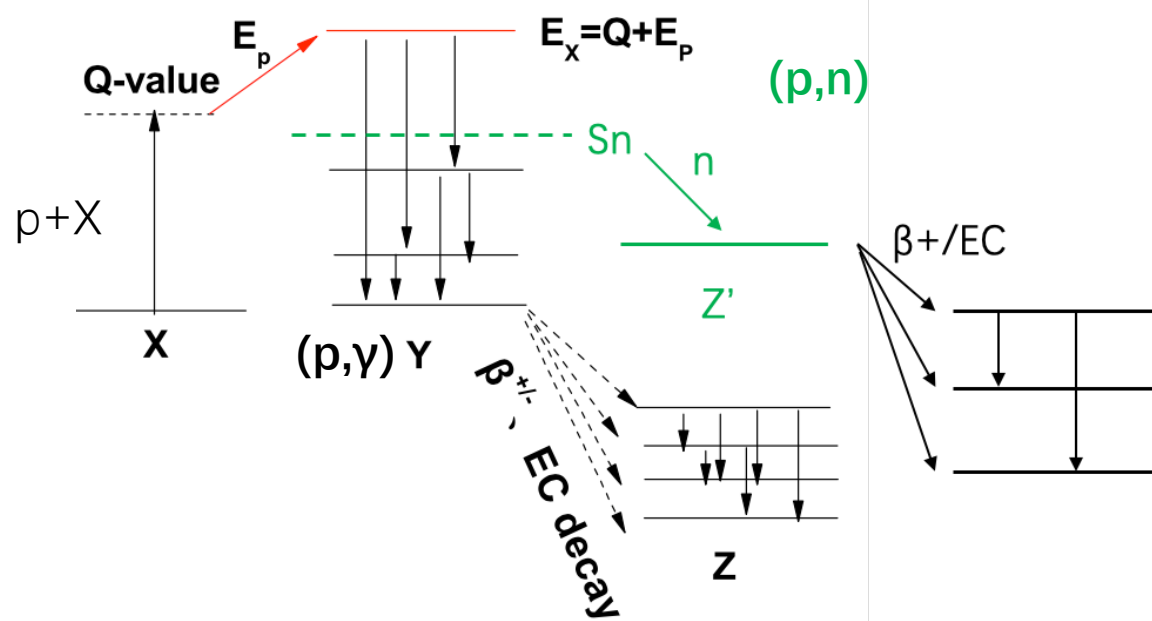


Credit: L.C. He, PhD thesis (2018)

Isotopes on which (p, γ) cross sections relevant for the γ -process have been measured. The upper part of the p -isotope mass region is not shown since there are no data available there.

Experiment vs theory relevant for astrophysics

Activation-decay gamma radiation



Hauser-Feshbach statistical model HF统计模型

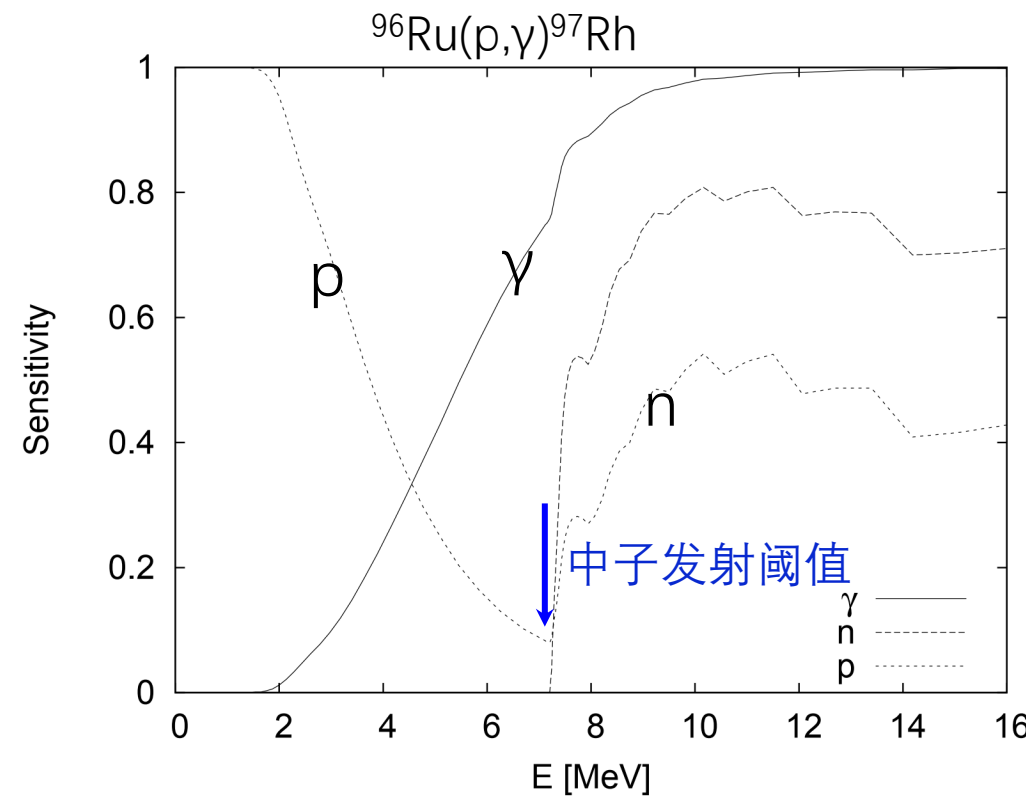
- Optical potential (proton width)
- γ -ray strength function
- Level density
- ...

$$\langle \sigma \rangle_{\text{HF}} \propto \frac{\langle \Gamma \rangle_i \langle \Gamma \rangle_o}{\langle \Gamma \rangle_{\text{tot}}}$$

i: input channel
o: output channel
tot: total width

- Determine $\sigma(p, \gamma)$ and $\sigma(p, n)$ by counting γ rays
- (p, γ) , (p, n) are crucial to determine the gamma and proton strength
- Level density: total width

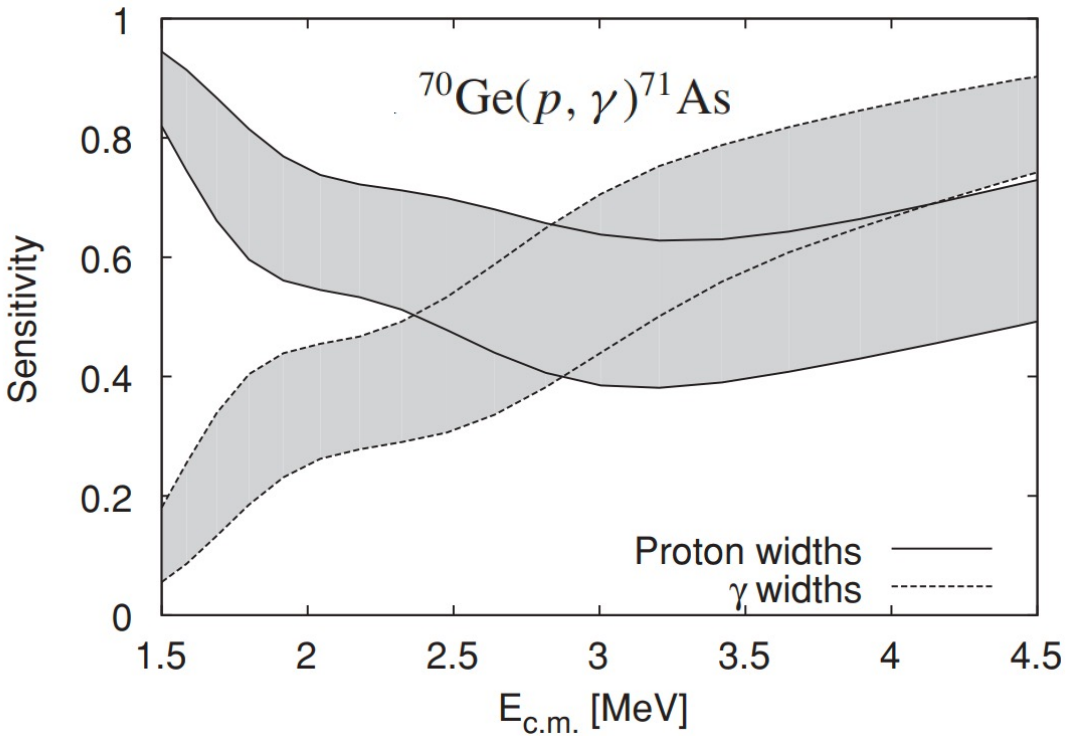
Sensitivity to inputs



Sensitivities when multiplying the transmission coefficients (averaged widths) by a factor of 2

Rauscher, IJMPE 20, 1071(2011)

$$\langle\sigma\rangle_{\text{HF}} \propto \frac{\langle\Gamma\rangle_i \langle\Gamma\rangle_o}{\langle\Gamma\rangle_{\text{tot}}}$$



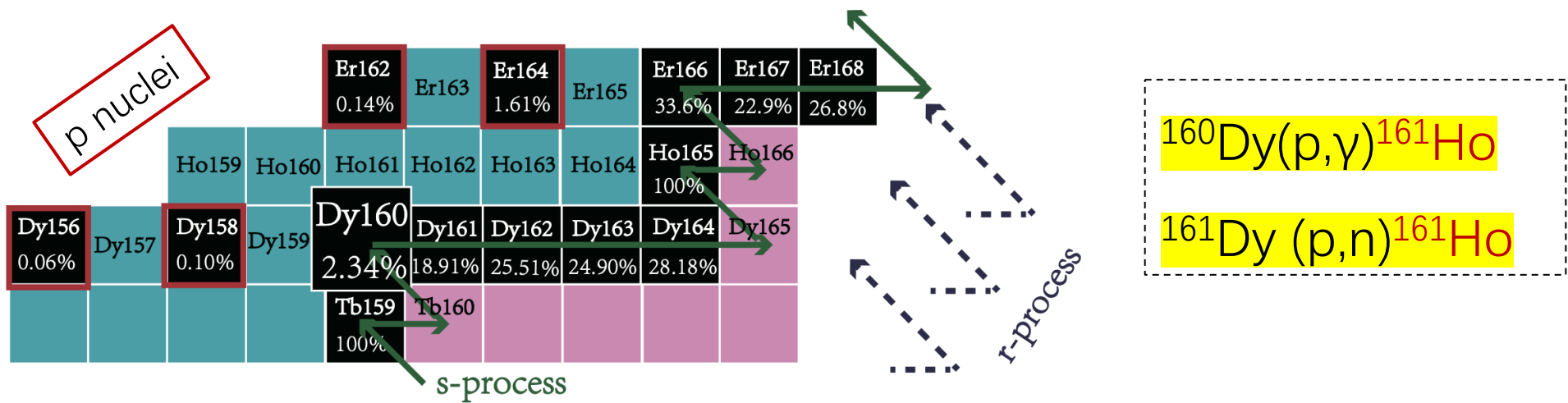
Sensitivities when multiplying the widths by 2 or 0.5

Kiss et al., PRC 76, 055807 (2007)

First experiment study on Dy(p, γ)

Difficulty: 7 stable isotopes, almost impossible to distinguish isotopes

→ (p, γ) and (p,n) can yield the same isotope at 3-7 MeV



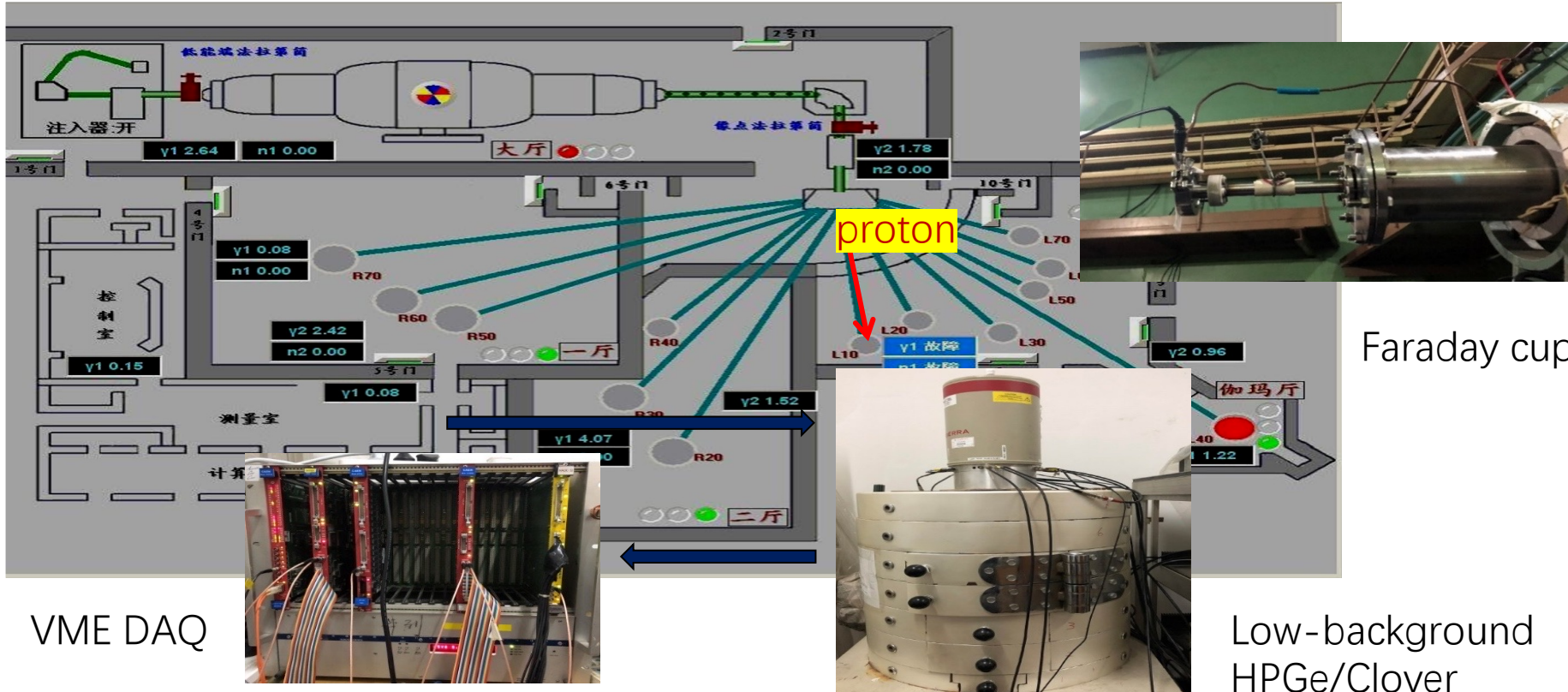
Solution:

Isotopic Abundances in the Natural Dy (${}^{\text{nat}}\text{Dy}$) and the Enriched ${}^{160}\text{Dy}$ Targets (${}^{160}\text{Dy}_2\text{O}_3$)

Type	Material	Isotopic Composition					
1	${}^{\text{nat}}\text{Dy}$	${}^{160}\text{Dy}(2.34\%),$	${}^{161}\text{Dy}(18.91\%),$	${}^{162}\text{Dy}(25.51\%),$	${}^{163}\text{Dy}(24.90\%),$	${}^{164}\text{Dy}(28.18\%)$	
2	${}^{160}\text{Dy}_2\text{O}_3$	${}^{160}\text{Dy}(51.82\%),$	${}^{161}\text{Dy}(13.87\%),$	${}^{162}\text{Dy}(5.79\%),$	${}^{163}\text{Dy}(3.05\%),$	${}^{164}\text{Dy}(1.68\%)$	

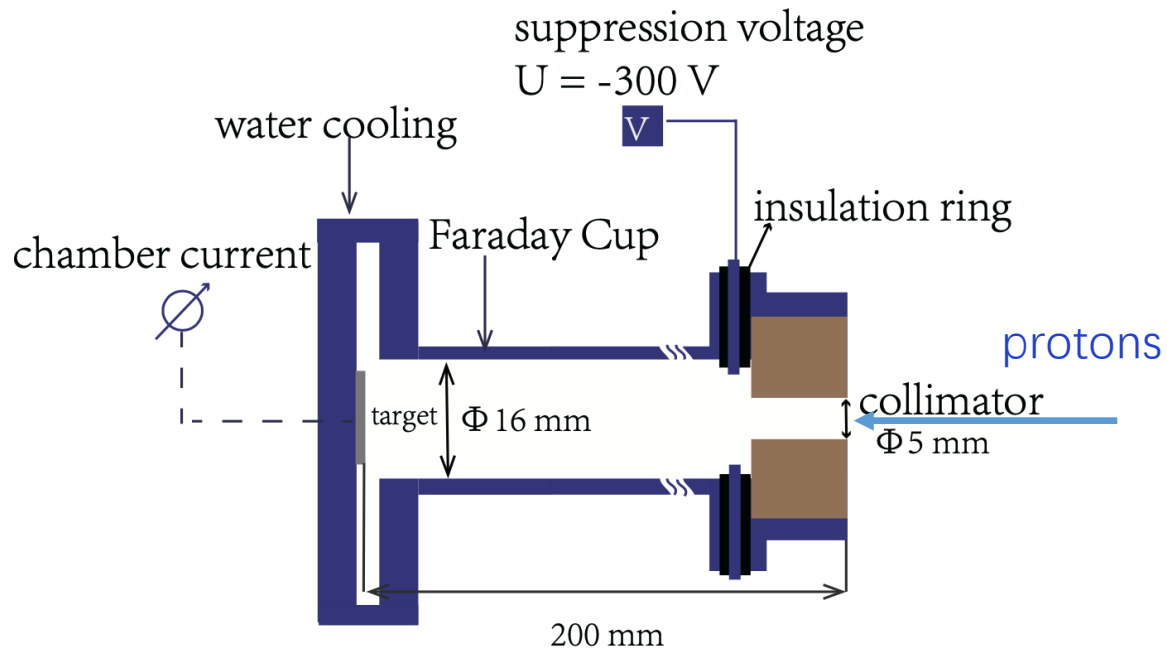
Experiment @ CIAE

Proton beams delivered by the 2×1.7 MeV and H1-13 tandem accelerators



- Timestamps of each event
- Dead time correction

Real-time beam counting



Dy targets

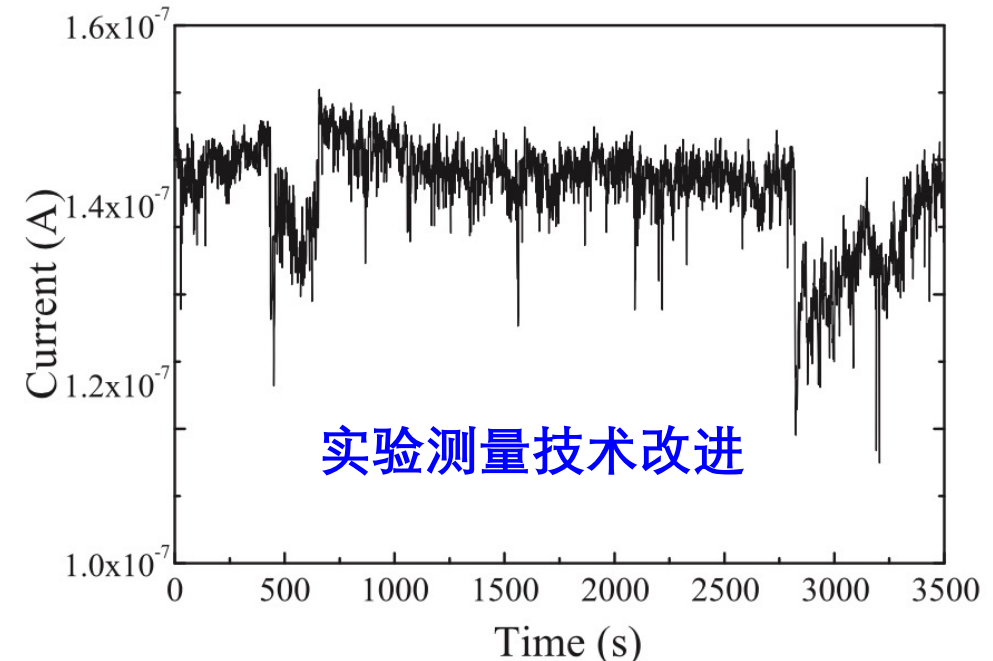
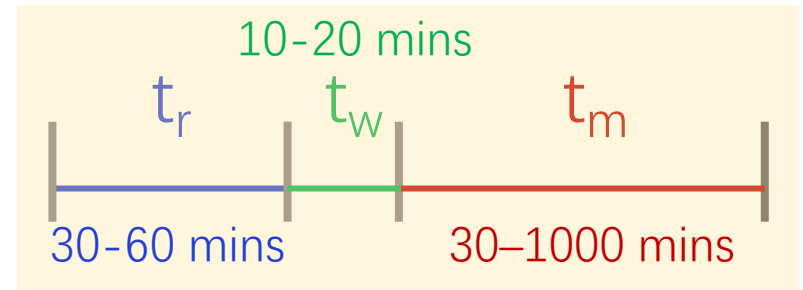
$1\text{-}2 \text{ mg/cm}^2$

Irradiated by
30-60 mins (t_r)

Collimated

Proton beams

3.4-7 MeV
150-700 nA



beam current digitized with a 50ms sampling

Beam fluctuation can lead to up to 35%
difference in the cs determination!

Cross section determinations

The activation method is constituted by the irradiation and the residual measurements of the experimental target. The rate of change in the number of radioactive nuclei is given by the difference of production and decay rate,

$$\frac{dN(t)}{dt} = \sigma(E)N_s I(t) - \lambda N(t), \quad 0 < t < t_b \quad (\text{A1})$$

where $N(t)$ and λ are the number and the decay constant of the object nucleus, $\sigma(E)$ the cross section of the reaction at the bombarding energy E , N_s the number of target nuclei, and $I(t)$ is the beam intensity at a time t . t_b is the irradiation time.

The number of reaction products is:

I(t): current as a function of time

$$N(t_b) = N_s \sigma(E) e^{-\lambda t_b} \int_0^{t_b} I(t) e^{\lambda t} dt, \quad (\text{A2})$$

In the present work, a waiting time t_w was needed to release the vacuum, dismount the target and place the target in the position for off-line measurement. Then the targets were measured for t_m (measurement time). The decayed γ rays emitted from the target is thus

$$n_\gamma = N(t_b) e^{-\lambda t_w} (1 - e^{-\lambda t_m}) \varepsilon_\gamma \eta_\gamma, \quad (\text{A3})$$

where ε_γ and η_γ are the detection efficiency and the gamma intensity, respectively.

Deduced from Eq. A2 and Eq. A3, the cross section of the reaction, $\sigma(E)$, is

$$\sigma(E) = \frac{n_\gamma}{N_s e^{-\lambda t_b} e^{-\lambda t_w} (1 - e^{-\lambda t_m}) \varepsilon_\gamma \eta_\gamma \int_0^{t_b} I(t) e^{\lambda t} dt}, \quad (\text{A4})$$

For the special case of a constant flux, $I(t) = I_0$, the above equations can be solved analytically. Eq. A4 can be rewritten to

$$\sigma(E) = \frac{\lambda n_\gamma}{N_s I_0 e^{-\lambda t_w} (1 - e^{-\lambda t_m}) (1 - e^{-\lambda t_b}) \varepsilon_\gamma \eta_\gamma} \quad (\text{A5})$$

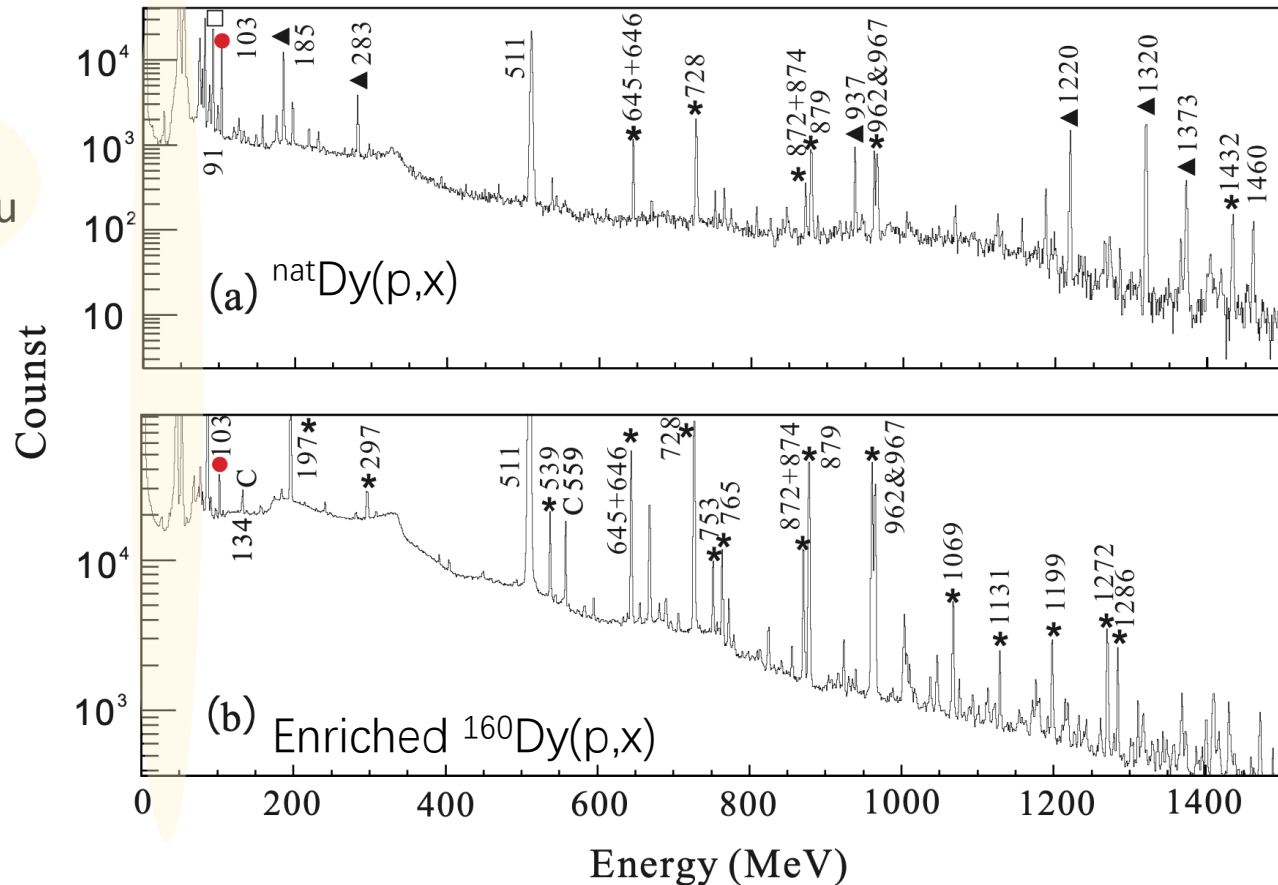
Parameters :

- Target : thickness, abun.
- Cooling during irradiation
- Beam current, $I(t)$
- Real-time measurement (20 Hz)
- γ -ray spectroscopy energy, counting eff., dead-time correction

Activation γ -ray spectra

Measured by Clover detector in a low-background system

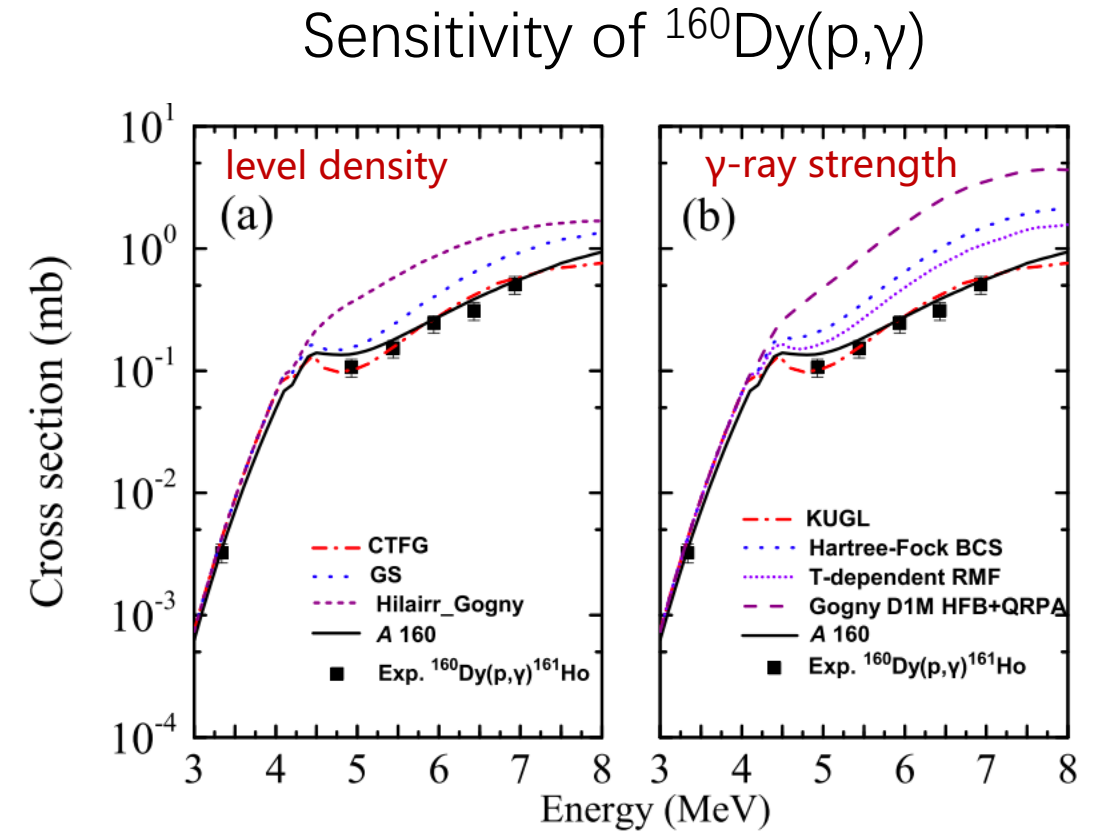
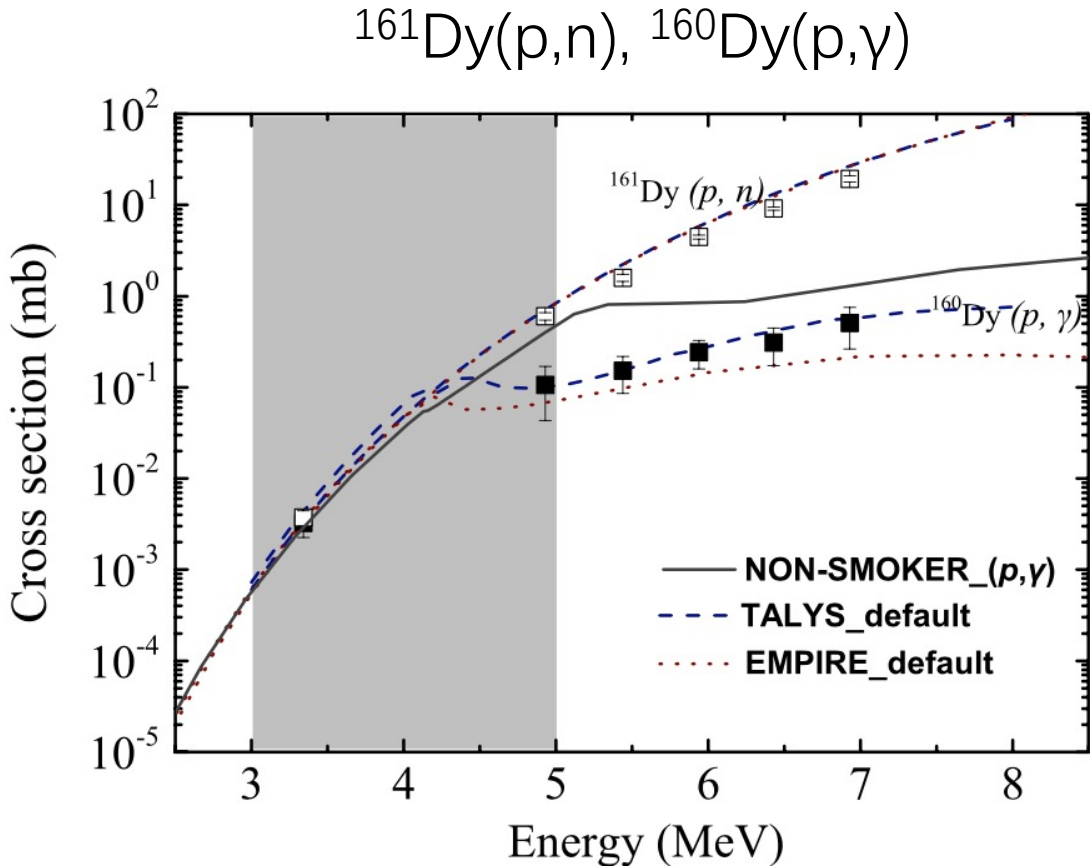
X-rays from
Ho, Dy and Au



- * : ${}^{160}\text{Ho}$
- : ${}^{161}\text{Ho}$ 103 keV
- ▲ : ${}^{162}\text{Ho}$
- : ${}^{164}\text{Ho}$
- C: contaminator

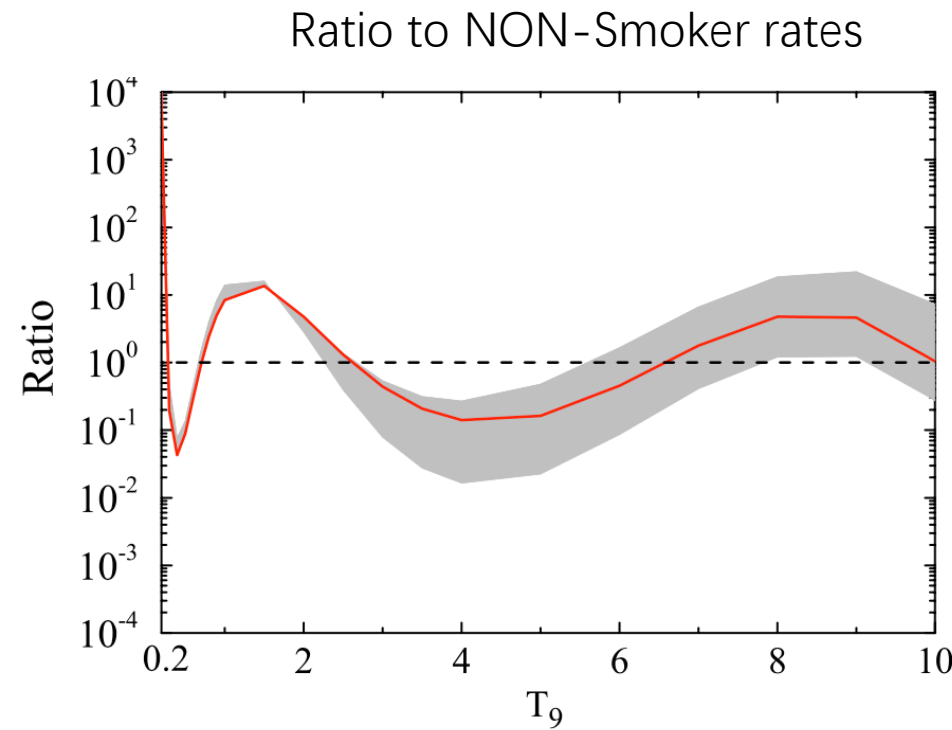
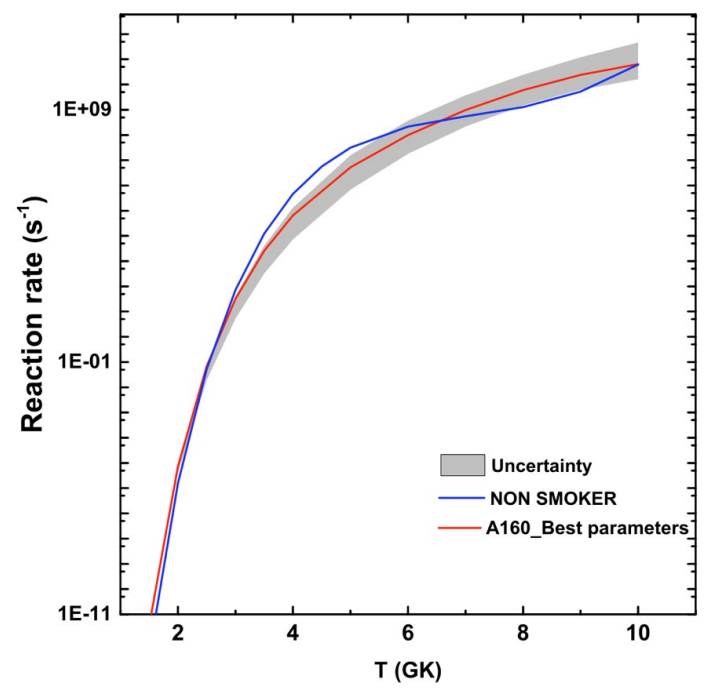
Different reactions can result in the same isotope, e.g., ${}^{160}\text{Dy}(p,\gamma){}^{161}\text{Ho}$, ${}^{161}\text{Dy}(p,n){}^{161}\text{Ho}$

Cross sections: exp. vs. models



(p,γ) : Deviation seen from the ~ 4 MeV (neutron threshold of ^{161}Ho) on

Stellar rate: $^{161}\text{Ho}(\gamma, \text{p}) ^{160}\text{Dy}$

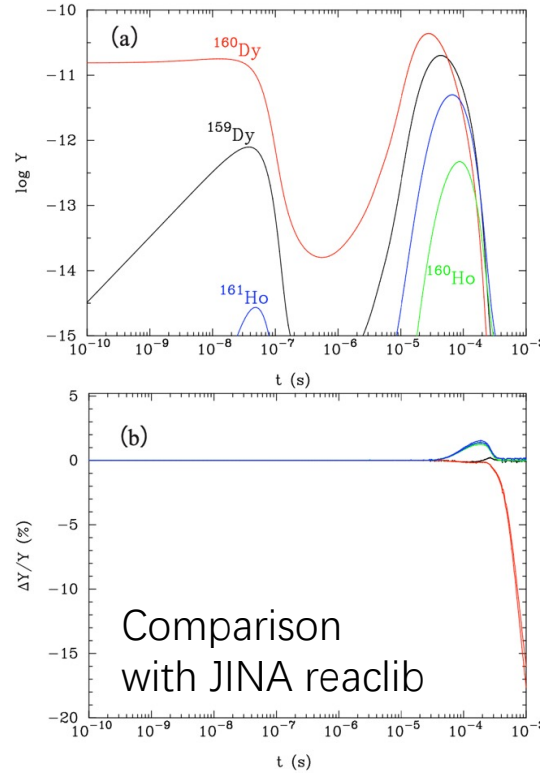


- The stellar reaction rates sharply depend on the temperature and span over 250 order of magnitudes in the temperature range of $T_9 = [0.1, 1.0]$.
- The ratios to the NON-SMOKER calculations are up to one order of magnitude.

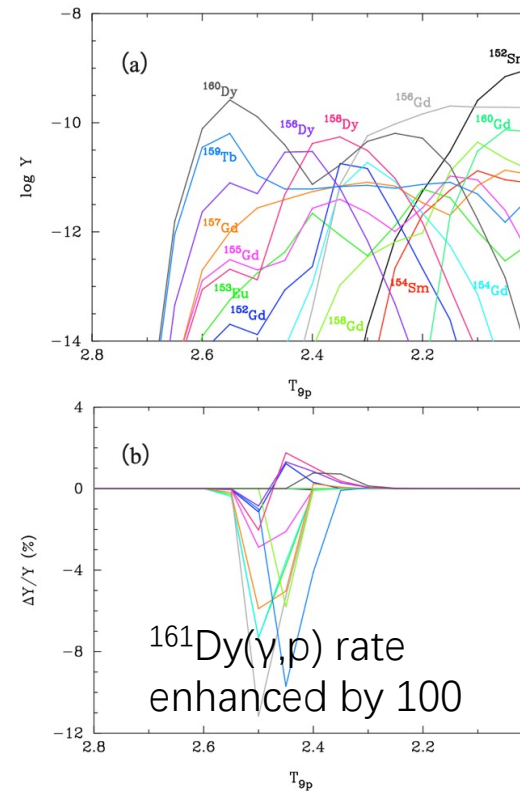
Nucleosynthesis calculation for A~160 p-nuclei

a network calculation using the updated $^{161}\text{Dy}(\gamma, \text{p})$ cross section assuming the γ -process layer in SNe Ia. (Kusakabe et al., ApJ 726, 25(2011))

Comparison with JINA reaclib



Impact of $^{161}\text{Dy}(\gamma, \text{p})$ and its uncertainty on the mass flow



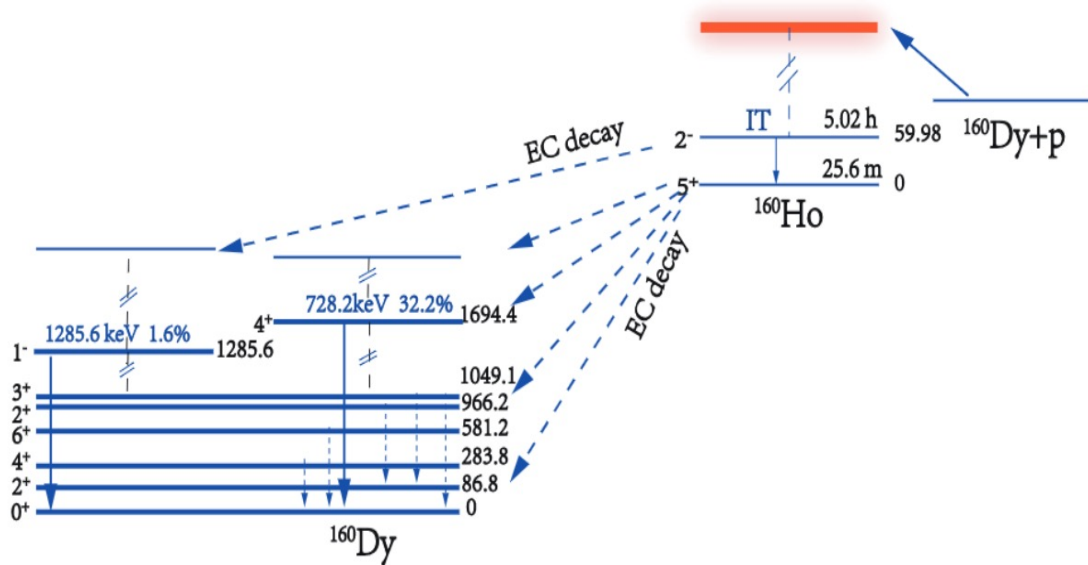
Sensitivity of $^{161}\text{Dy}(\gamma, \text{p})$ rate on the isotope abundance

- Cross sections are precise enough for the γ -process calculations.
- It has a minor effect on the yields of ^{160}Dy and accordingly the p-nuclei, $^{156,158}\text{Dy}$.

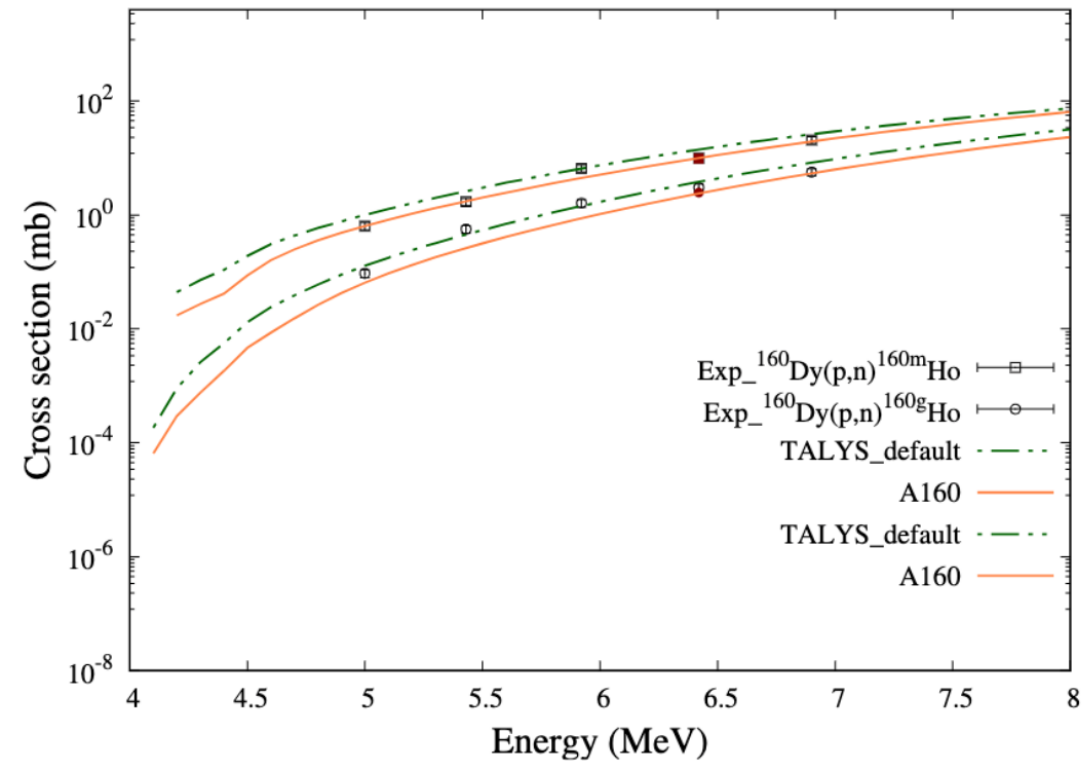
$^{160}\text{Dy}(\text{p},\text{n})/(\text{p},\text{g})$

$$\langle\sigma\rangle_{\text{HF}} \propto \frac{\langle\Gamma\rangle_i \langle\Gamma\rangle_o}{\langle\Gamma\rangle_{\text{tot}}}$$

First evaluation of the proton-width, gamma-width in this mass range



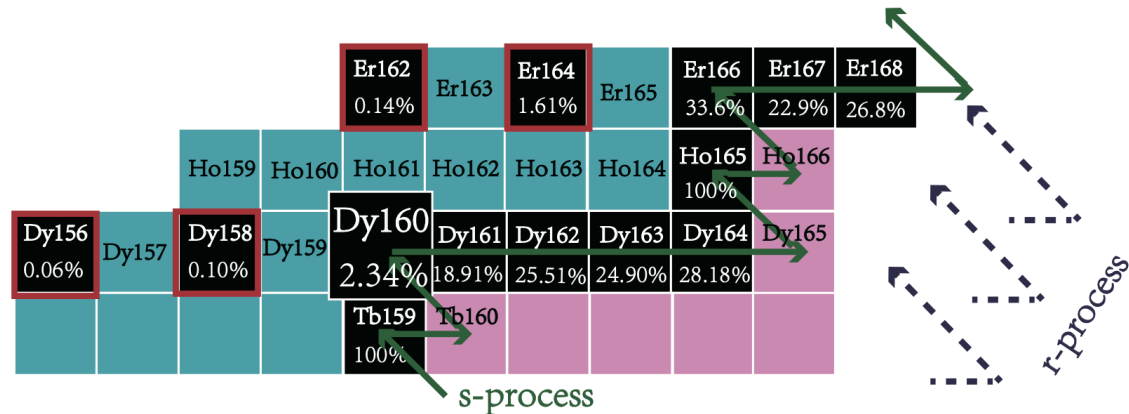
分析复杂 : $^{160}\text{Dy}(\text{p},\text{n})^{160\text{g,m}}\text{Ho}$



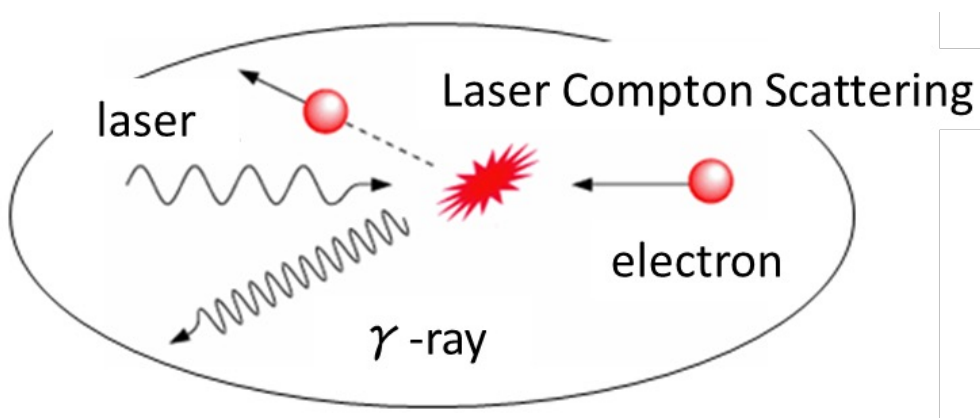
Ready for discussions with theorist

Perspective

$(\gamma, n/p)$ vs $(p/n, \gamma)$



□ 系统测量 $^{162-164}\text{Dy}$ (p, n) vs (p, γ) 截面



□ 基于上海光源开展光核反应的直接研究

稀有核素 ^{138}La 的起源

- 可能产生机制包括 γ 过程和 ν -过程
- 对 γ 过程的理解，可约束 ν -过程贡献

γ 过程 $\left\{ \begin{array}{l} ^{139}\text{La}(\gamma, n)^{138}\text{La} \text{ 产生} \\ ^{138}\text{La}(\gamma, n)^{137}\text{La} \text{ 破坏} \end{array} \right.$

实验数据 ✓

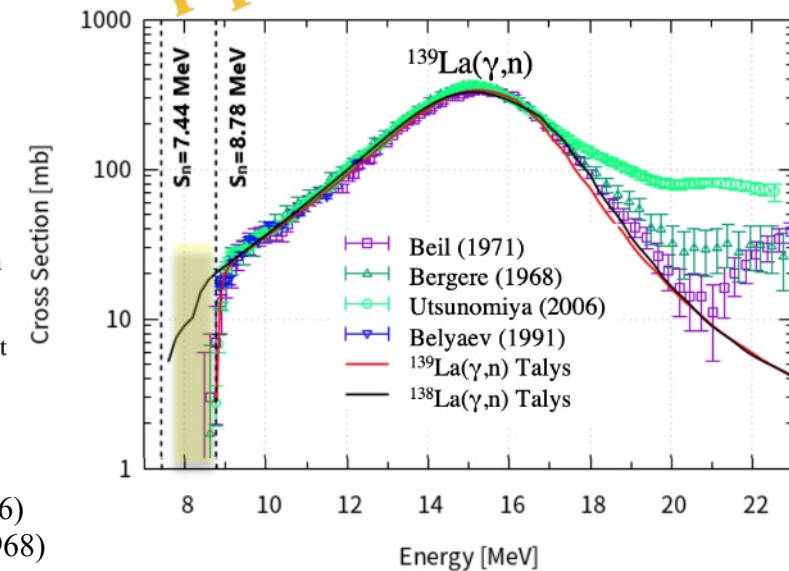
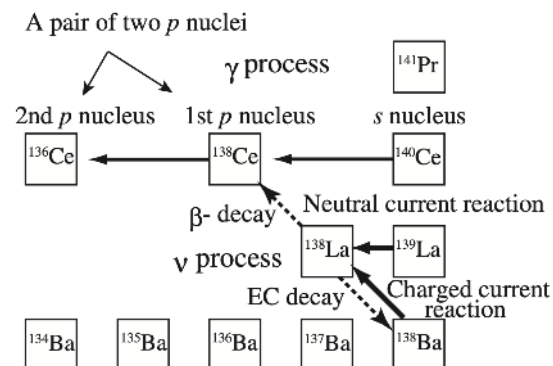
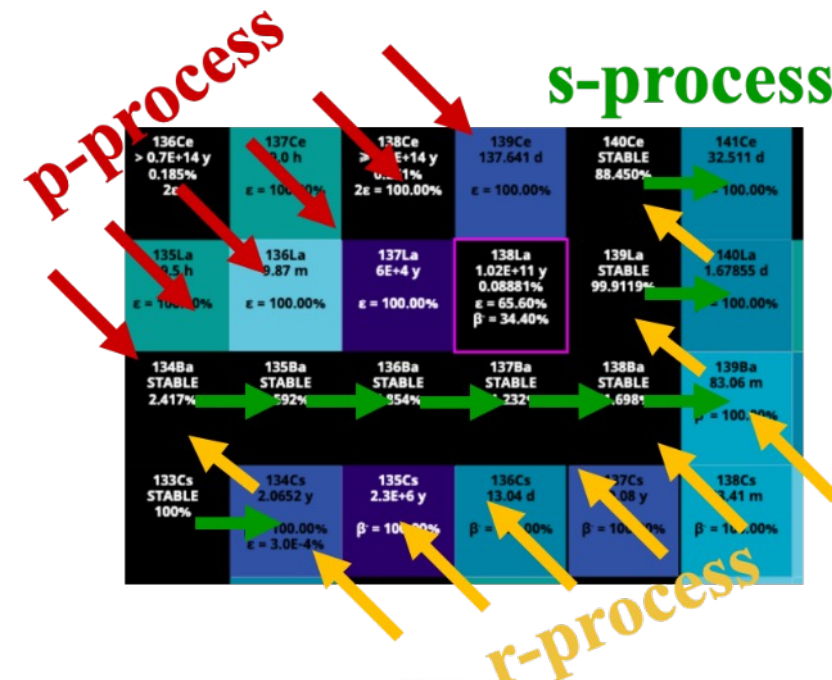
无实验数据

研究目标

- 高精度测量 $^{139}\text{La}(\gamma, n)$
- 在近中子发射阈首次测量 $^{138}\text{La}(\gamma, n)$

可行性及关键问题

- 利用 ^{138}La 比 ^{139}La 中子发射阈低1.3 MeV的特点，测量 $^{138}\text{La}(\gamma, n)$ ，预期产额为0.94/s。
- 如何压低测量系统的中子本底（关键）



Utsunomiya et al., PRC74, 025806 (2006)

Bergere et al., Nucl.Phys. A121, 463 (1968)

Beil et al., Nucl.Phys. A172, 426 (1971)

Belyaev et al., Izv.Akad.Nauk SSSR, Ser.Fiz. 55, 953 (1991)

Hayakawa, et al., PRC 77(2008) 065802

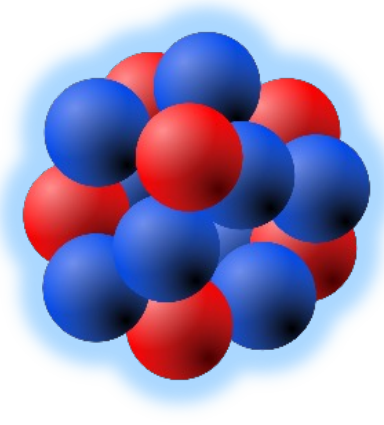
Charge-changing reaction and neutron skin-thickness

电荷改变反应及中子皮厚度

Size: bulk property in nuclei

The nuclear size is often studied in terms of the second moment of the corresponding **density distribution** of a nucleus in its ground state.

$$\langle r_q^2 \rangle = \int d\mathbf{r} \rho_q(\mathbf{r}) r^2 \quad q=n, p$$



Also referred as **root-mean-square (rms) radius** of neutrons and protons.

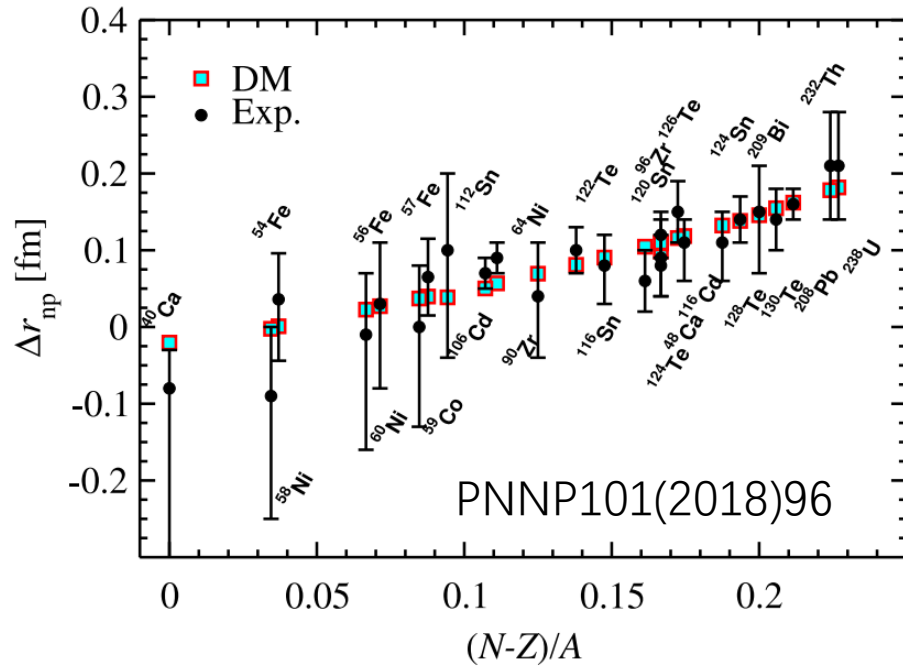
- **Matter density:** $\rho_n + \rho_p \longrightarrow$ **matter rms radius**

The proton and neutron distributions may not be exactly the same at the surface of (stable) nuclei.

- **Neutron skin thickness:** $\Delta r_{np} \equiv \langle r_n^2 \rangle^{1/2} - \langle r_p^2 \rangle^{1/2}$

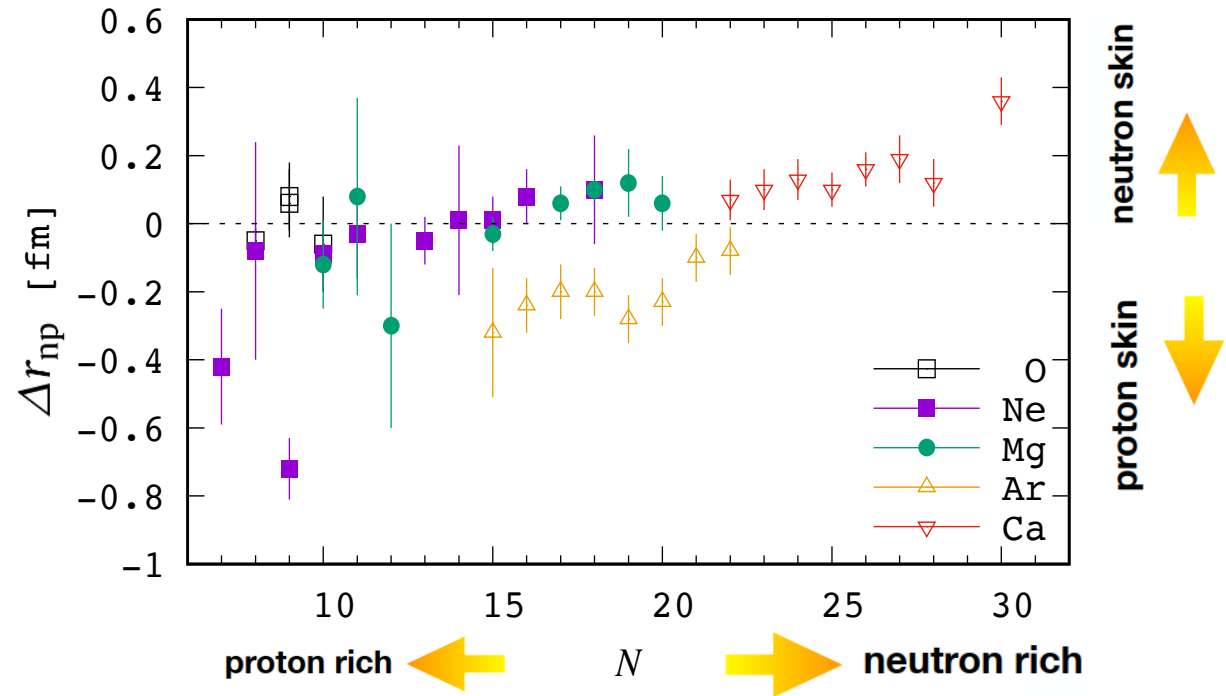
Neutron-skin thickness

$$\Delta r_{\text{np}} \equiv \langle r_n^2 \rangle^{1/2} - \langle r_p^2 \rangle^{1/2}$$



Data from antiprotonic atom experiments

Protons and neutrons develop differently in Nuclei



Data deduced from different types of experiments

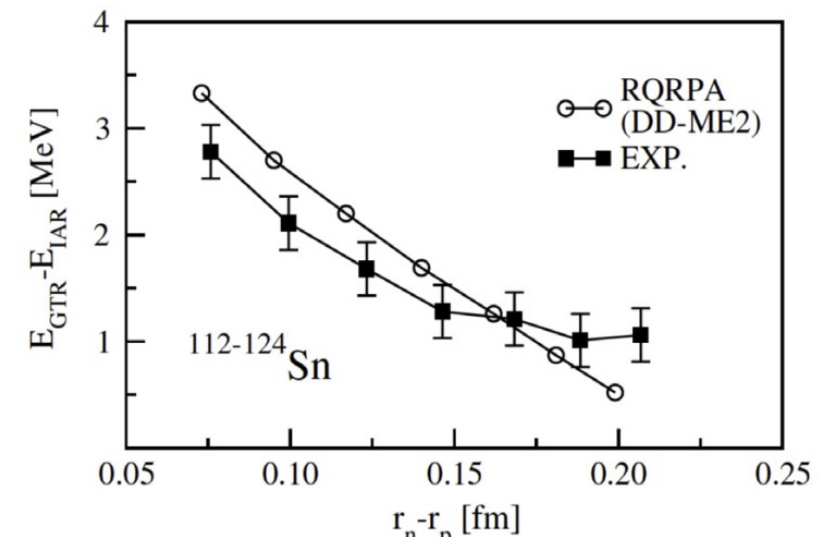
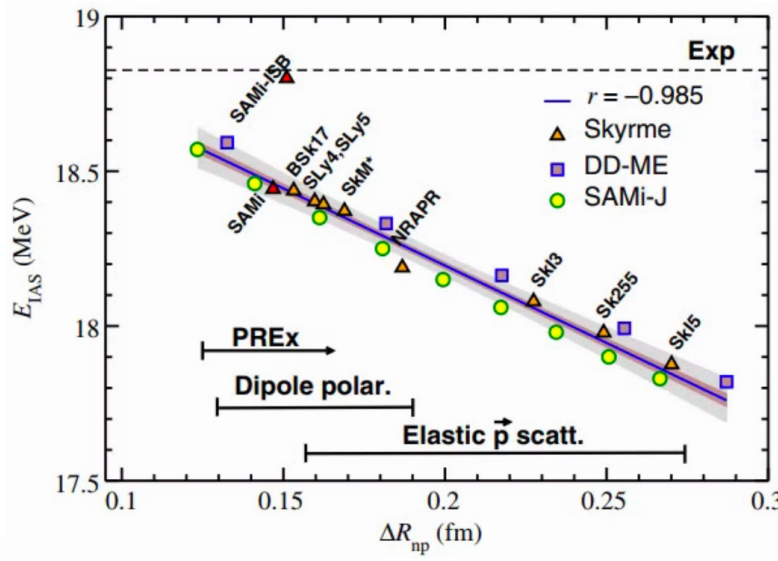
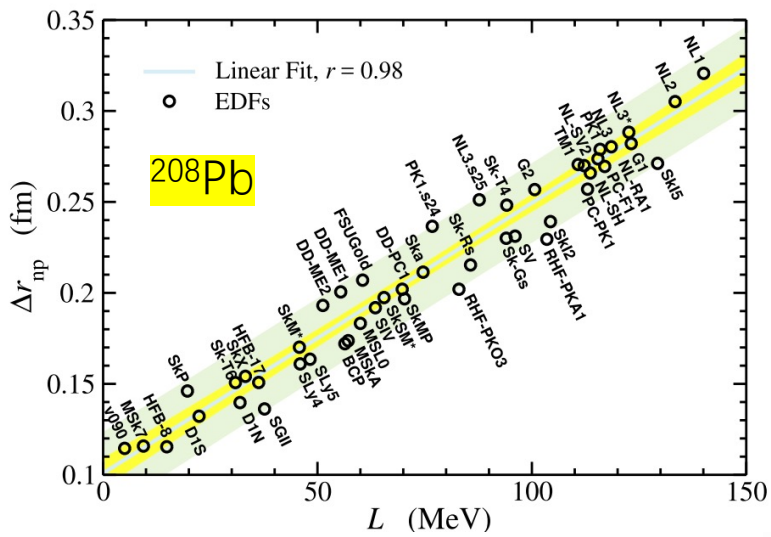
The thickness, studied experimentally and theoretically for decades, remains a frontier in current nuclear physics, and new experiments are proposed worldwide.

Δr_{np}

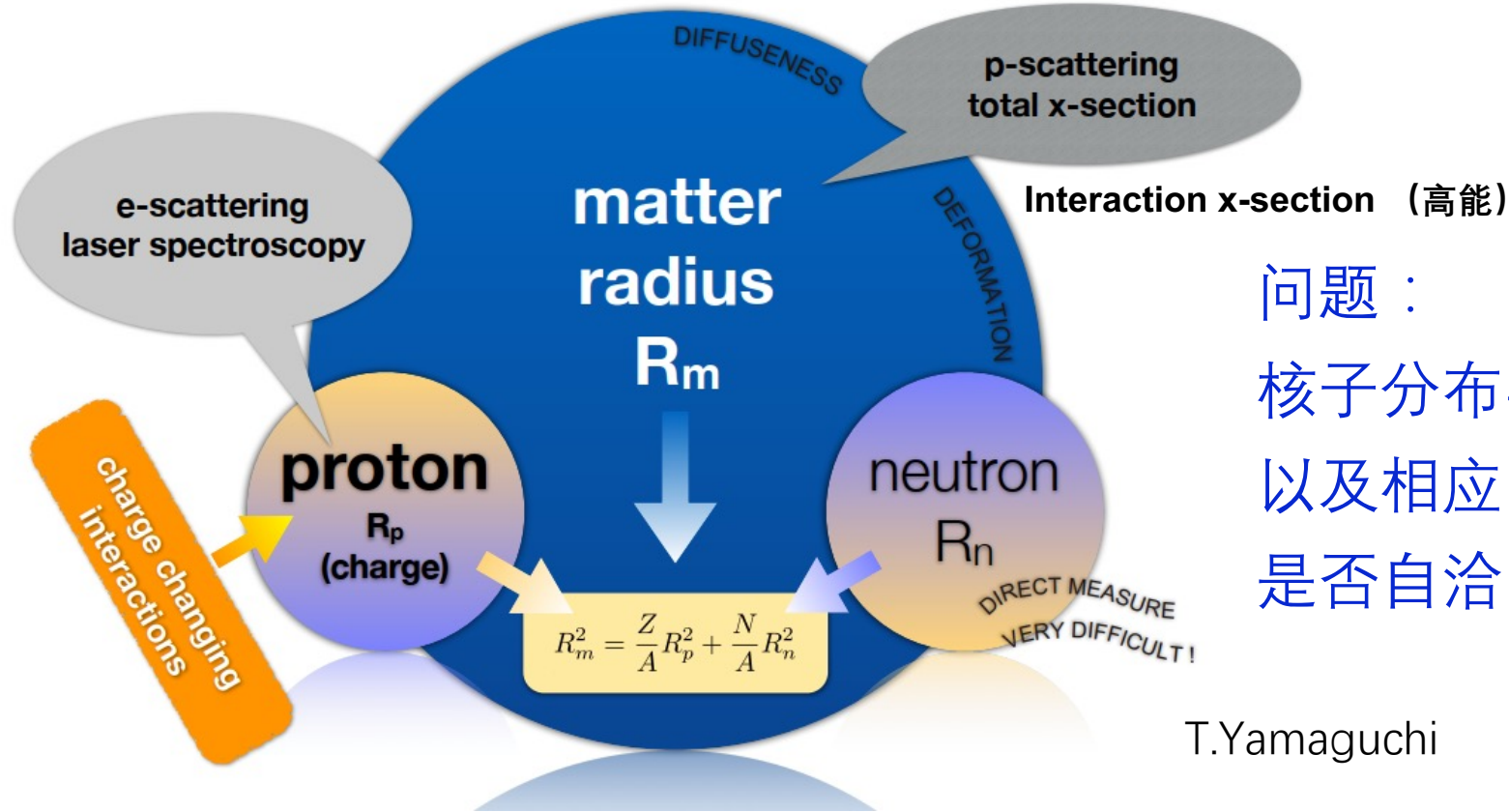
Δr_{np} of atomic nuclei are correlated with many interesting physics.

Symmetry energy: $S(\rho) = J + [L \frac{\rho - \rho_0}{3\rho_0} + \frac{1}{2} K_{\text{sym}} (\frac{\rho - \rho_0}{3\rho_0})^2 + \mathcal{O}[(\rho - \rho_0)^3]]$

the slope of the symmetry energy at saturation



Direct determination of $\Delta r_{np} \equiv \langle r_n^2 \rangle^{1/2} - \langle r_p^2 \rangle^{1/2}$



问题：

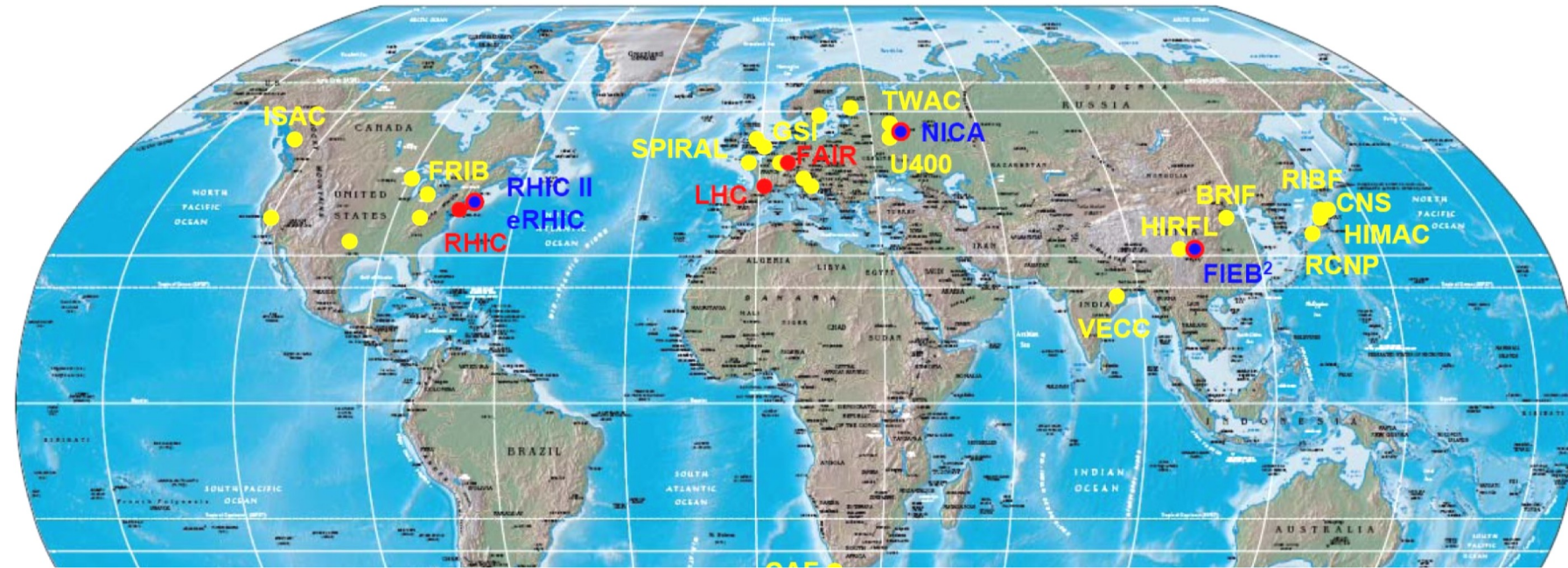
核子分布半径（实验探针）
以及相应的理论半径
是否自洽？

T.Yamaguchi

Hadronic probes, nucleon or heavy ions, require model assumptions to deal with the strong force. It in principle can be applied to exotic nuclei.

重离子加速器+放射性次级束流装置

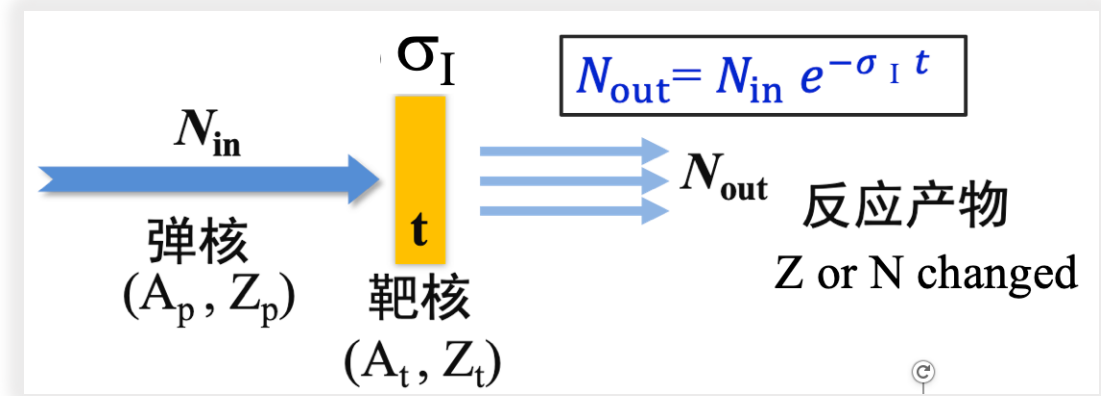
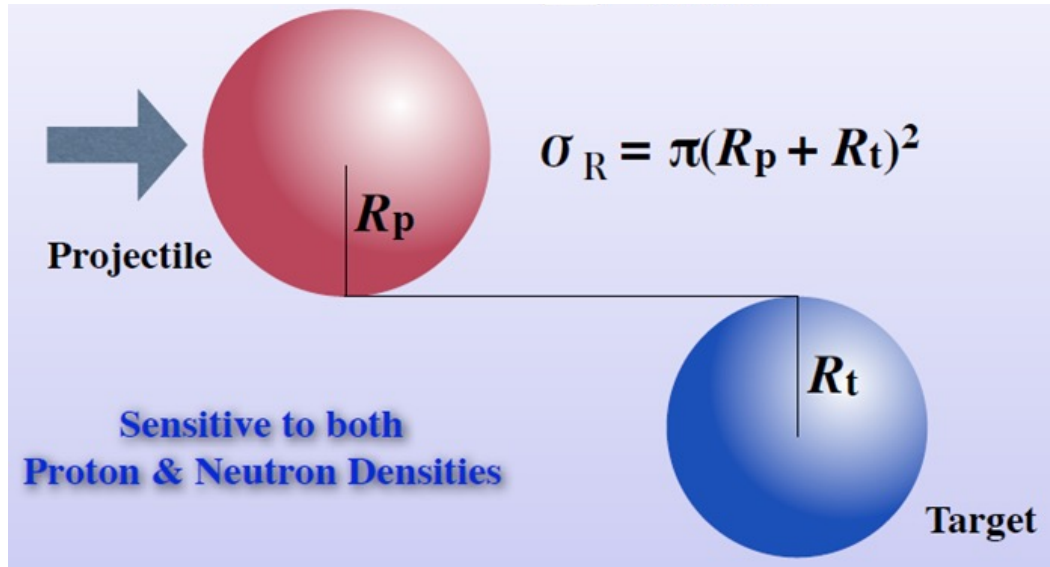
□ 放射性次级束流线：GSI/FRS, RIKEN/BigRIPS, HIRFL/RIBLL2



加速器：加速重离子，累计高流强；不同类型加速器，能区不同

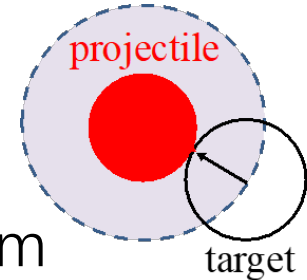
分离器：大大扩大研究对象，产生宇宙中曾经产生的原子核，甚至某种程度上扮演者“上帝”角色造出新核素

Reaction cross section of nuclear collisions



At high energy, Interaction x-section σ_I , $\sigma_I = \sigma_R - \sigma_{inelastic} \approx \sigma_R$

Cross section and nucleon density/rms radii



Glauber model for interaction (reaction) cross sections works very well from 30A to 1000A MeV. Energy dependence of the cross section provided a mean to determine the density distribution of nucleons.

Optical limit (an example)

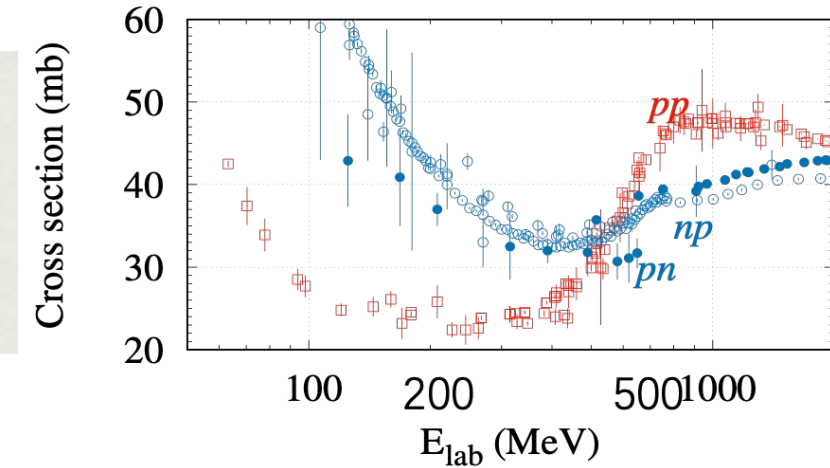
$$\sigma_I(P,T) = \int [1 - T(\mathbf{b})] d\mathbf{b}$$

$$T(\mathbf{b}) = \exp[-\sigma_{pp} \int \{\rho_{Pp}(\mathbf{r} - \mathbf{b}) \cdot \rho_{Tp}(\mathbf{r}) + \rho_{Pn}(\mathbf{r} - \mathbf{b}) \cdot \rho_{Tn}(\mathbf{r})\} d\mathbf{r}] \\ - \sigma_{pn} \int \{\rho_{Pp}(\mathbf{r} - \mathbf{b}) \cdot \rho_{Tn}(\mathbf{r}) + \rho_{Pn}(\mathbf{r} - \mathbf{b}) \cdot \rho_{Tp}(\mathbf{r})\} d\mathbf{r}]$$

σ_{pp}, σ_{pn} : nucleon-nucleon total cross section

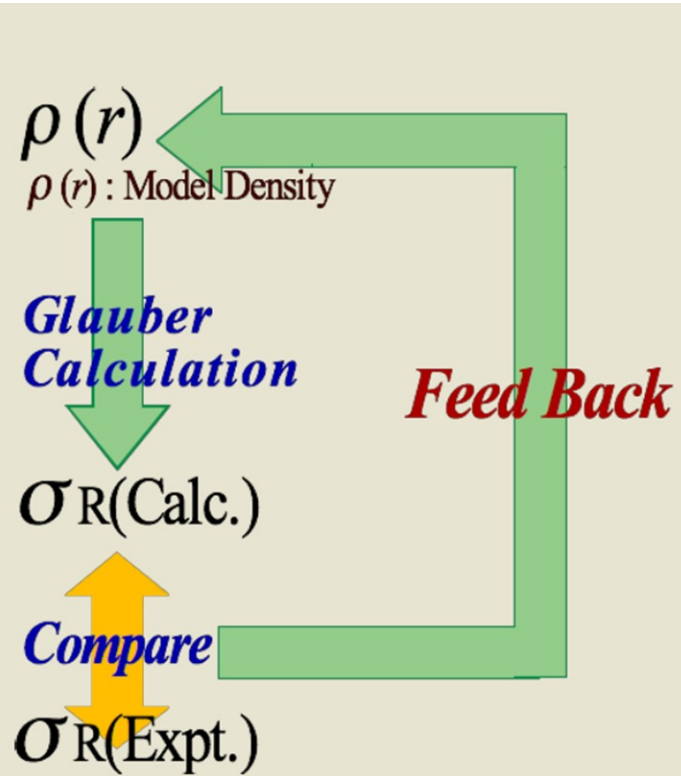
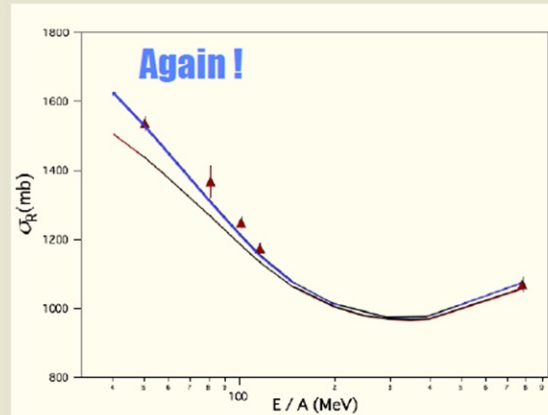
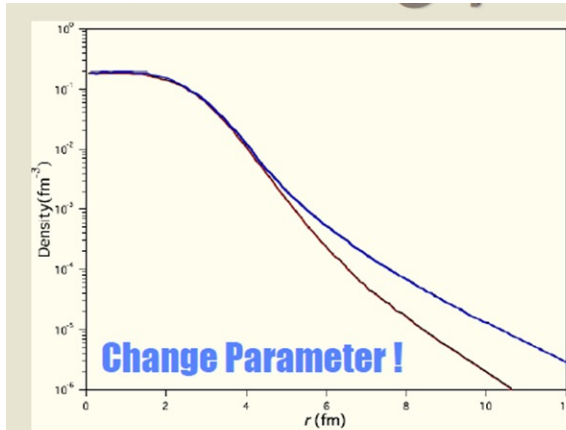
ρ_{Pp}, ρ_{Pn} : proton, neutron distribution of projectile

ρ_{Tp}, ρ_{Tn} : proton, neutron distribution of target



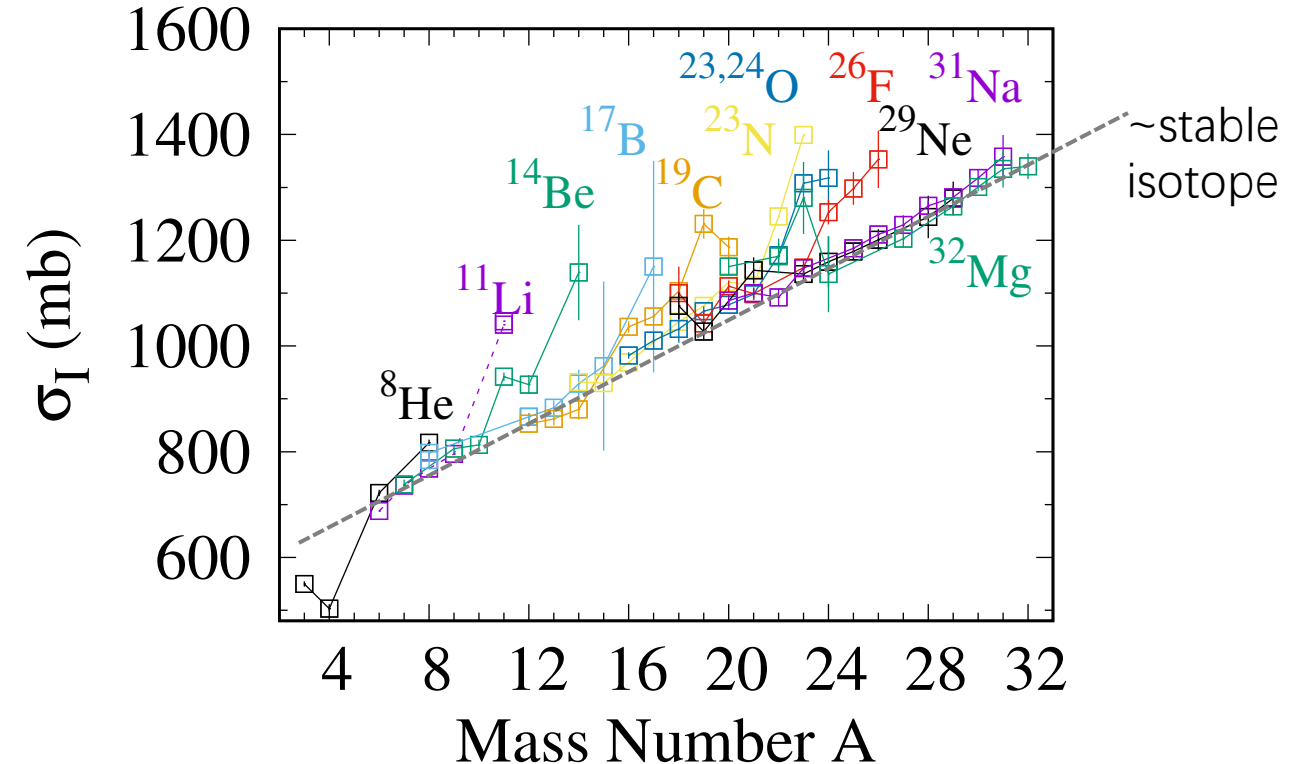
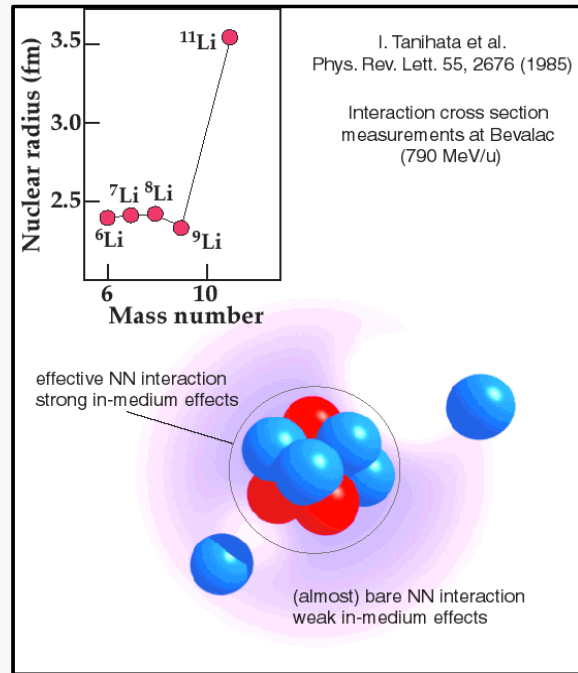
>200 MeV/nucleon: Eikonal model
(sudden approximation, Eikonal approximation)

How to deduce nucleon density or radii



Practically it can reproduce well the experimental σ_t data at 100 AMeV and above.

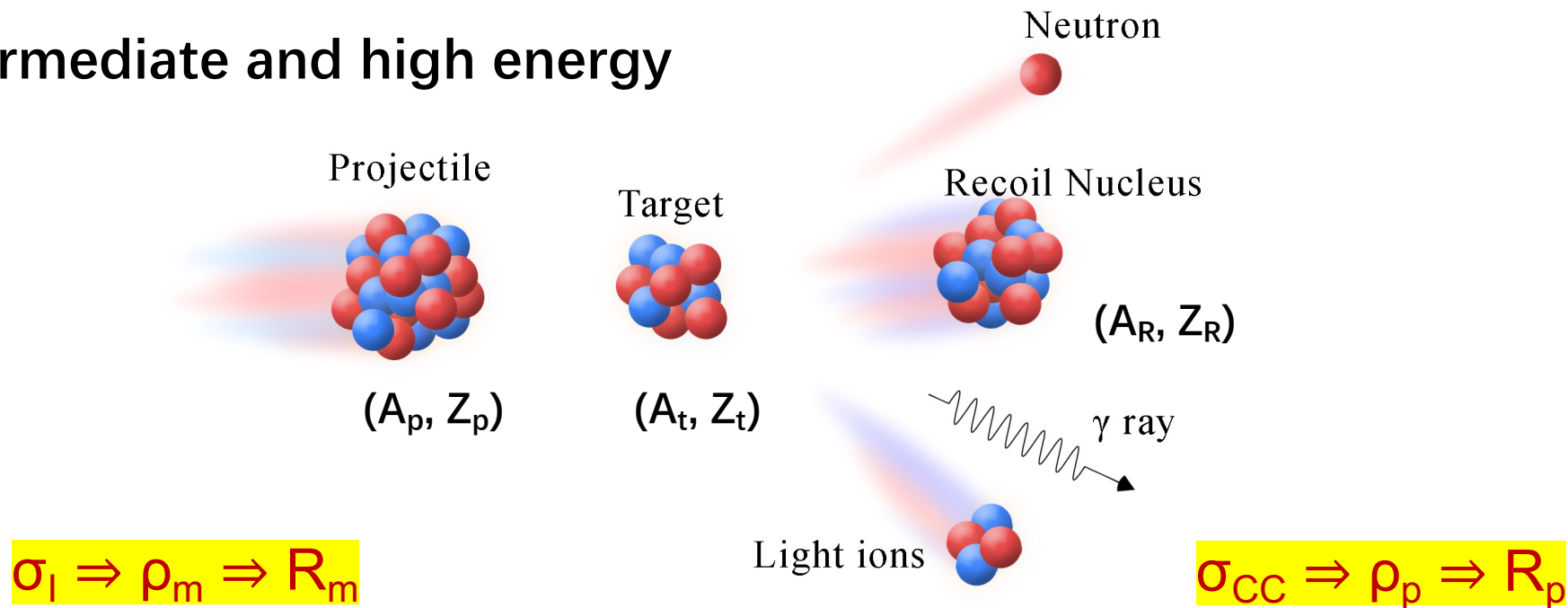
Systematic studies of interaction cross sections



It has been one of the most effective way to extract the rms matter radii of exotic nuclei.
Providing first hand information for most exotic light nuclei.

Interaction x-section vs charge-changing x-section

At intermediate and high energy



the reaction probability of **changing nuclear species** (A or Z) after collision, and are correlated with the **matter** (proton+neutron) density distribution in projectile

the reaction probability of **changing element** (Z) after collision, and are correlated with the proton density distribution in projectile

Cross section and nucleon density/rms radii

Cross section can be formulated in a microscopic Glauber model, relying only on the nucleon density distribution in the projectile and target nuclei and the bare nucleon-nucleon interaction.

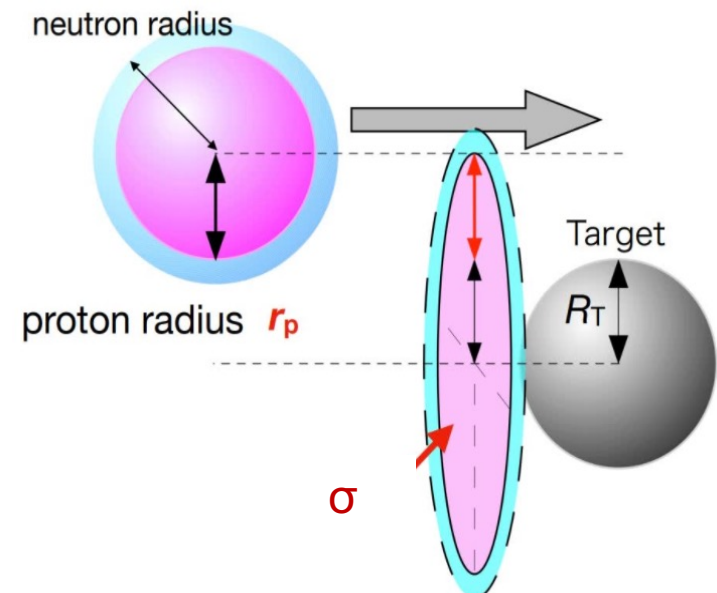
Optical limit (an example)

$$\sigma_I(P,T) = \int [1 - T(b)] d\mathbf{b}$$
$$\sigma_{cc} = 2\pi \int b[1 - T^p(b)] d\mathbf{b}$$
$$T(\mathbf{b}) = \exp[-\sigma_{pp} \int \{\rho_{Pp}(\mathbf{r} - \mathbf{b}) \cdot \rho_{Tp}(\mathbf{r}) + \rho_{Pn}(\mathbf{r} - \mathbf{b}) \cdot \rho_{Tn}(\mathbf{r})\} d\mathbf{r}]$$
$$- \sigma_{pn} \int \{\rho_{Pp}(\mathbf{r} - \mathbf{b}) \cdot \rho_{Tn}(\mathbf{r}) + \rho_{Pn}(\mathbf{r} - \mathbf{b}) \cdot \rho_{Tp}(\mathbf{r})\} d\mathbf{r}]$$

σ_{pp}, σ_{pn} : nucleon-nucleon total cross section

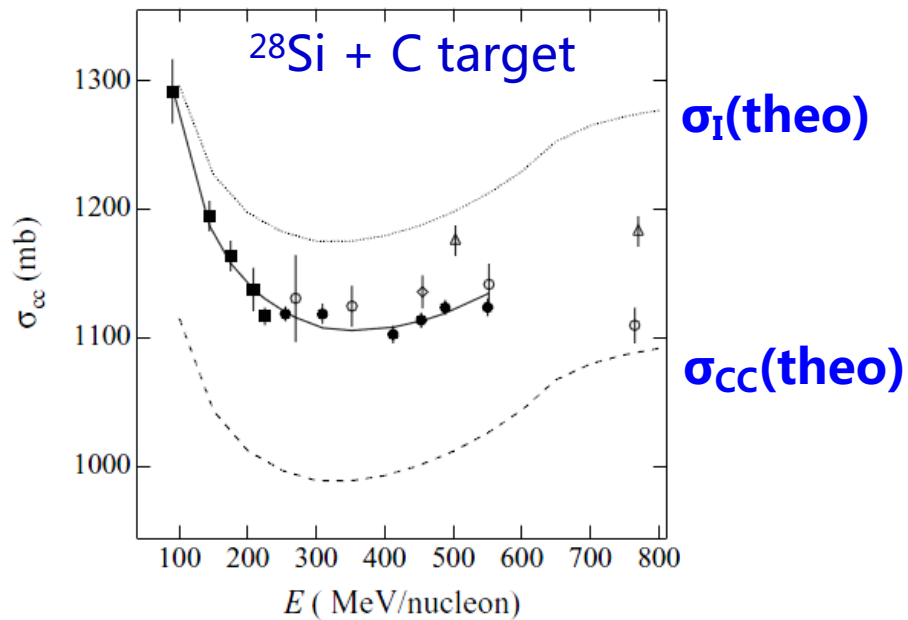
ρ_{Pp}, ρ_{Pn} : proton, neutron distribution of projectile

ρ_{Tp}, ρ_{Tn} : proton, neutron distribution of target

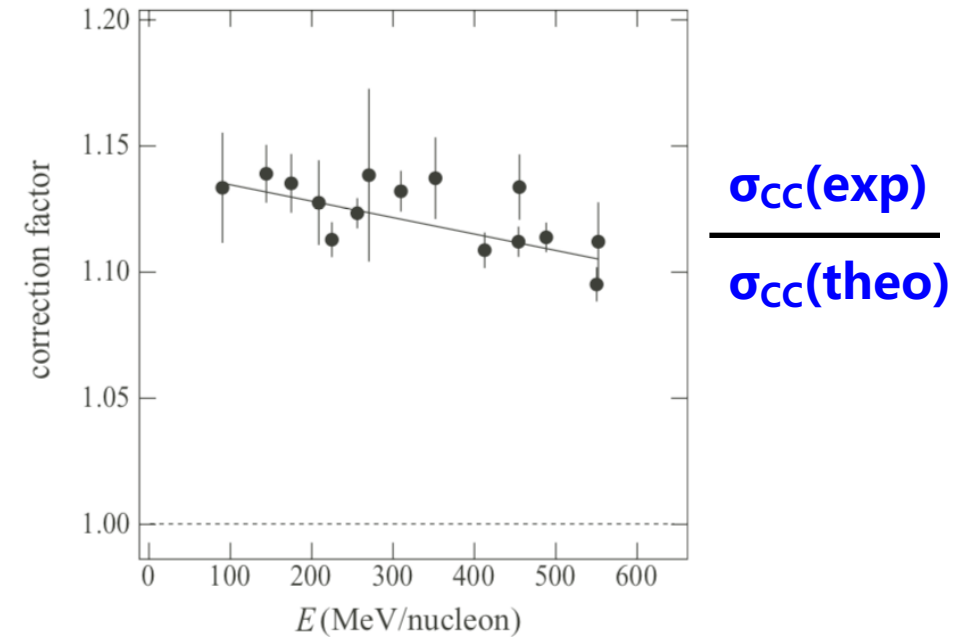


R_p from σ_{CC} of exotic nuclei

■ systematic investigation at HIMAC



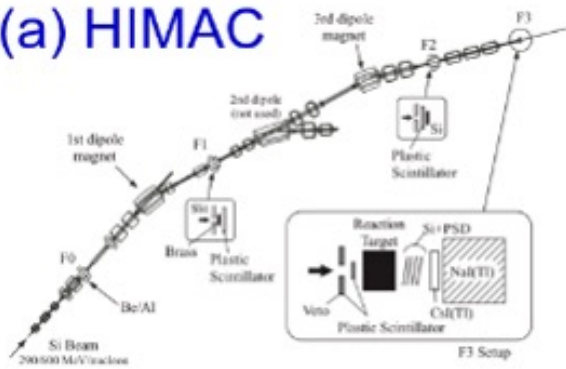
Yamaguchi-PRC 82, 014609 (2010)
Yamaguchi-PRL107,032502(2011)



- Energy-dependent correction factor needed for the zero-range optical-limit Glauber-type calculation to reproduce the experimental data
- The Glauber model successfully relates the σ_{CC} to R_p .

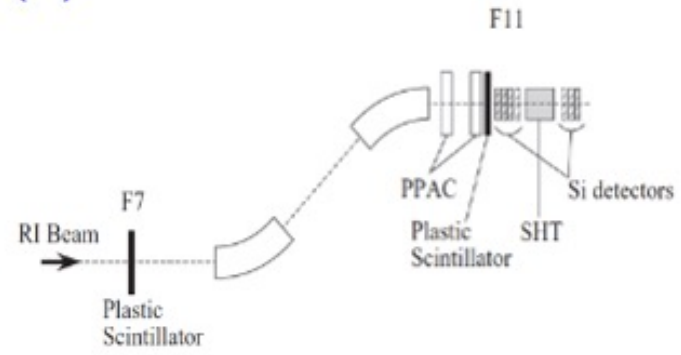
Experiments at HIMAC, RIKEN, GSI, RCNP

(a) HIMAC



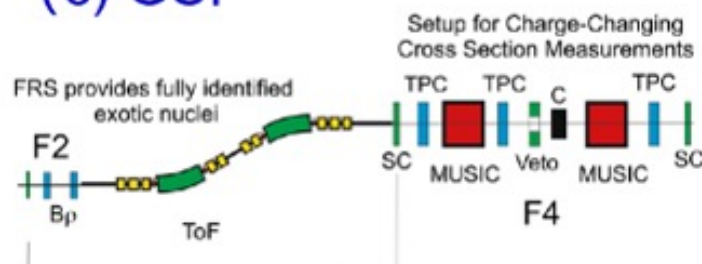
~300 AMeV

(b) RIKEN



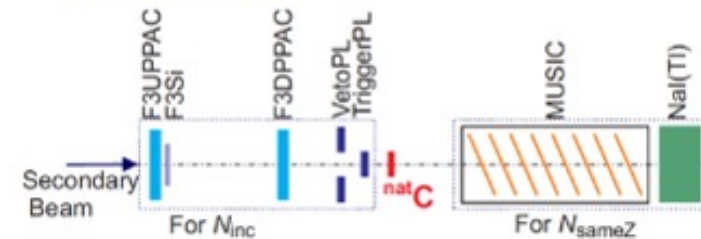
~300 AMeV

(c) GSI



~900 AMeV

(d) RCNP

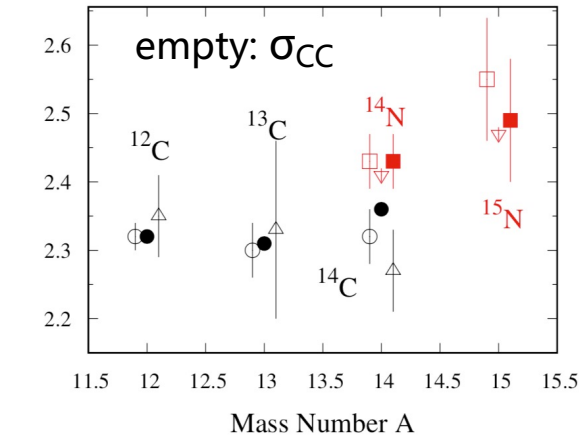
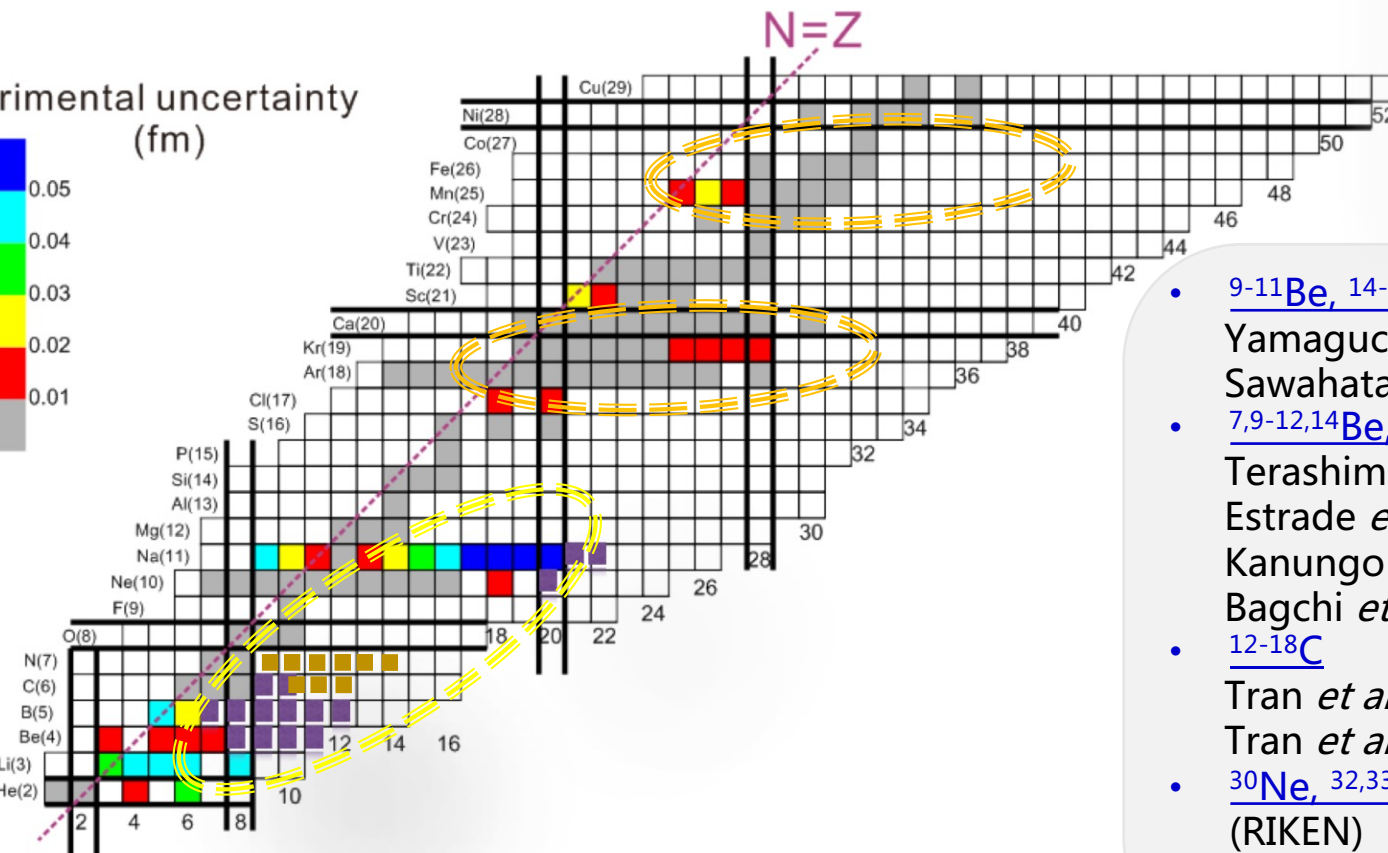
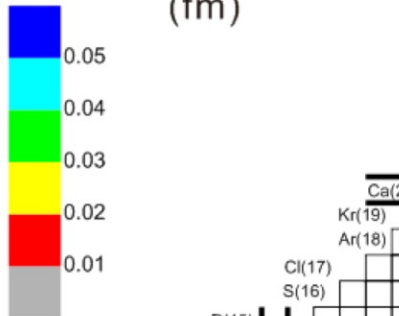


~40 AMeV

$\langle r^2 \rangle_p^{1/2}$ of unstable nuclei studied by σ_{CC}

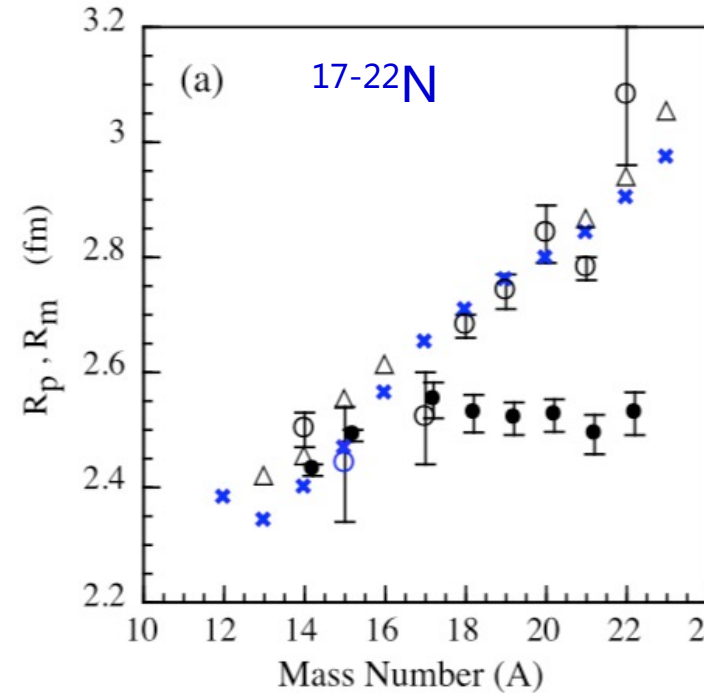
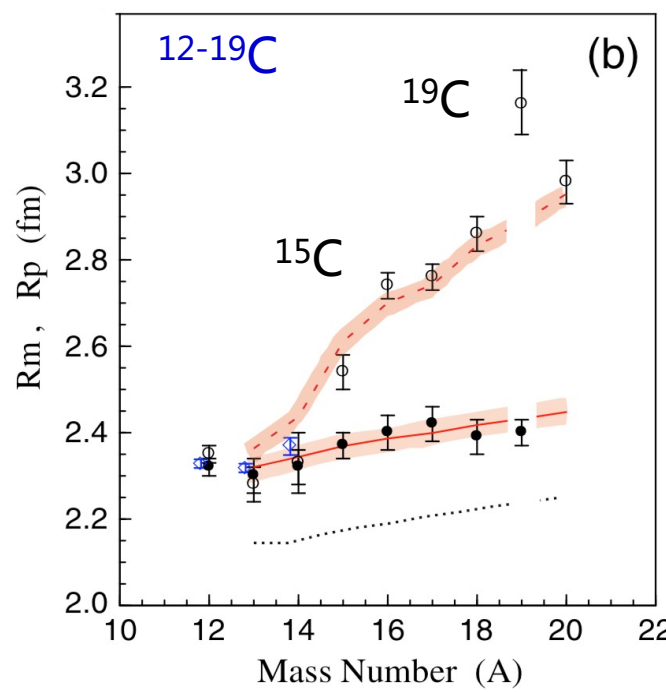
■ mostly in p-sd shell nuclei

Experimental uncertainty (fm)



- ^{9-11}Be , $^{14-16}\text{C}$, $^{16-18}\text{O}$ ~ 300 A GeV (HIMAC)
Yamaguchi *et al.*, PRL 107, 032502(2011)
Sawahata et al., NPA 961 (2017) 142
- $^{7,9-12,14}\text{Be}$, $^{12-17}\text{B}$, $^{12-19}\text{C}$, $^{17-22}\text{N}$ ~ 1 A GeV (GSI)
Terashima *et al.*, PTEP 2014, 101D02
Estrade *et al.*, PRL113, 132501 (2014)
Kanungo *et al.*, PRL117, 102501(2016)
Bagchi *et al.*, PLB790, 251(2019)
- $^{12-18}\text{C}$ ~ 45 A MeV (RCNP)
Tran *et al.*, PRC 94, 064604(2016)
Tran *et al.*, Nat. Comm. 9, 1594(2018)
- ^{30}Ne , $^{32,33}\text{Na}$, $^{42-51}\text{Ca}$ ~ 240 A MeV (RIKEN)
Ozawa *et al.*, PRC 89, 044602(2014)
Tanaka et al., PRC106(2022)014617

Experiments at 900 MeV/u at GSI

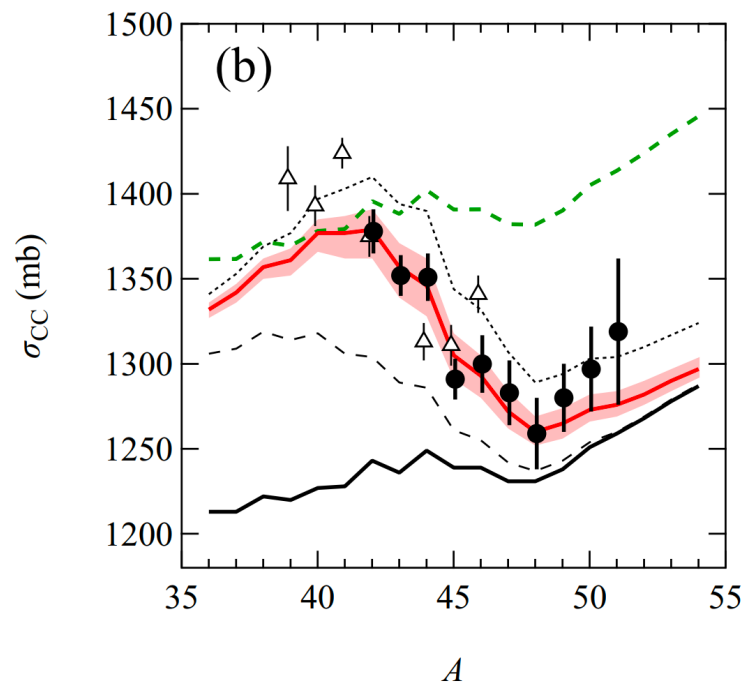
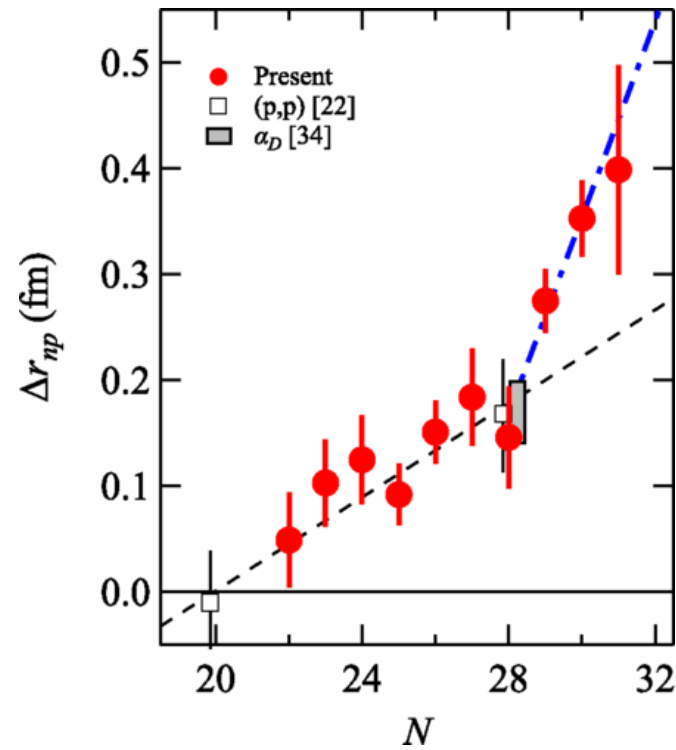
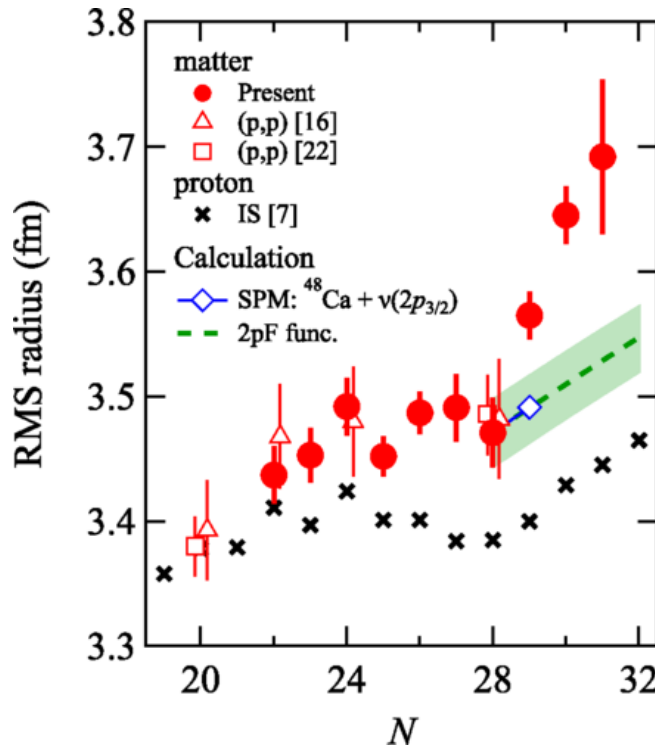


通过“调整”GM，再现稳定核半径，再外推得到奇特核半径

Q : how reliable is this Determination?

- Neutron surface: 0.2 fm (^{15}C) ~ 1 fm (^{19}C)
- Halo radius in ^{19}C : 6.4(7) fm from core+neutron model: as large as ^{11}Li
- kink at $N=14$ for N isotopes? ^{22}N neutron halo-like structure?

σ_I and σ_{CC} of Ca isotopes at RIKEN

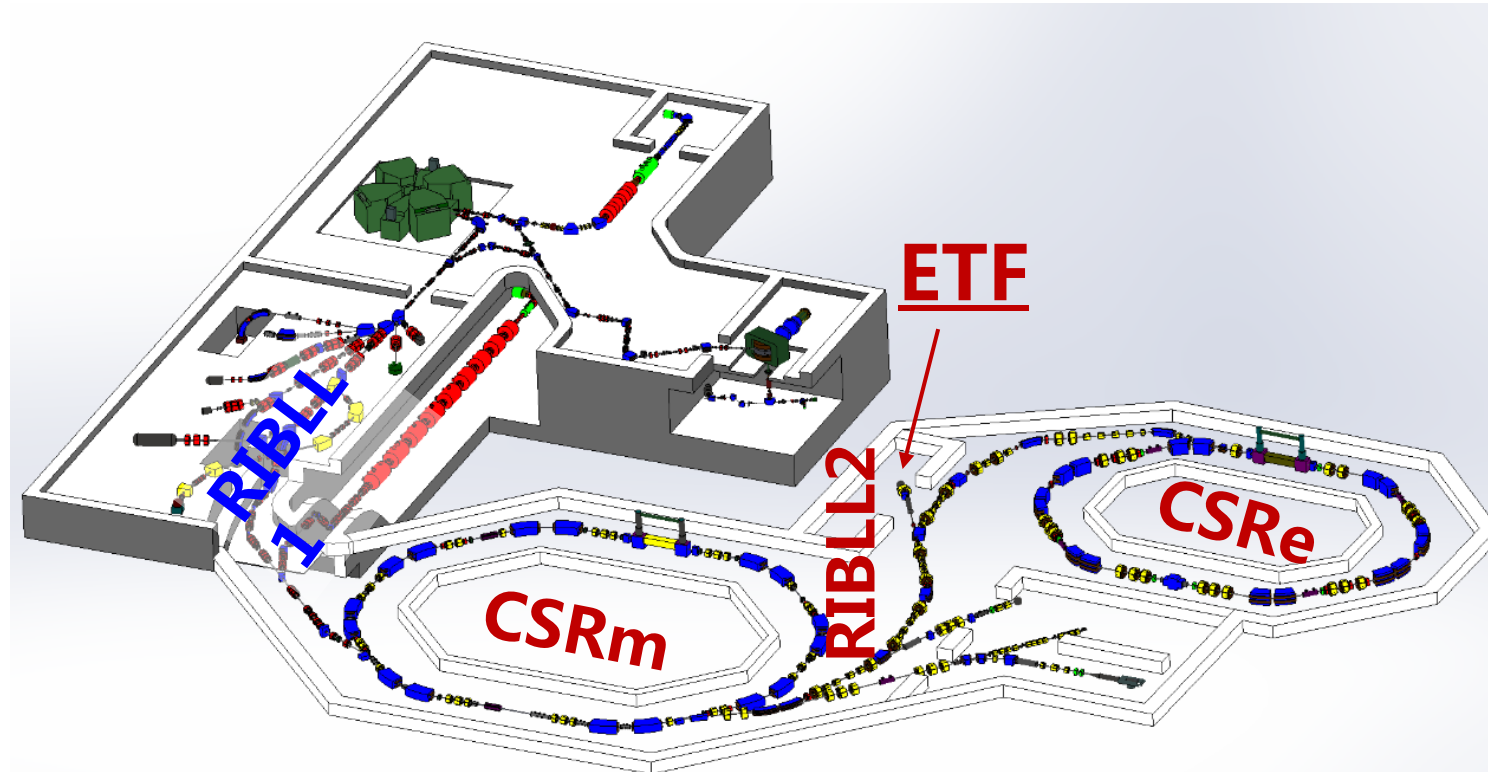


Ruiz *et al.* Nat. Phys. (2016)

M. Tanaka et al., PRL124(2020)102501
PRC106(2022)014617

RIBLL2 - Second Radioactive Ion Beam Line at HIRFL

RIBLL2 was using routinely as a beam transfer line from CSRm to CSRe. To exploit its full ability and to investigate HFRS at HIAF has been one of our group focus since 2015.



Beam delivered for
Slow extraction
 ^{16}O @360 MeV/u ,
 ^{18}O @400 MeV/u ,
 ^{40}Ar @320 MeV/u ,
 ^{78}Kr @300 MeV/u ,
 $\sim 10^8$ particles/spill

J.W. Xia et al. The heavy ion cooler-storage-ring project (HIRFL-CSR) at lanzhou. Nucl. Instrum. Meth. A 488 (2002) 11
BHS et al., Towards the full realization of the RIBLL2 beam line at the HIRFL-CSR complex, Sci. Bull. 63(2018)78
Y. Sun et al., The charged fragment detector system of the External Target Facility, NIMA927(2019)390

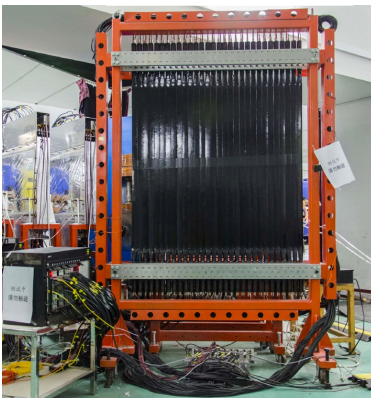
Detector development

MUSIC



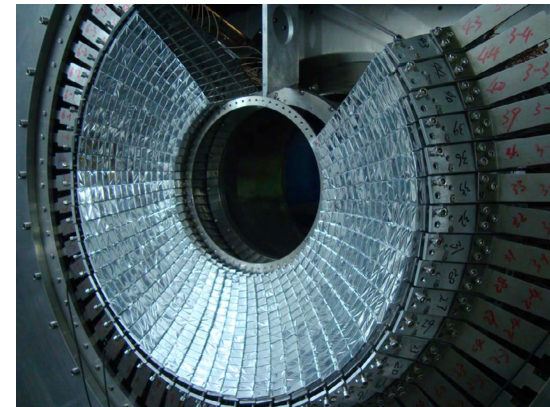
Zhang-IMA795(2015)389
Zhao-NIMA930(2019)95

TOF wall



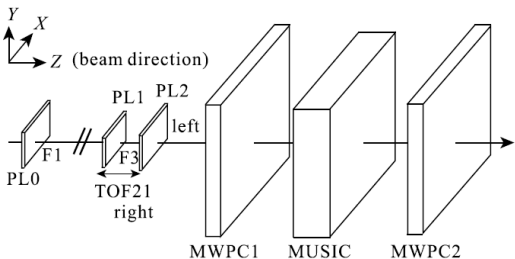
Y.Sun-NIMA893(2018)68

CsI(Tl) γ array



Yue-NIMB317(2013)653

TOF detector



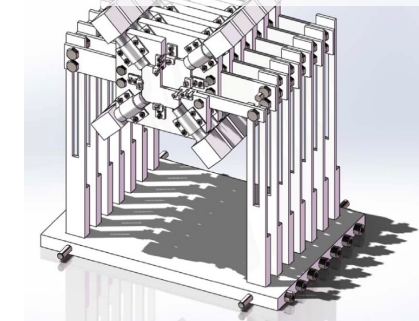
Zhao-NIMA823(2016)41
Lin-CPC41(2017)066001

MWDC array



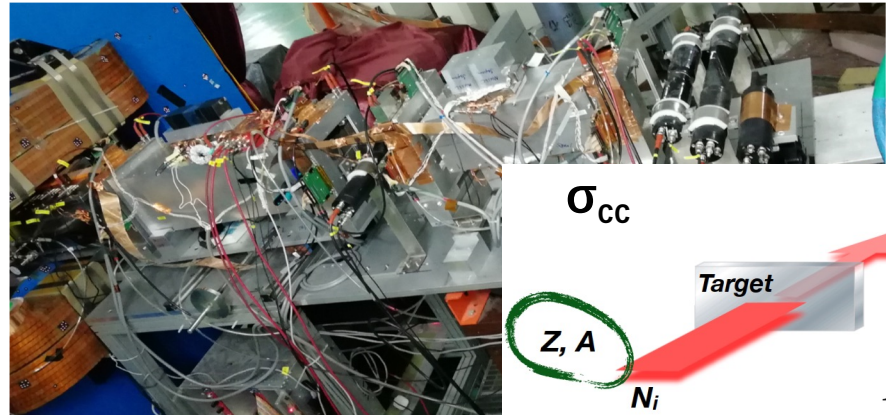
Y.Sun-NIMA894(2018)72;
NIMA985 (2021)164682

CsI(Tl) detector telescope



Yan-NIMA843(2017)5

ETF: 2021



σ_{cc}

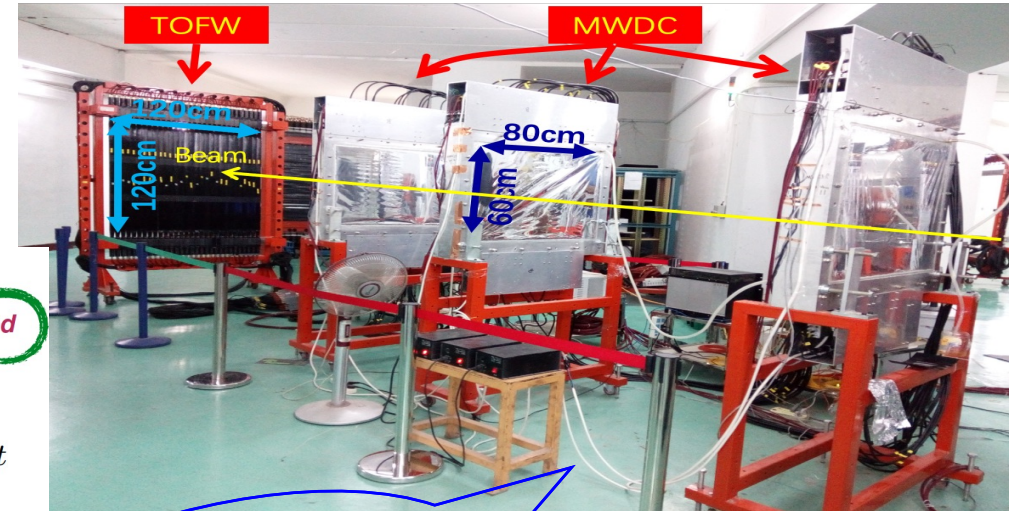
Target

Z, A

N_i

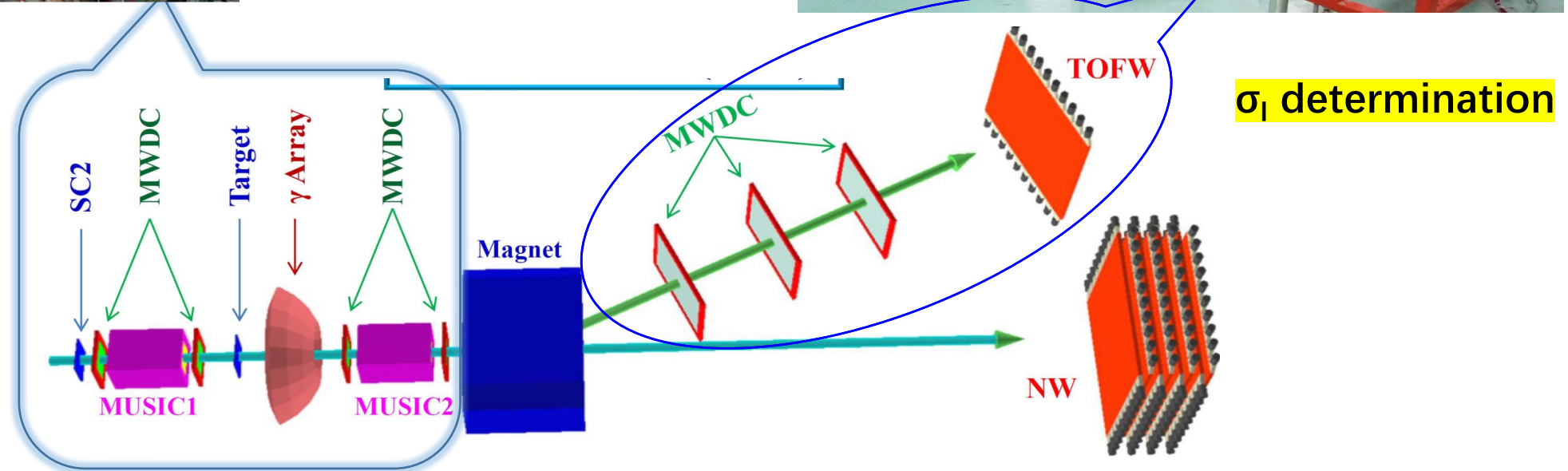
$$N_o = N_i e^{-\sigma_{cc} t}$$

N_o only Z identified



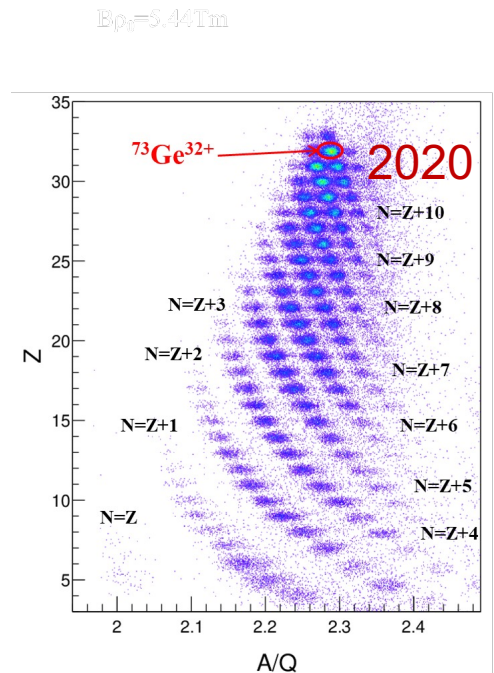
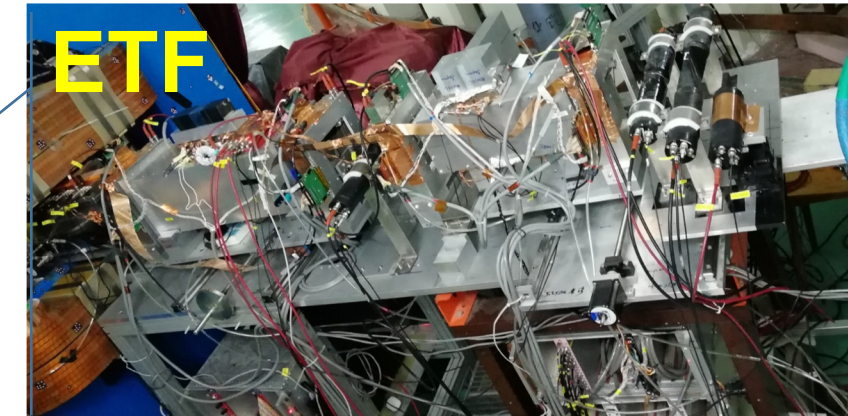
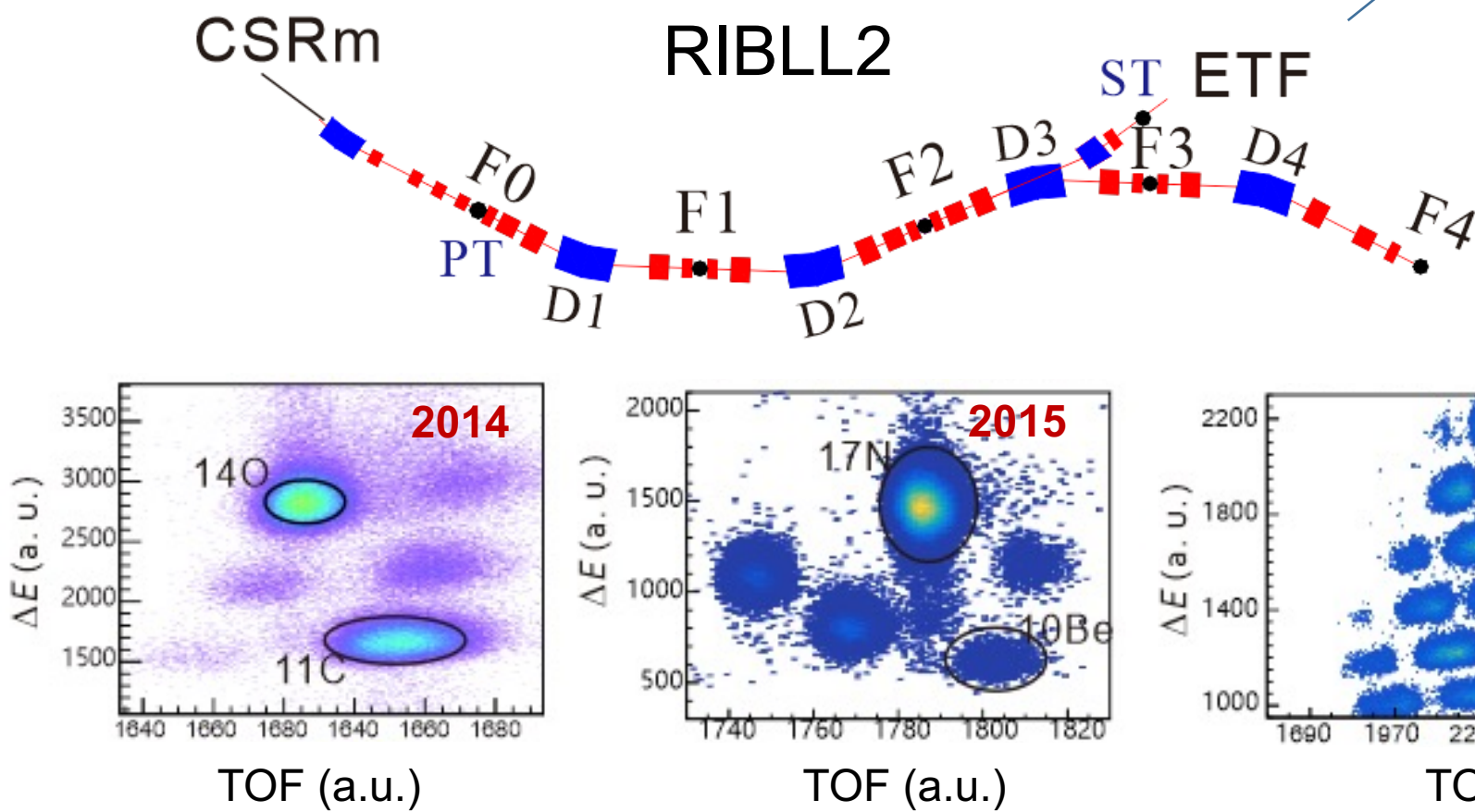
TOF-dE-Bp

Half-RIBLL2



Y. Z. Sun, et al., Nucl. Inst. Meth. A 927 (2019) 390

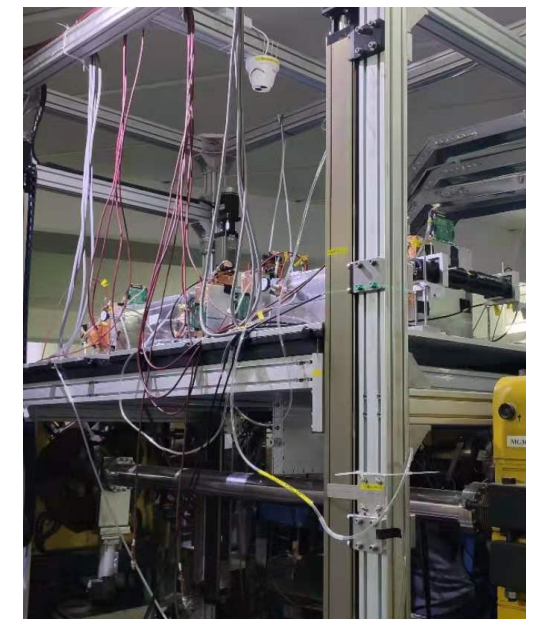
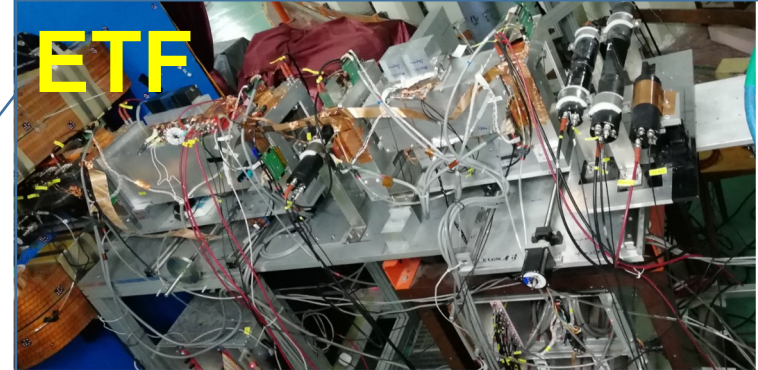
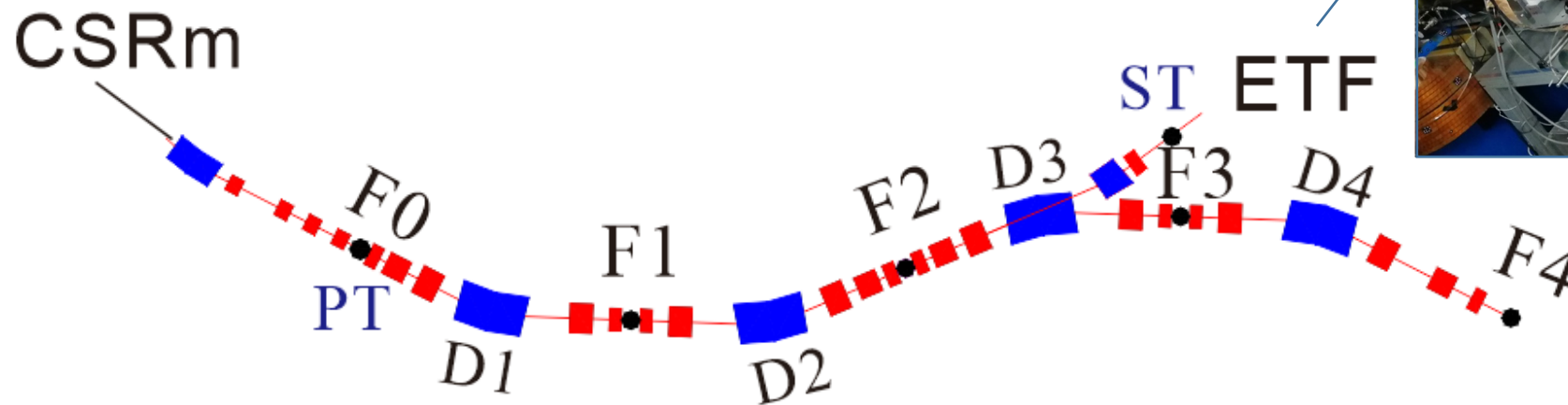
RIBLL2: Particle identification



Increasing resolving power (light mass to intermediate mass range)

BHS et al., Sci. Bul. (2018); F. Fang et al., Nucl. Phys. Rev. (2021)

RIBLL2 upgrade and F4



- Upgrade all the focal plans
- Install beam diagnosis system for primary beam and RIB beams
- Ion-optical optimization
- New F4 platform: increased TOF pathlength from 26m to 42 m

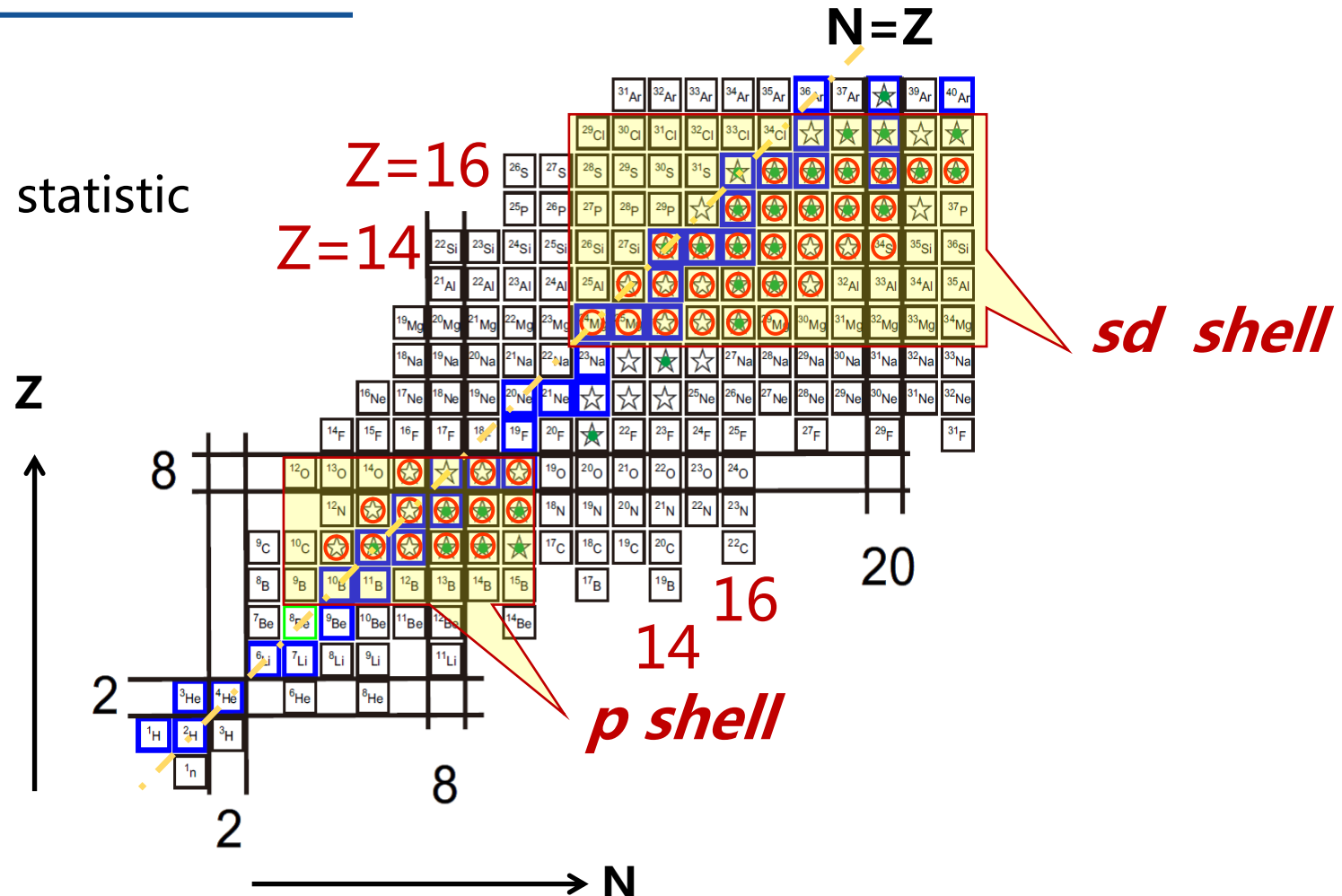
Courtesy: Yong Zheng, Xueheng Zhang, H. Ong

CCCS measurements at $\sim 300\text{MeV/nucleon}$ (2015-)

★ ~60 nuclei

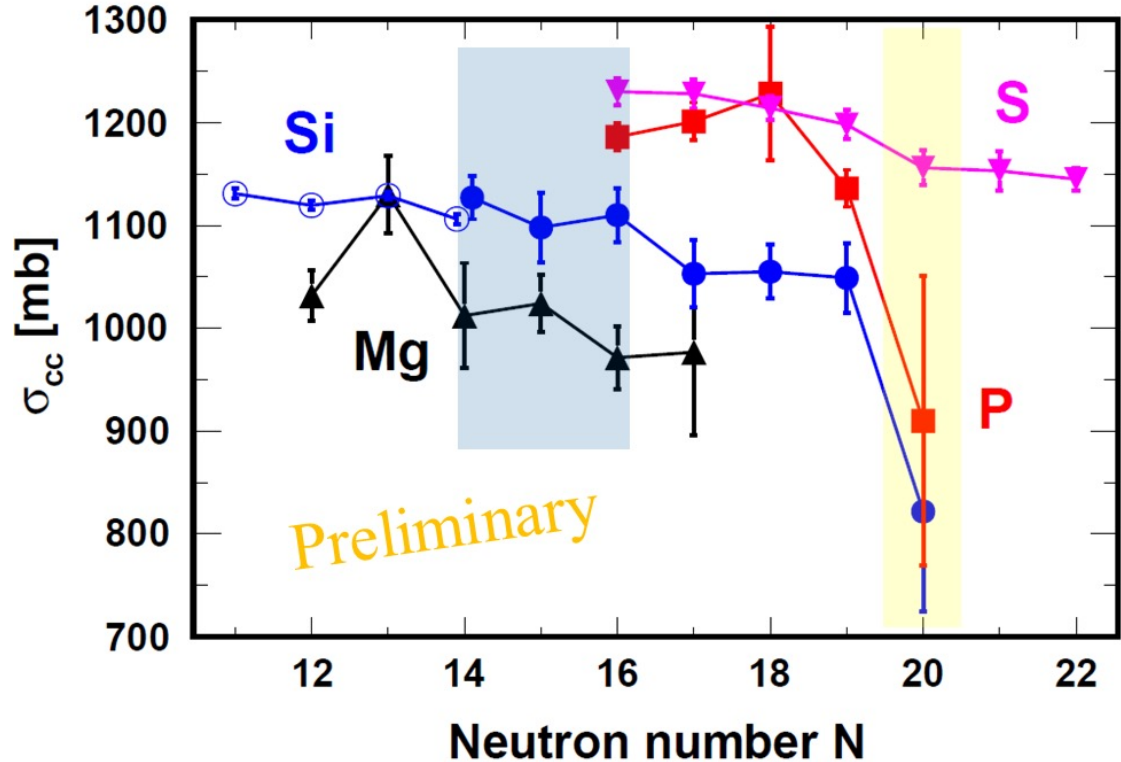
★ ~10 nuclei with good statistic

★ Preliminary results



J. Zhao, BHS, Nuclear Physics Review (Chinese edition), 35(2018)362
BHS, Science Bulletin 65, 3886 (2020)

New data in *sd* shell



Systematic data;

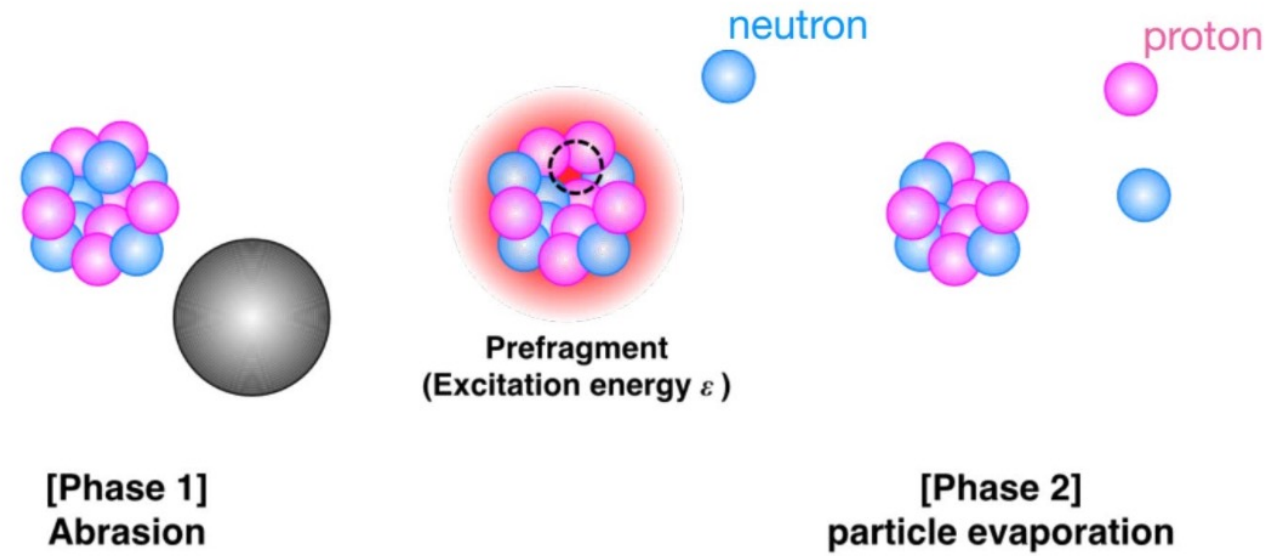
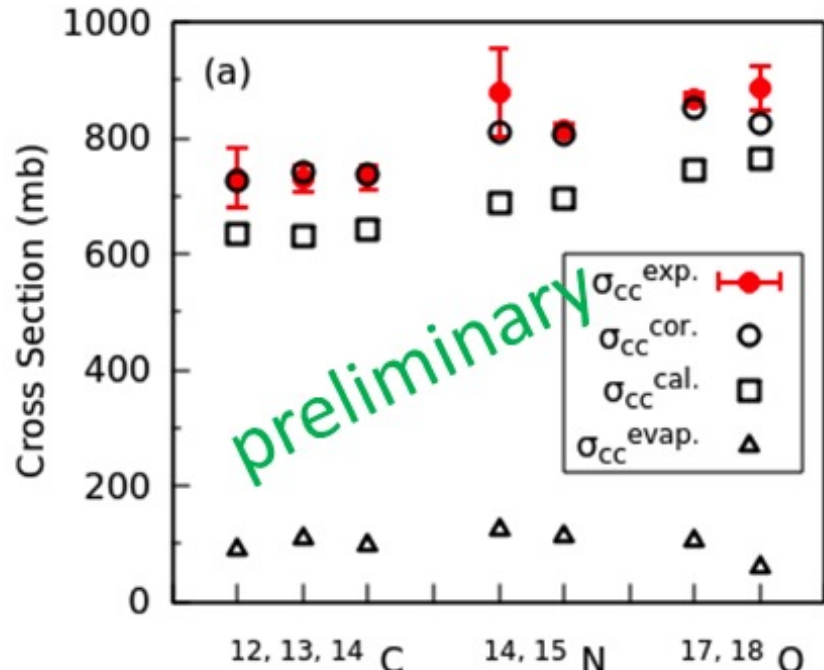
$N=20$ kink is seen, but $N=14$,
 16 needs a better statistic

Data with improved statistic
(2021)

HIMAC-Data (empty) , $^{25-28}\text{Si}$: NPA961,142(2017)

Courtesy: Guang-Shuai Li, Xiu-Lin Wei, Xiao-Dong Xu

New data in stable C, N and O isotopes

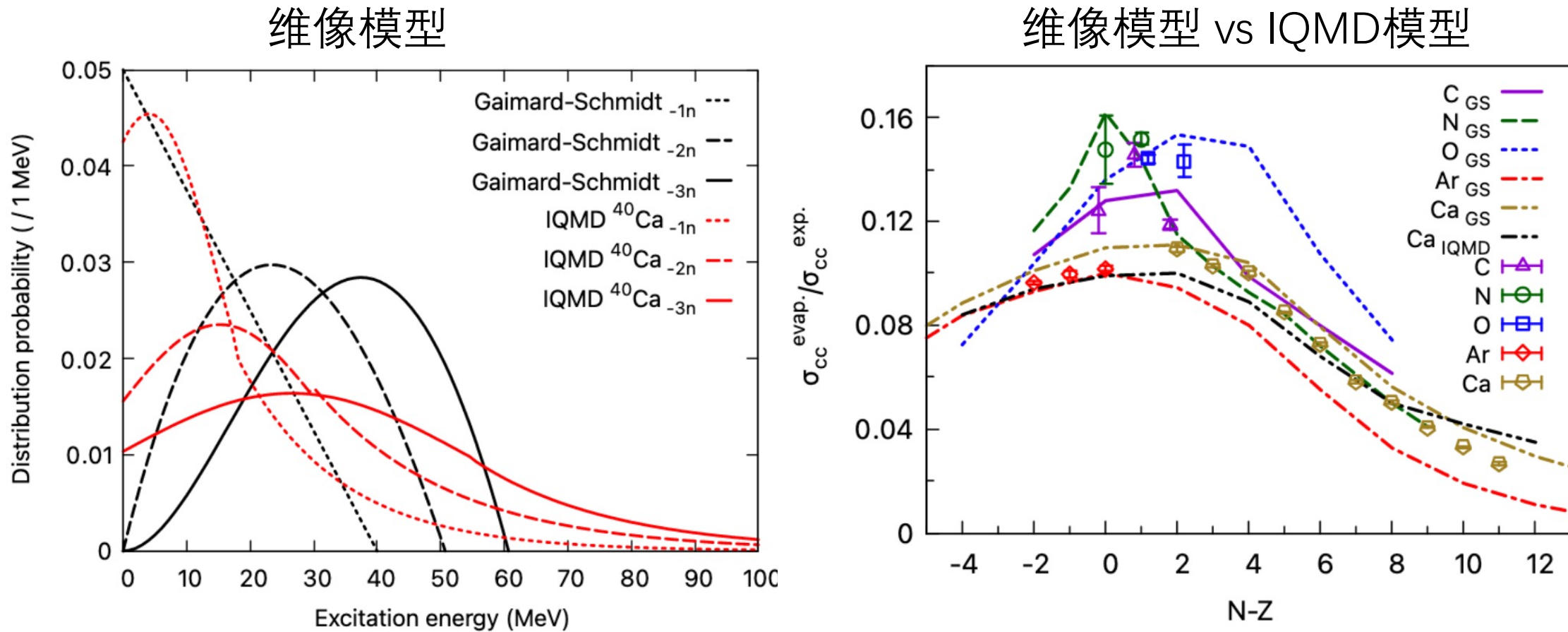


Courtesy: M. Tanaka

Glauber model cannot reproduce the cross section, while by including proton evaporation process , can well explain the discrepancy between experiment and theory.

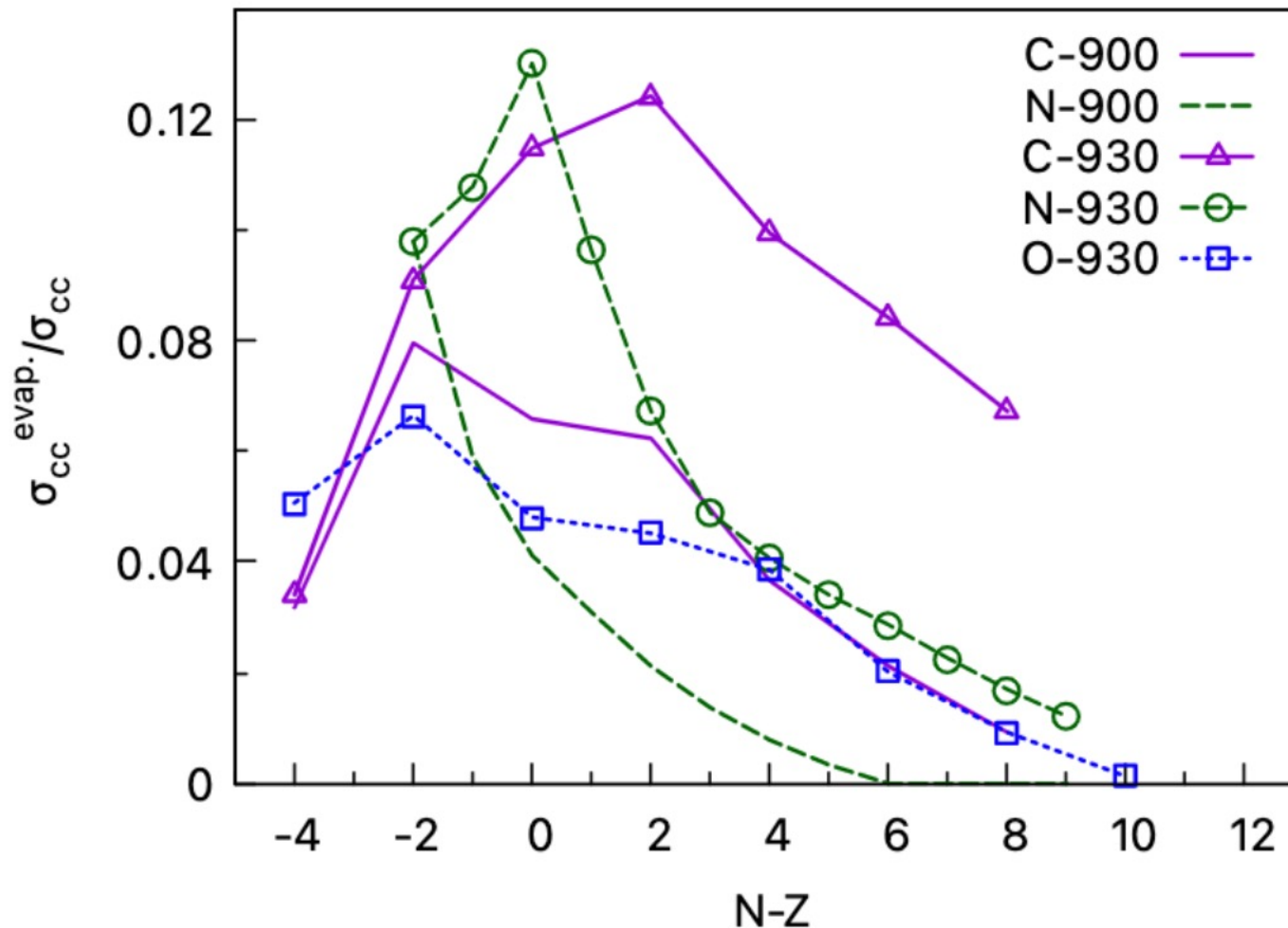
J. Zhao, BHS, J.Y. Xu et al., in preparation

neutron induced charged particle evaporation



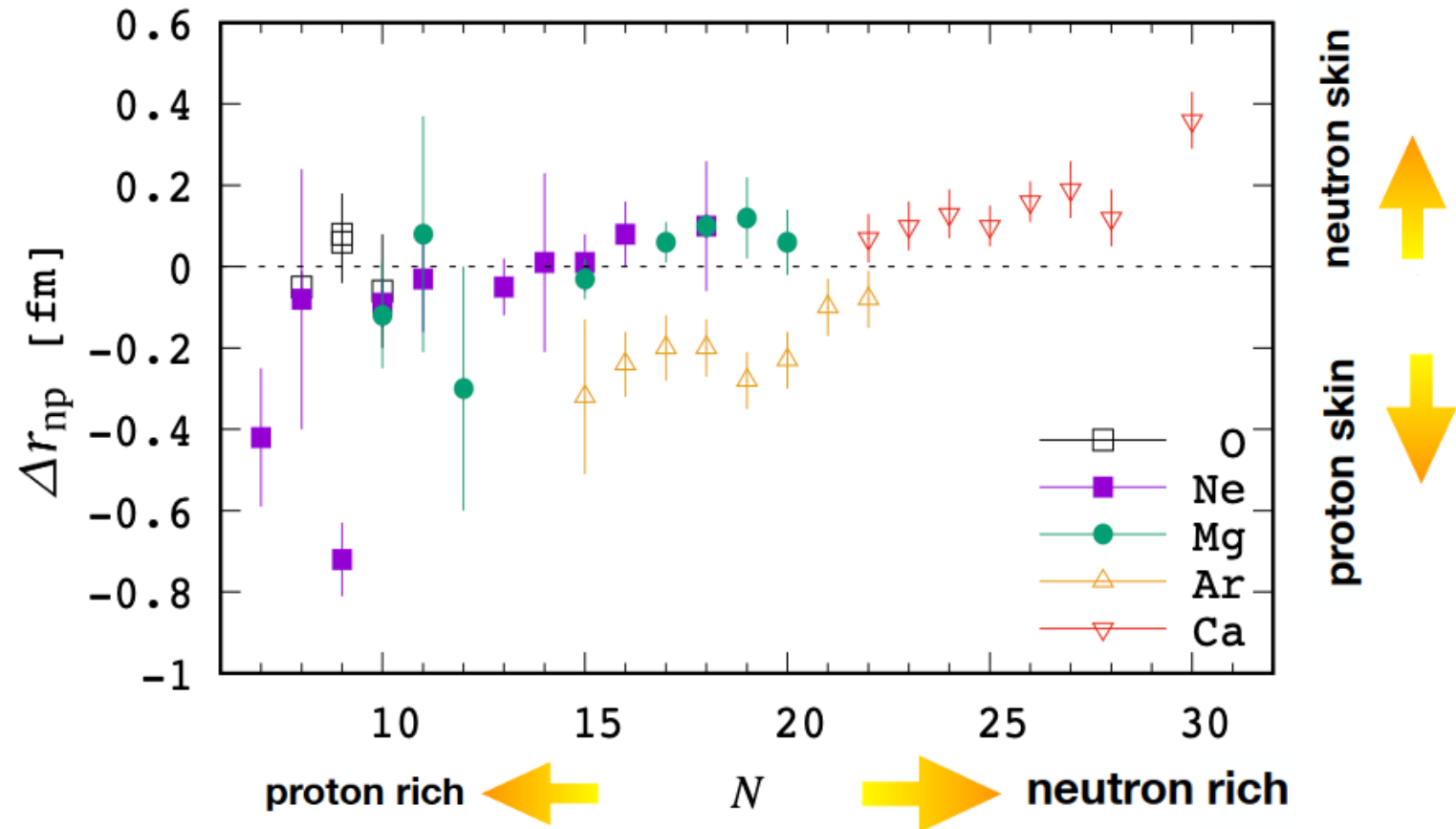
J. Zhao, BHS, J.Y. Xu et al., in preparation

Isospin dependent ?

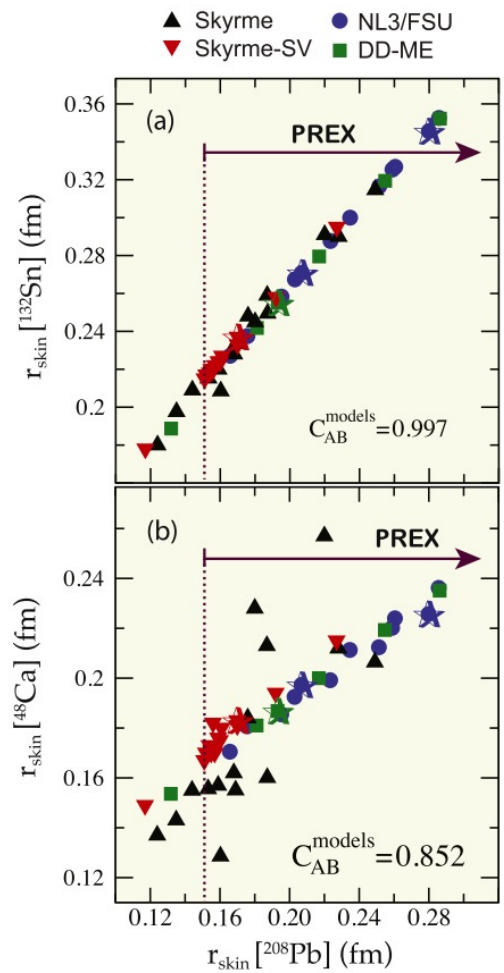


J. Zhao, BHS, J.Y. Xu et al., in preparation

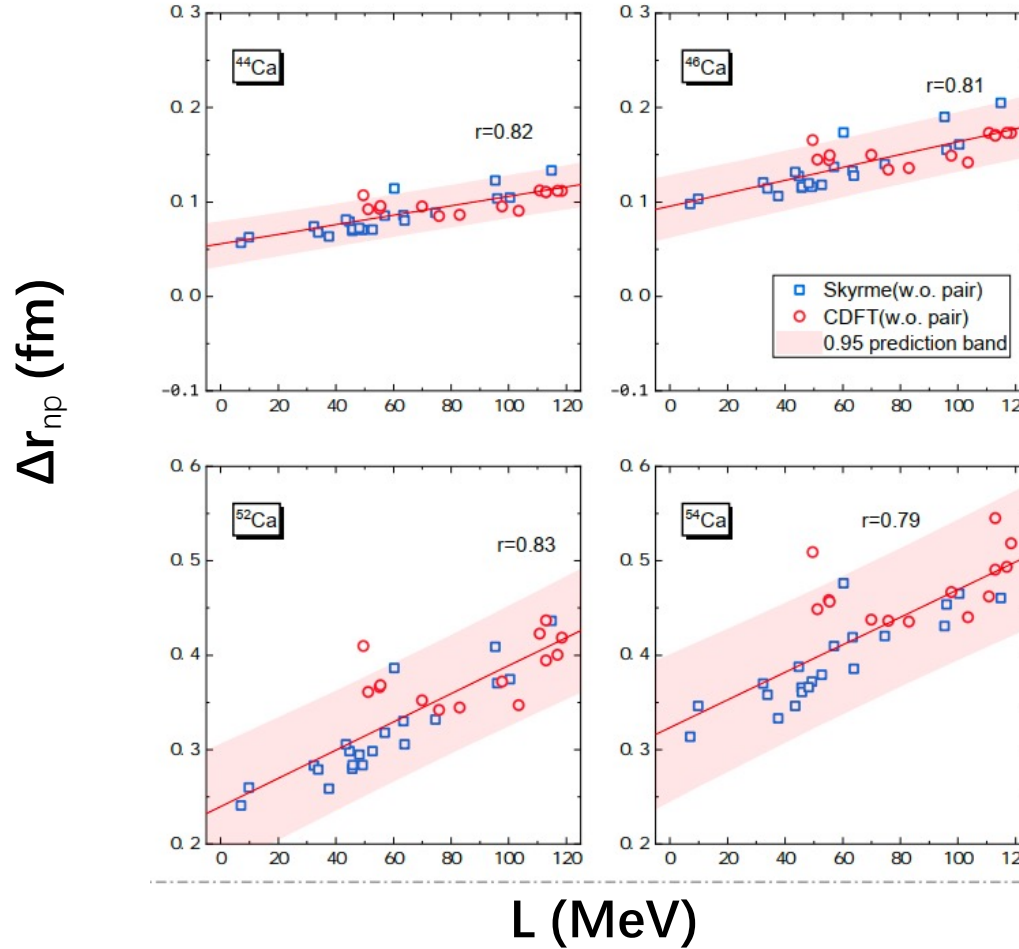
Are the Δr_{np} of light nuclei useful to constrain L ?



Seems not good enough ...

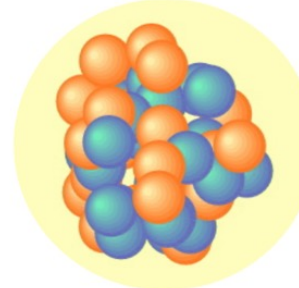
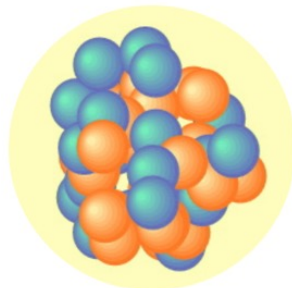


Calculations done by Y.F. Niu group



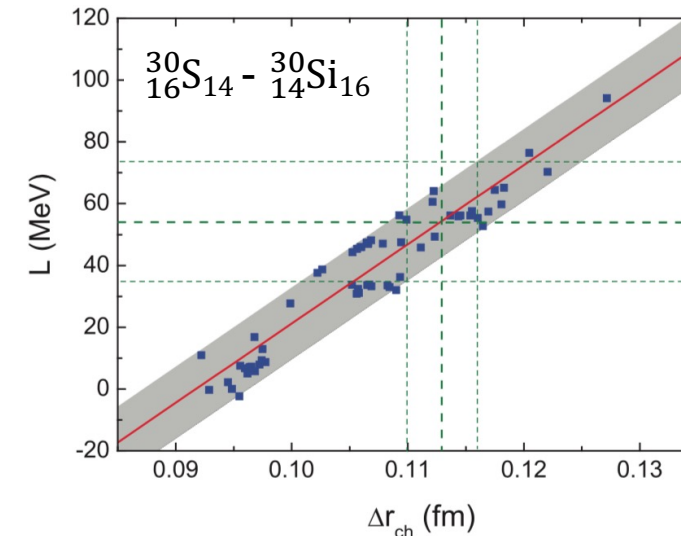
Linearity between L and skin thickness holds better in medium and heavy nuclei.

Mirror nuclei as a laboratory to probe EOS



isospin symmetry
nearly identical properties

$$R_{\text{skin}}(Z, N) \equiv R_n(Z, N) - R_p(Z, N)$$
$$\approx R_p(N, Z) - R_p(Z, N) \equiv R_{\text{mirr}}(Z, N).$$

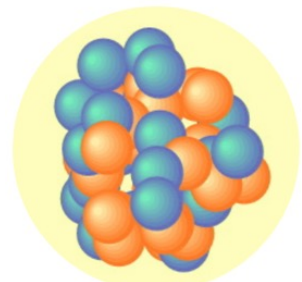


Wang & Li, PRC **88**, 011301(R) (2013)

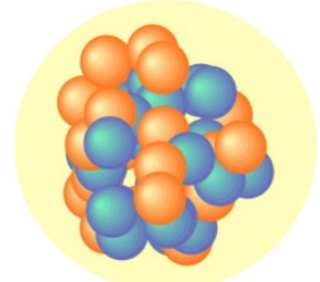
The differences in the charge radii of mirror nuclei are shown to be proportional to the derivative of the symmetry energy L at nuclear matter saturation density.

Brown, PRL 119, 122502(2017) ; Yang & Piekarewicz, PRC97,014314(2018)

Constrain EOS by CCCS difference of mirror nuclei



30Si

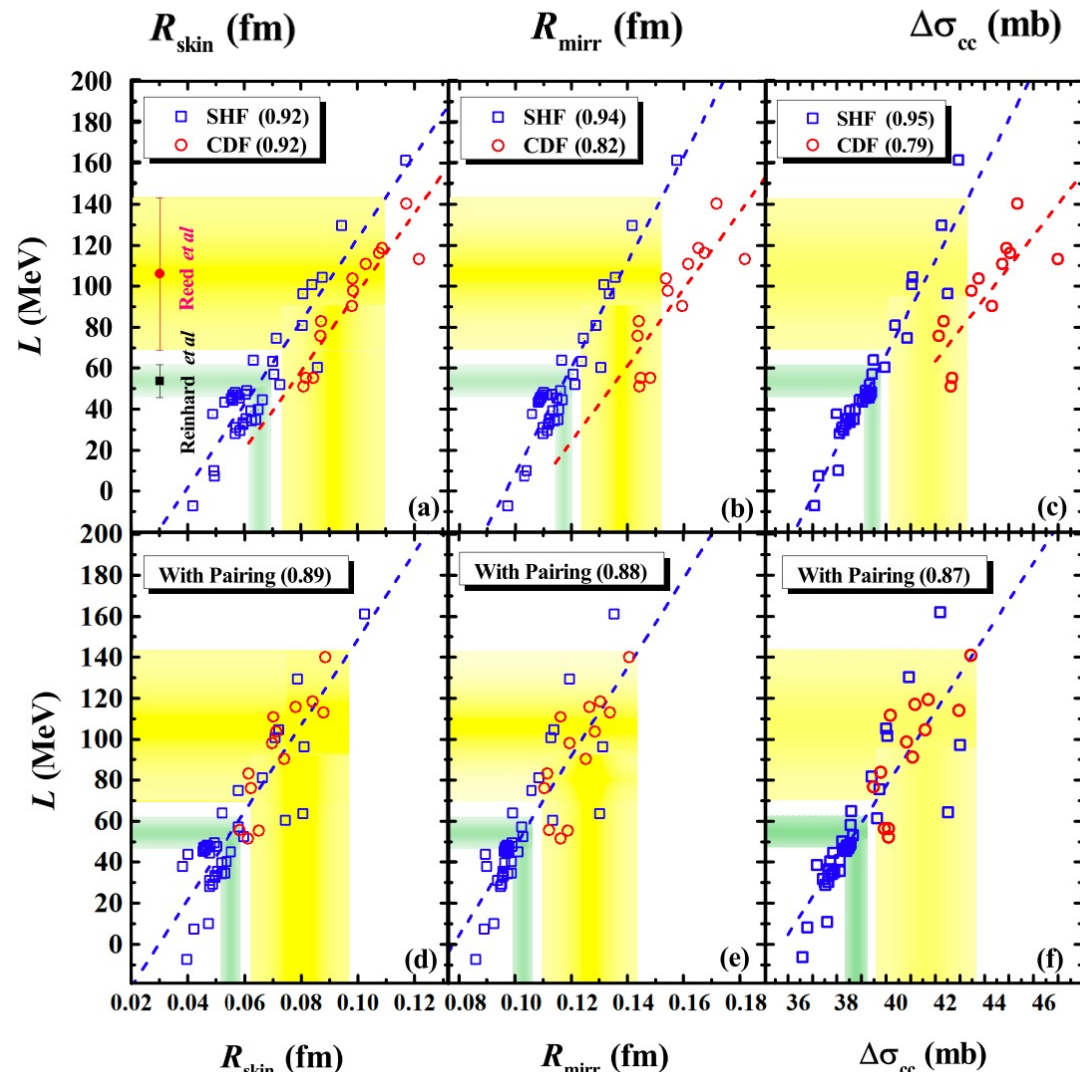


30S

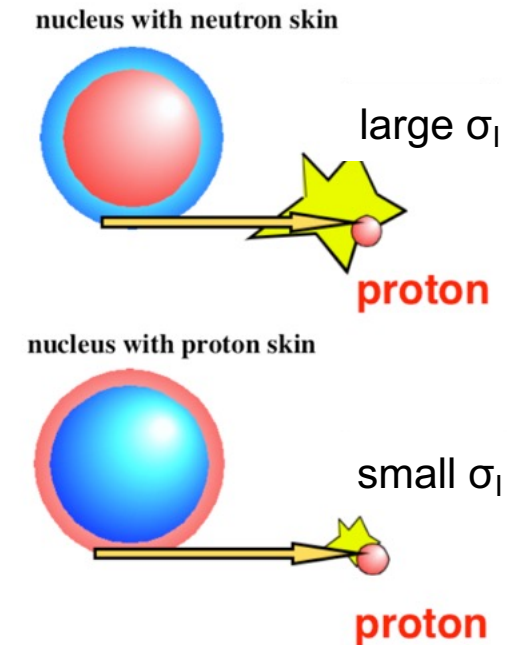
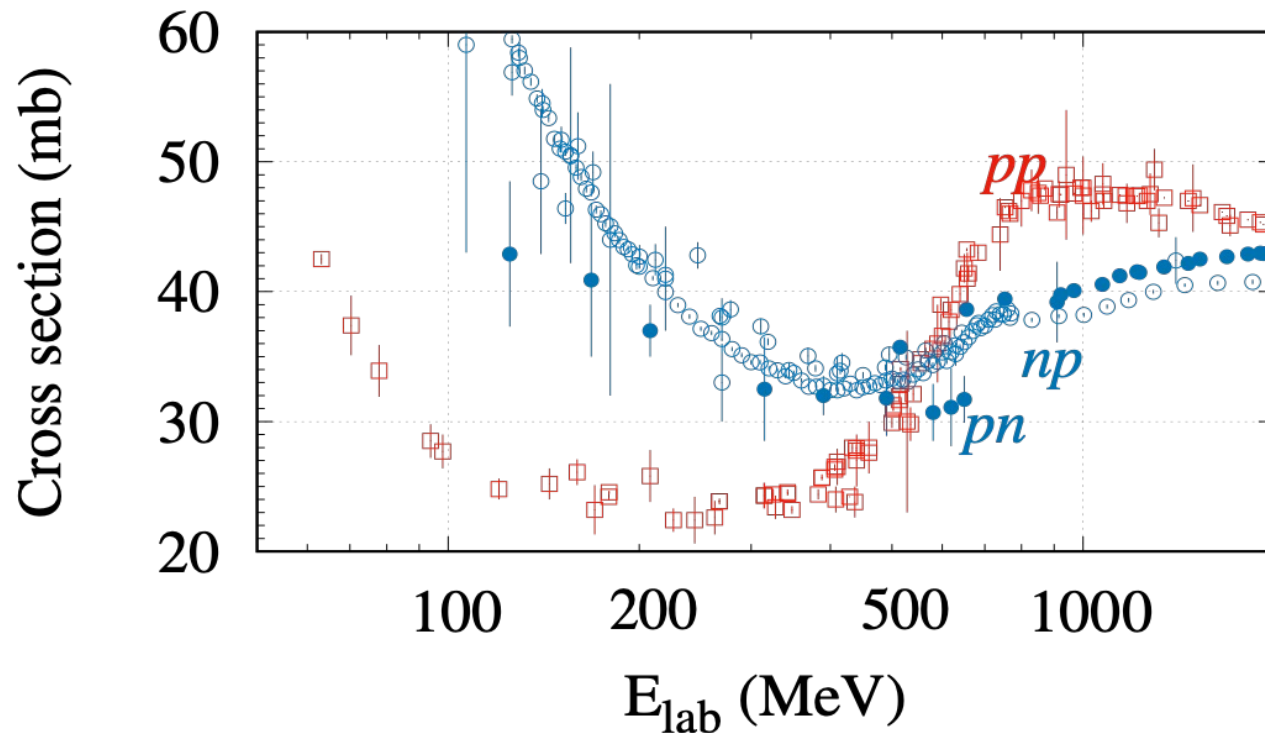
Mirror nuclei + same target

$$\Delta\sigma_{cc} \approx 2\pi(1 + af^2)[R_{\text{targ}}^{\text{mat}} + afR_{\text{proj}}^{\text{prot}}(Z, N) - c]R_{\text{mirr}}$$

$$\begin{aligned} R_{\text{skin}}(Z, N) &\equiv R_n(Z, N) - R_p(Z, N) \\ &\approx R_p(N, Z) - R_p(Z, N) \equiv R_{\text{mirr}}(Z, N). \end{aligned}$$



Target combination : ^2H , ^{12}C vs ^1H

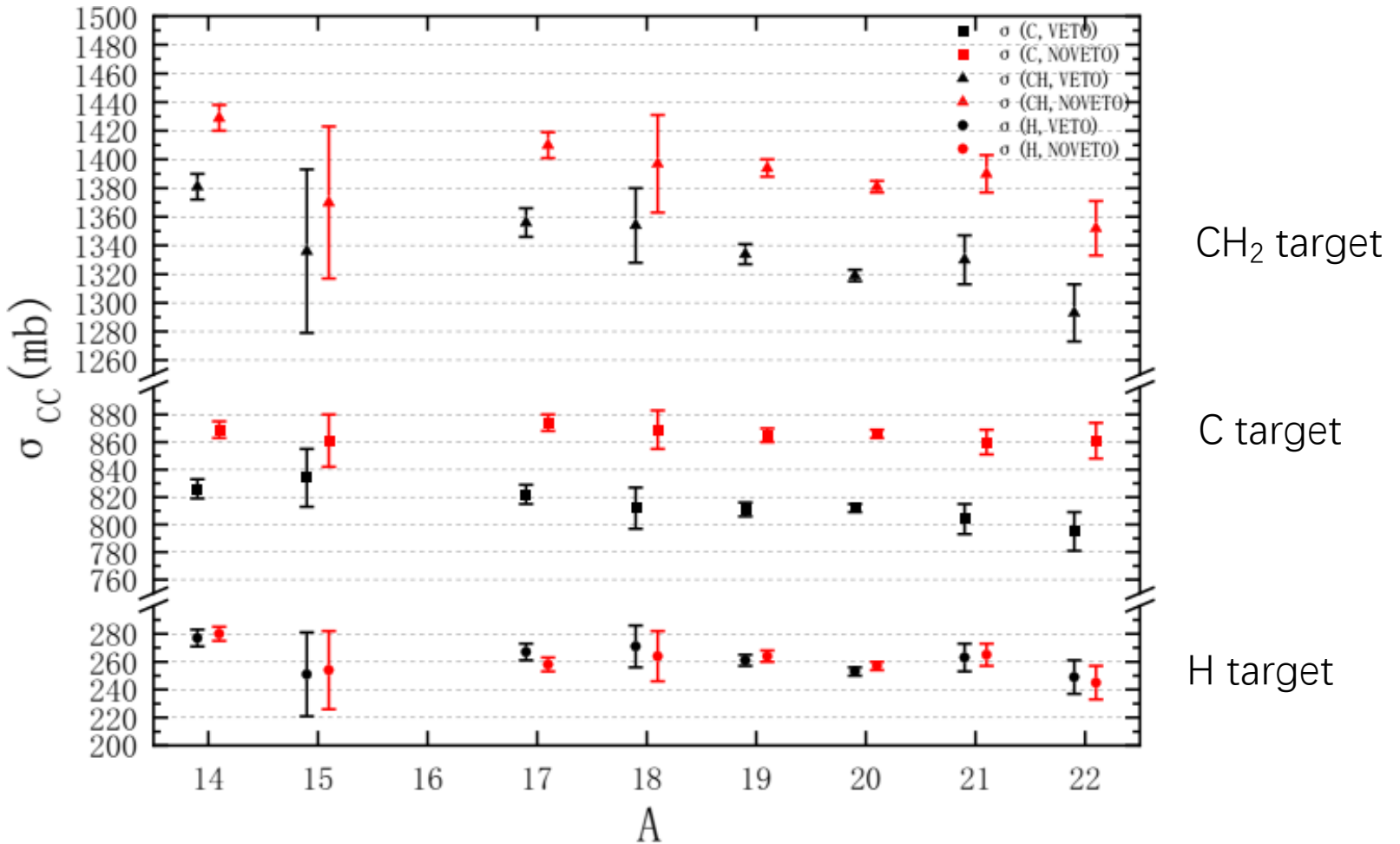


H/D target: best target to disentangle r_p and r_n , isospin effect.
proton/deuteron target can be used to deduce neutron skin thickness

Solid hydrogen target is in developing.

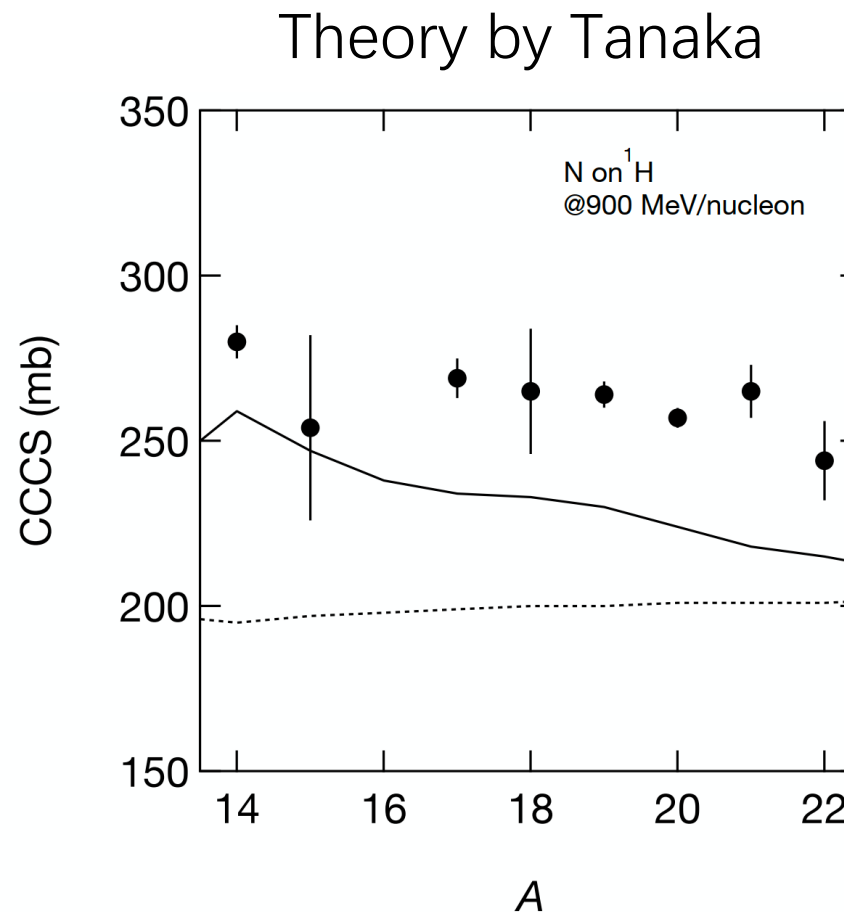
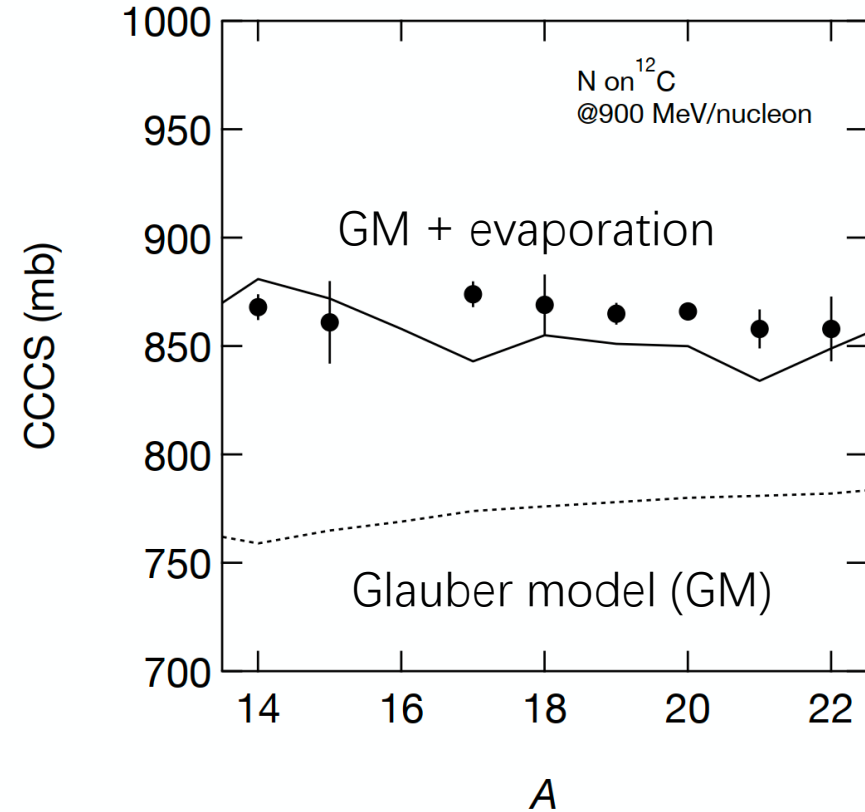
Horiuchi, Suzuki, Uesaka, Miwa, PRC102, 054601(2020)

First results on ^1H at 900 MeV/u at GSI



张寂潮等 , in preparation

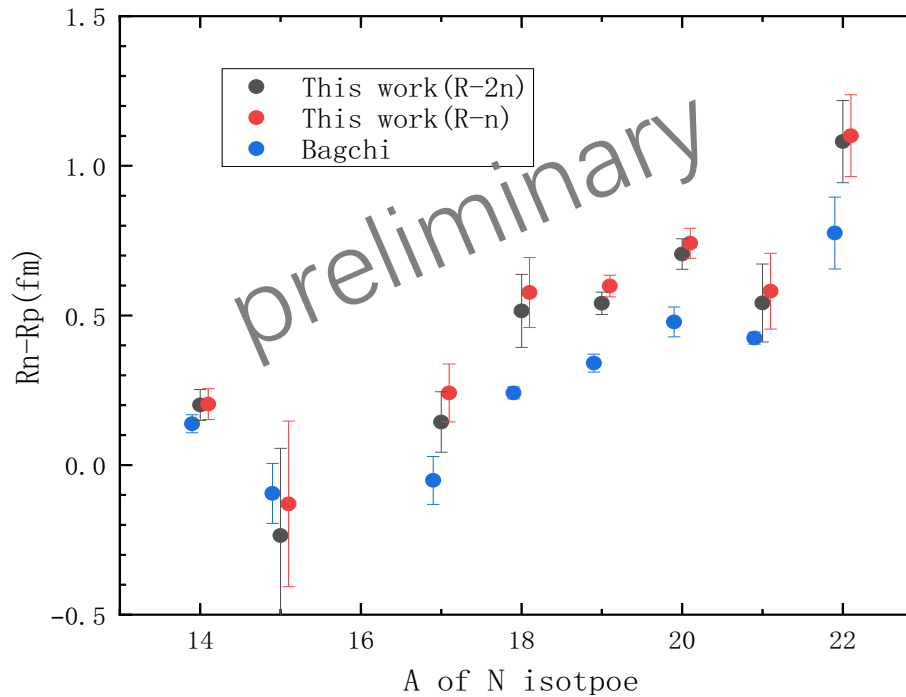
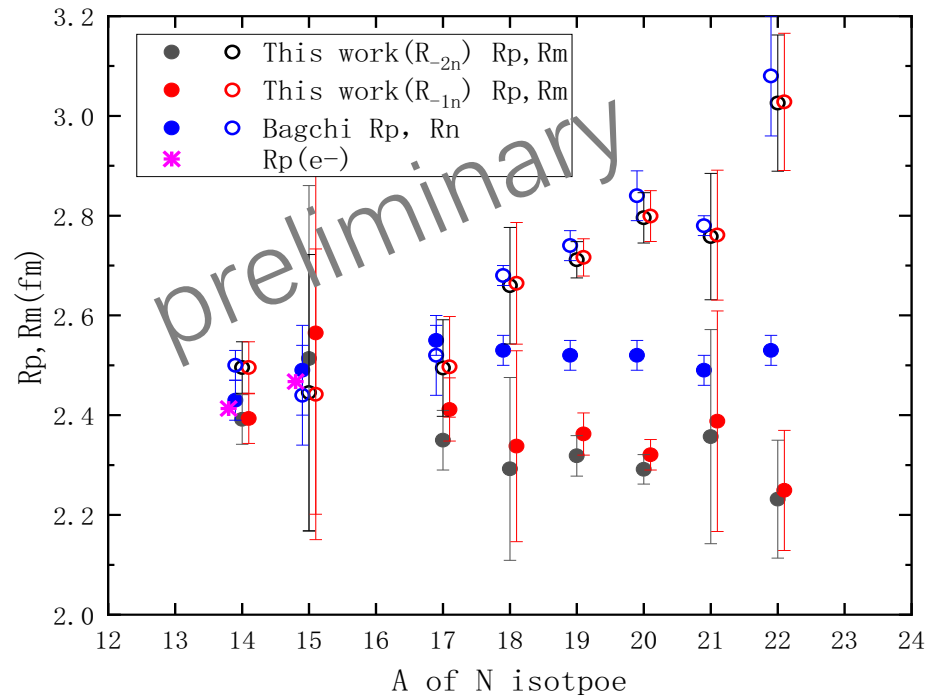
Problem with H-target data



Even considering the evaporation process cannot explain the data!

In discussion with theoretician

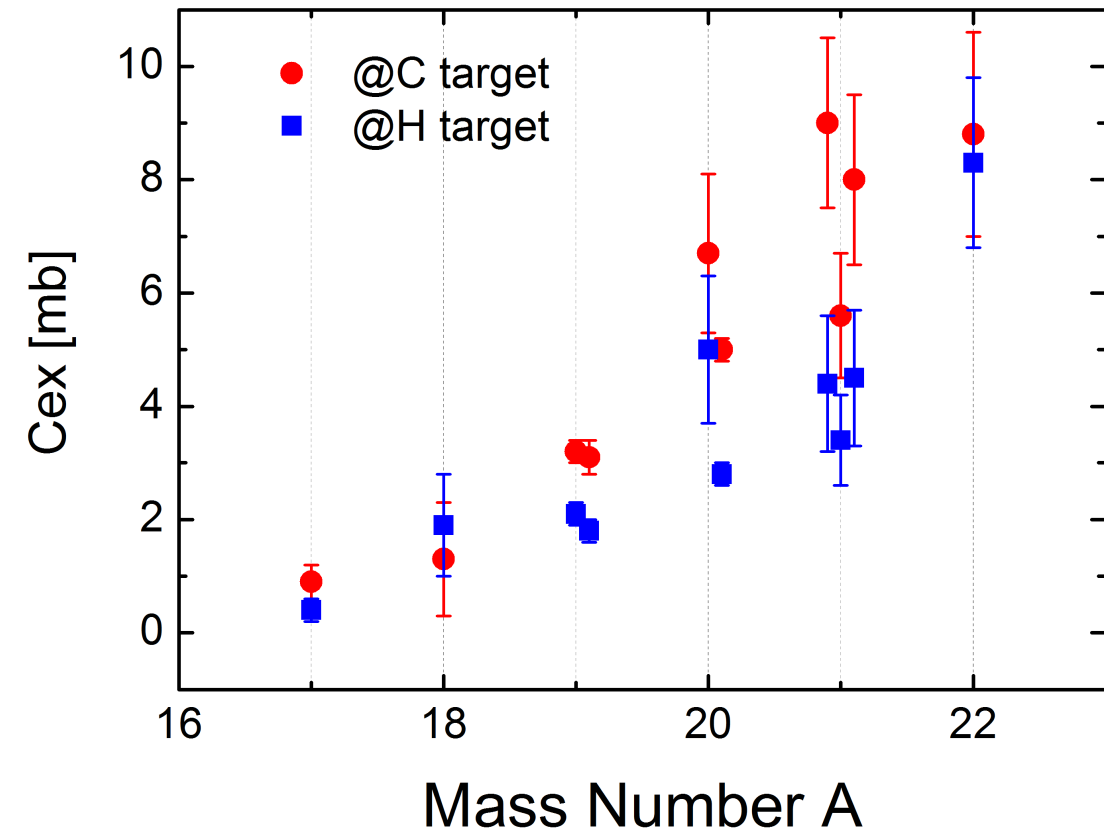
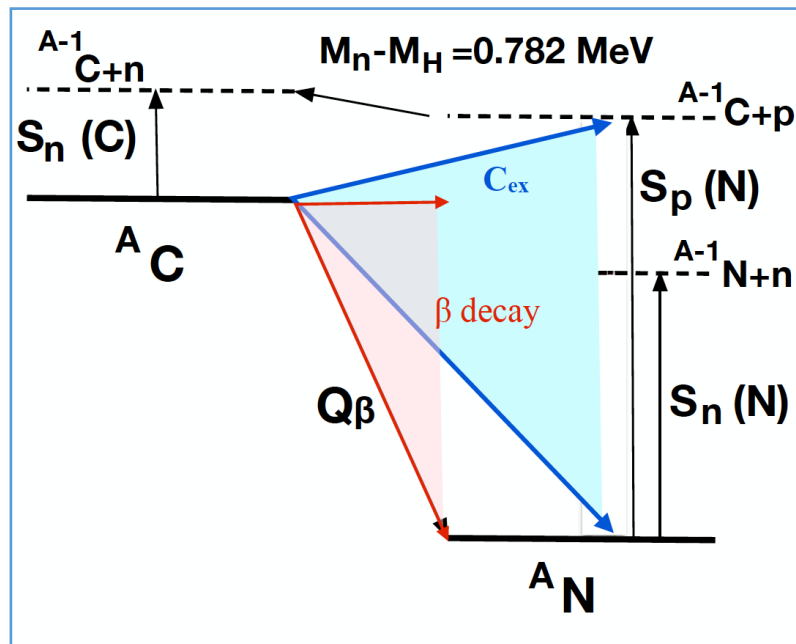
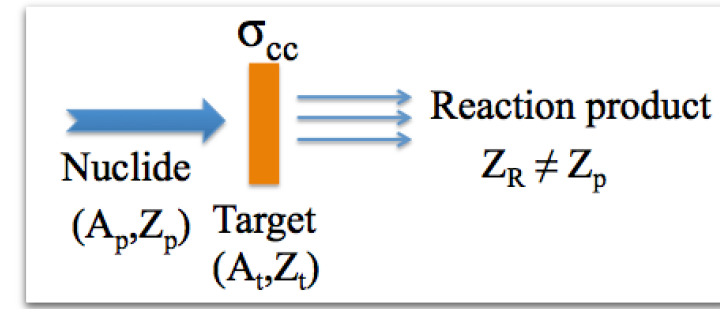
Developing a new approach to deduce rms radii



张寂潮等 , in preparation

电荷改变总截面的实验测量
“一种研究贝塔衰变总强度的可能新方法”

Total (p,n) charge-exchange reaction

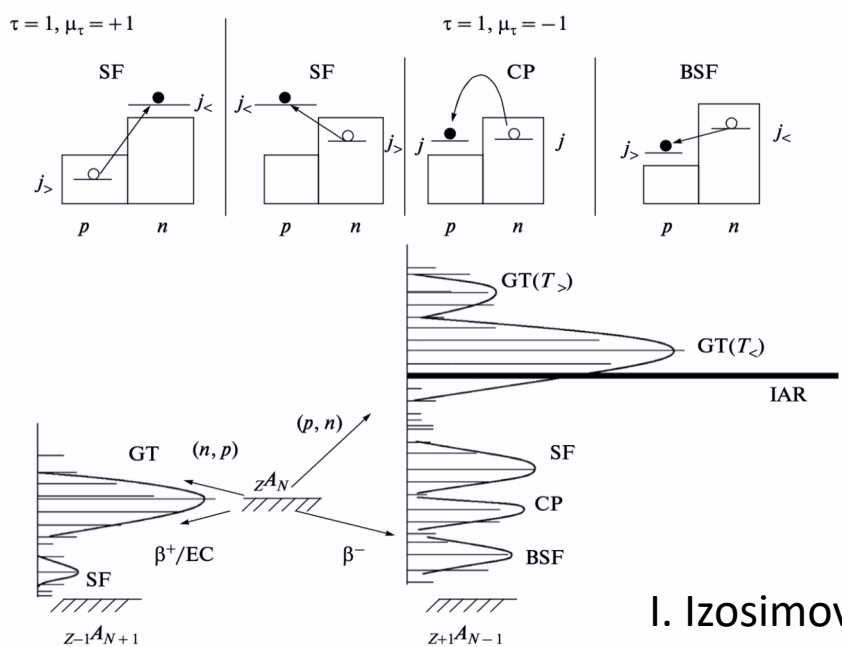


Assuming (p,n) to excited states above one-proton emission threshold, then only proton emission

β 衰变强度

原子核结构

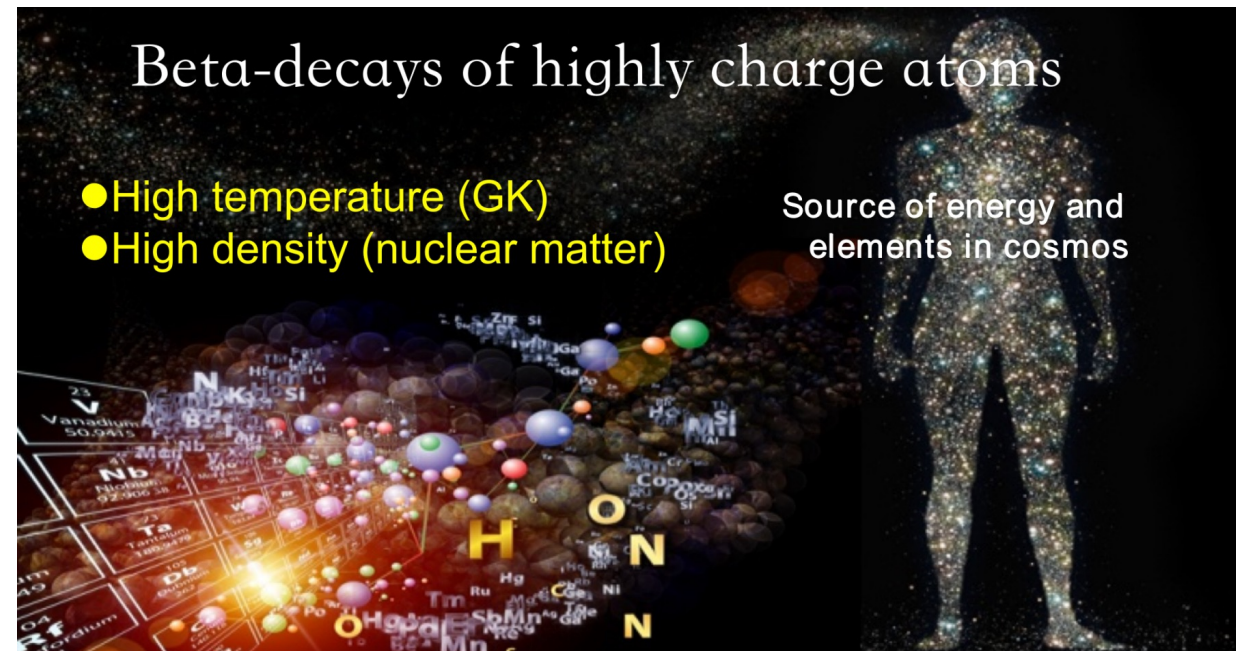
- Gamow-Teller strength vs Ex: T_z 系统学
- Gamow-Teller quenching
- Test theoretical models



$$\text{Sum Rule: } S_- - S_+ = 3(N - Z)$$

核天体物理

- 原子核半衰期寿命可能发生变化
- 丰中子原子核的电子俘获（中子星、超新星）
- β -decay beyond Q_β windows



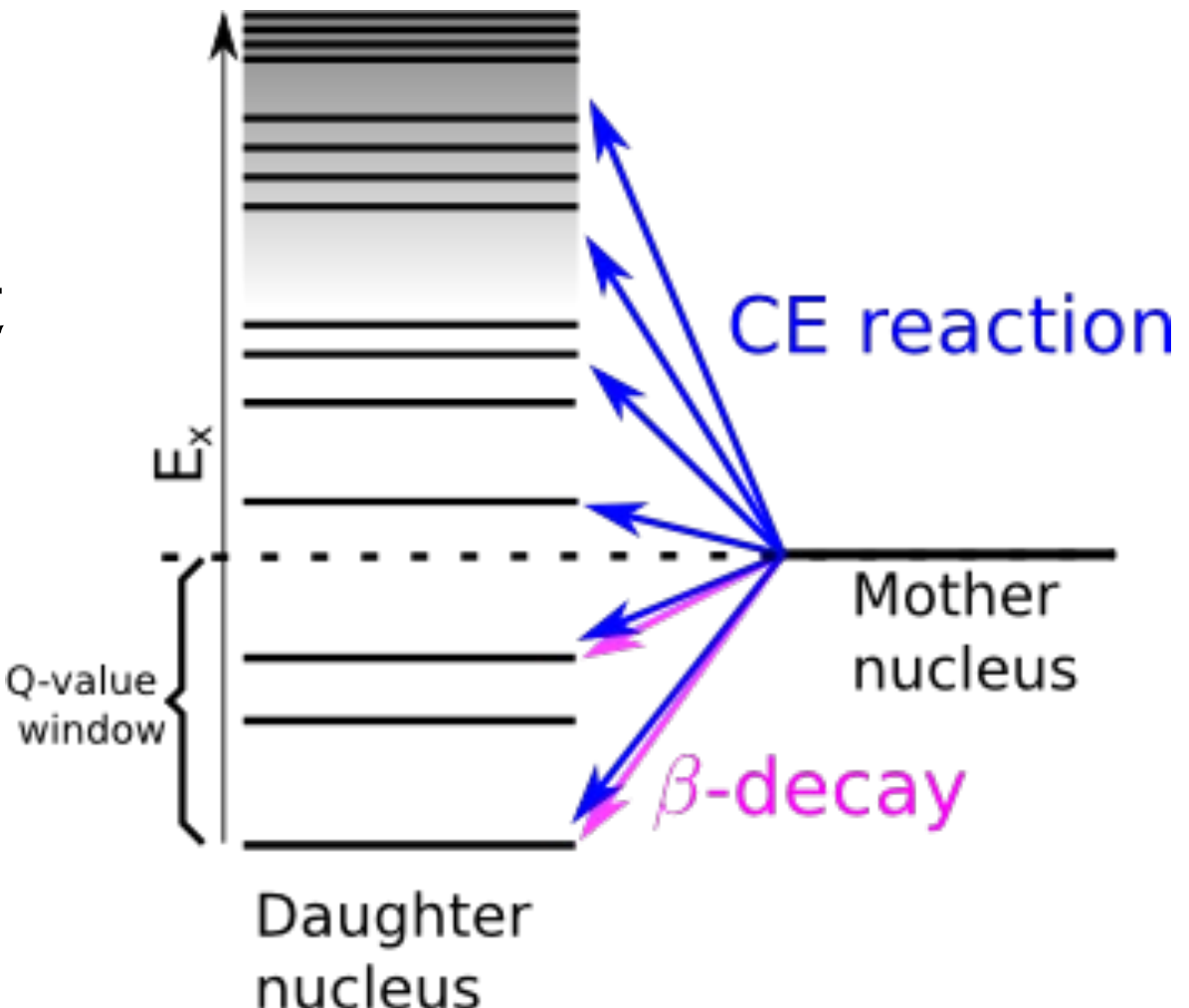
β 衰变强度的测量

β 衰变：

Q_β 窗口内衰变强度较大的跃迁

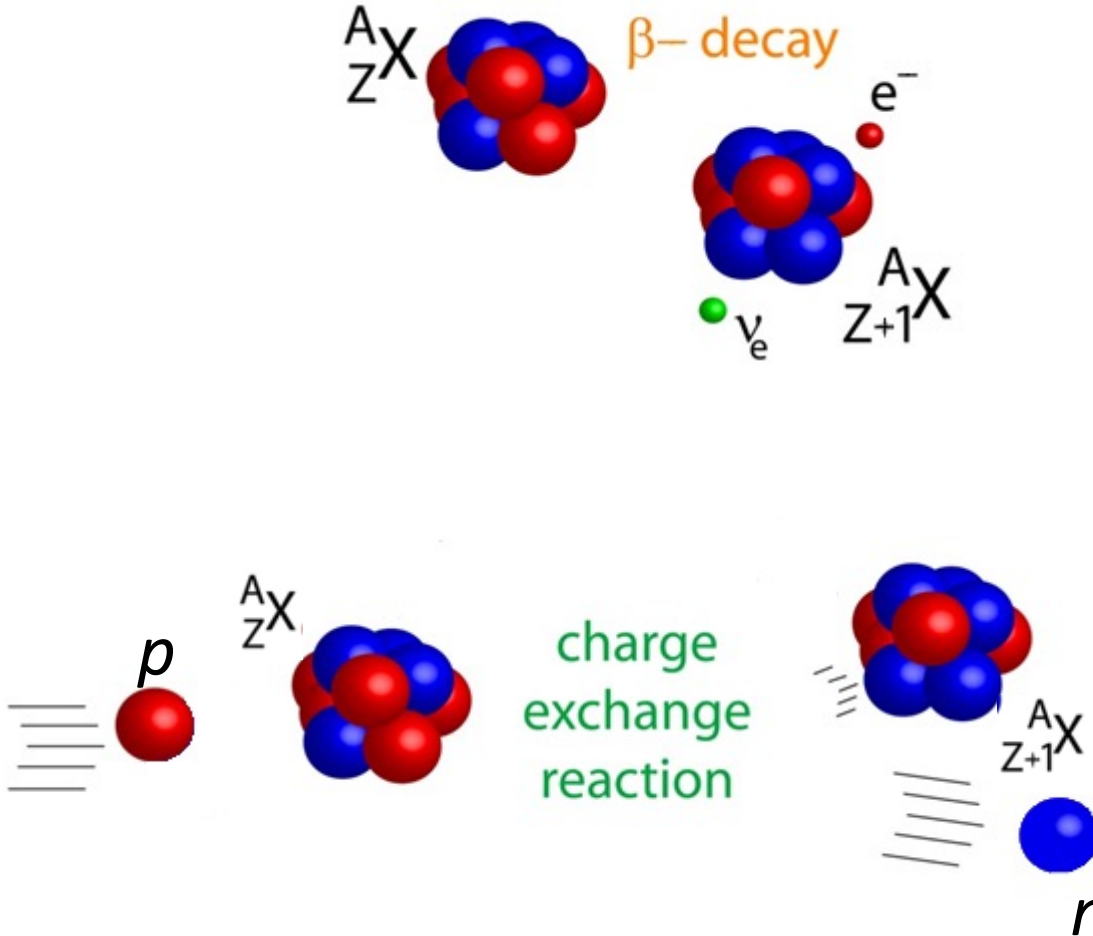
电荷交换反应：

可以测量高于 Q_β 窗口的跃迁



$$I_\beta = S_\beta \times F(Z, E)$$

电荷交换反应与 $B(GT)$



β -衰变: ${}^A_Z Y \rightarrow {}_{Z+1}^{A+1} X$

衰变强度: $B(GT)$

$$\left[\frac{d\sigma}{d\Omega} \right]_{(q=0)} = \hat{\sigma} B(GT)$$

零动量转化条件下

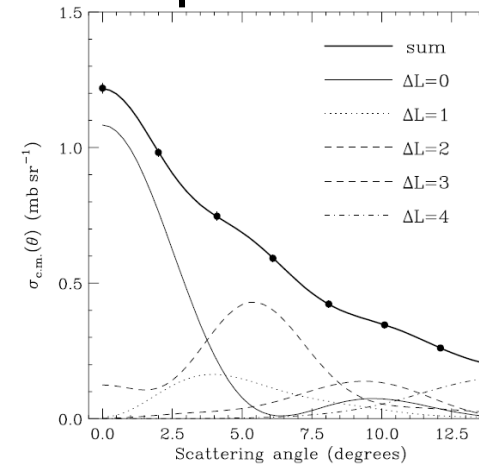
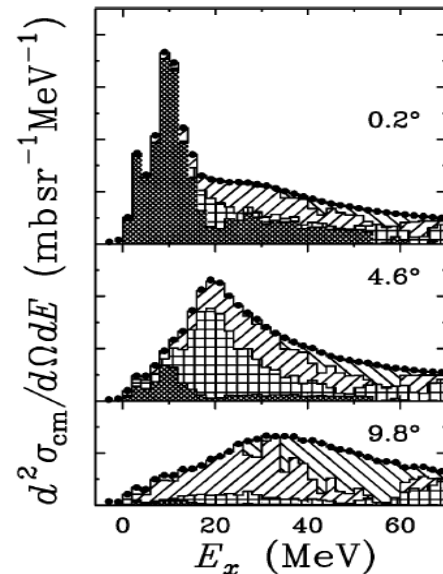
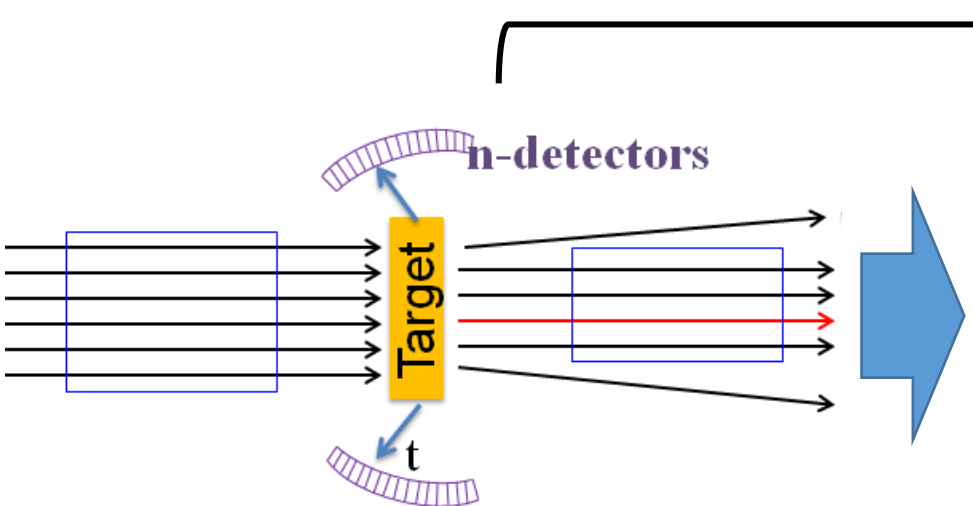
$$\text{反应微分截面: } \left[\frac{d\sigma}{d\Omega} \right]_{(Q, \theta)}$$

电荷交换反应: ${}^A_Z X (p, n) {}_{Z+1}^{A+1} Y$ et al.

不稳定核(p, n)反应截面测量

$$\hat{\sigma} B(\text{GT}) = \frac{d\sigma}{d\Omega}(q=0) = [d\sigma/d\Omega(Q, 0^\circ)]_{\text{exp}} \times \left[\frac{d\sigma/d\Omega(q=0)}{d\sigma/d\Omega(Q, 0^\circ)} \right]_{\text{DWBA}}$$

利用DWBA计算



M.Sasano, PRC 79(2009)024602

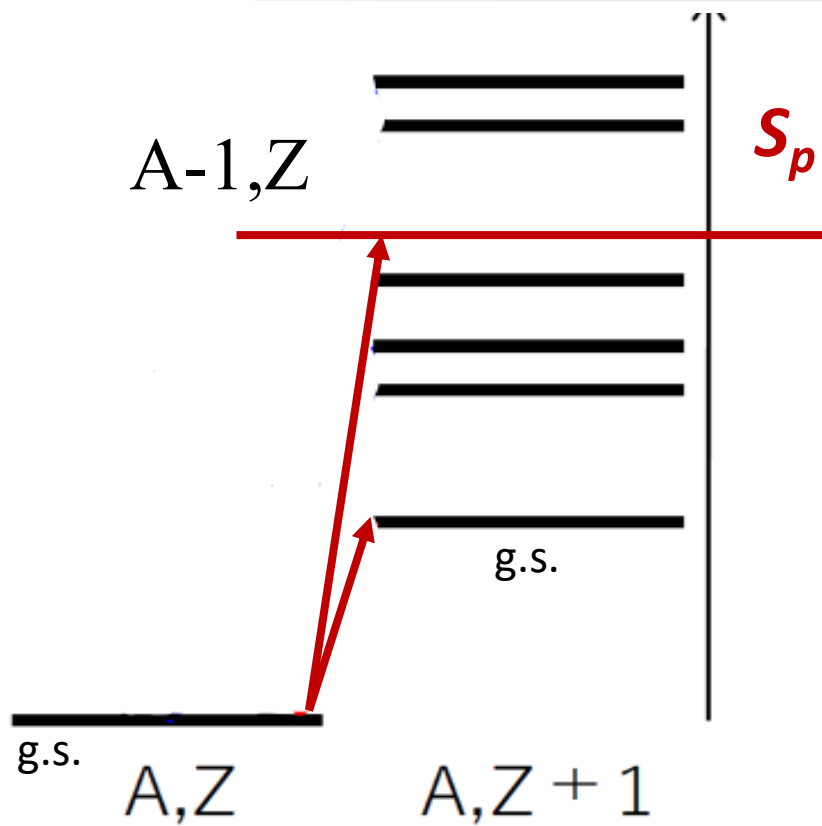
$$\sigma^{\text{calc}}(\theta) = \sum_{\Delta L=0}^4 a_{\Delta L} \sigma_{\Delta L}^{\text{calc}}(\theta)$$

- + 高分辨率谱仪
- + 利用逆动力学反推
- + 同时需要测反应产生的中子和反冲核的装置

- + 测量关于角度和能量的双微分截面谱
- + 对束流的流强和时间存在很高要求

- + 外推到0度角
- + 利用MDA计算出 $\Delta L = 0$ 的贡献

测量电荷交换反应总截面



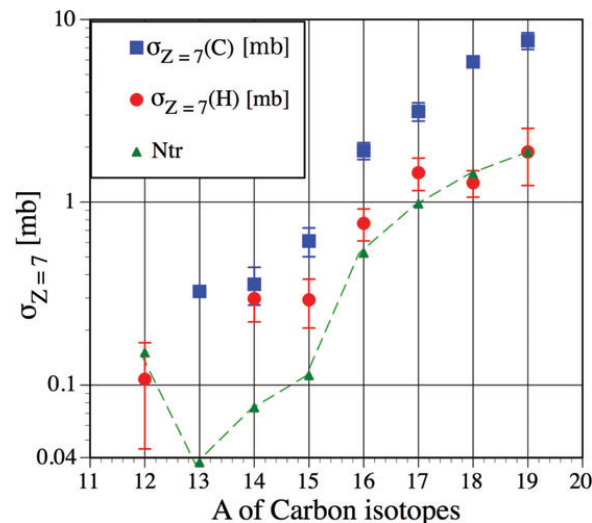
方法优势：

可以测量至 Q_β 窗口以上的能级。

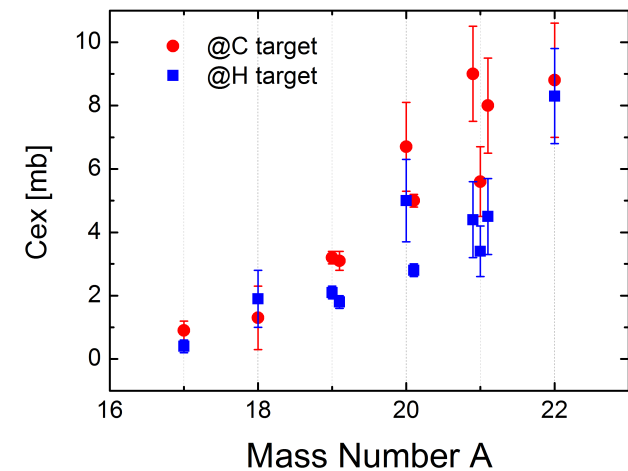
可以对不稳定核展开测量。

可以展开系统学研究

$$\begin{aligned}
 & \left[\sum_{g.s.}^{\text{Sp}} \int_{0^\circ}^{\text{Accepte angle}} \frac{d\sigma}{d\Omega} d\Omega \right]_{\text{GT}} \\
 & \times \frac{\left[\frac{d\sigma}{d\Omega} \right]_{(q=0), \text{DWBA}}}{\left[\sum_{\text{Ex}=0}^{\text{Sp}} \int_{0^\circ}^{\text{Accepte angle}} \frac{d\sigma}{d\Omega} d\Omega \right]_{\text{GT, DWBA}}} = \hat{\sigma} \sum B(\text{GT})
 \end{aligned}$$

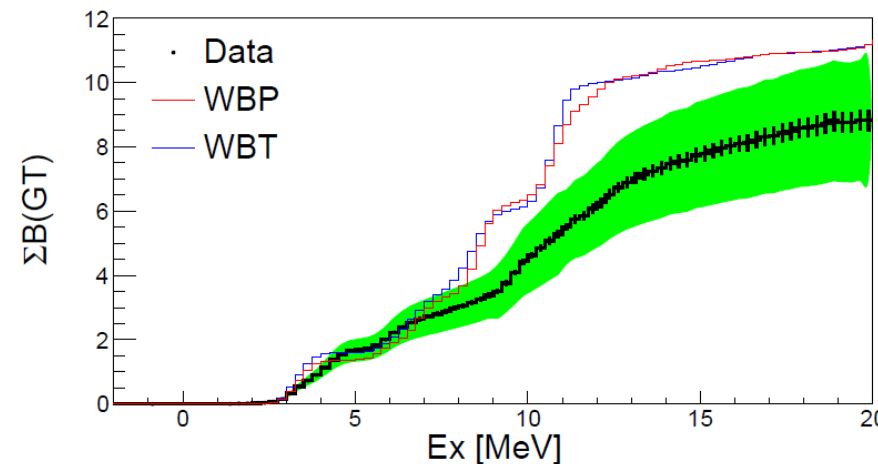
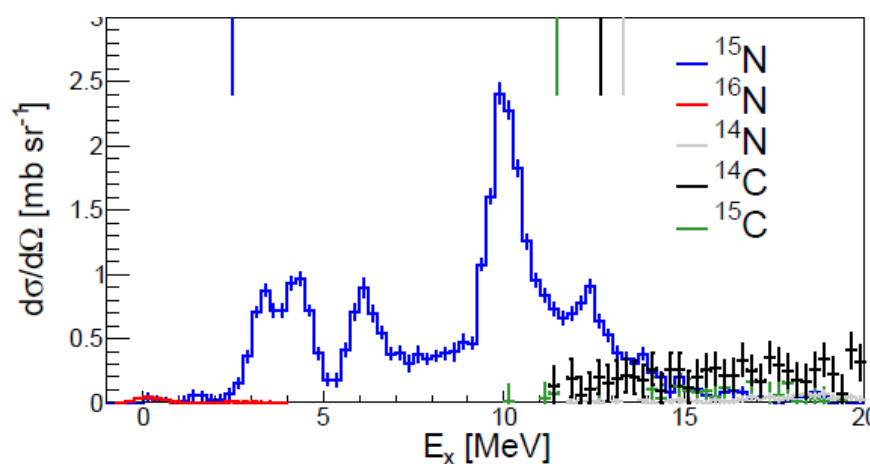
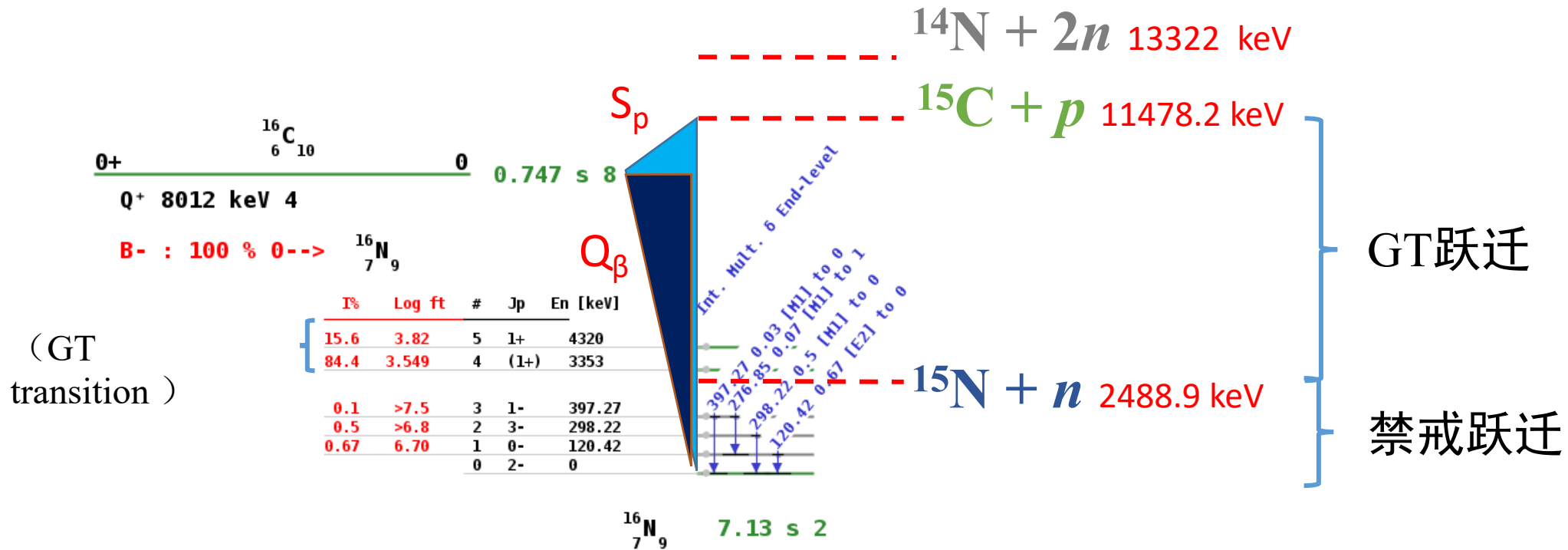


I. Tanihata, et al., PTEP.
2016, 043D05



Feng Wang, PhD thesis,
Beihang Univ(2018).

proof-of-principle experiment: $^{16}\text{C}(p,n)^{16}\text{N}$



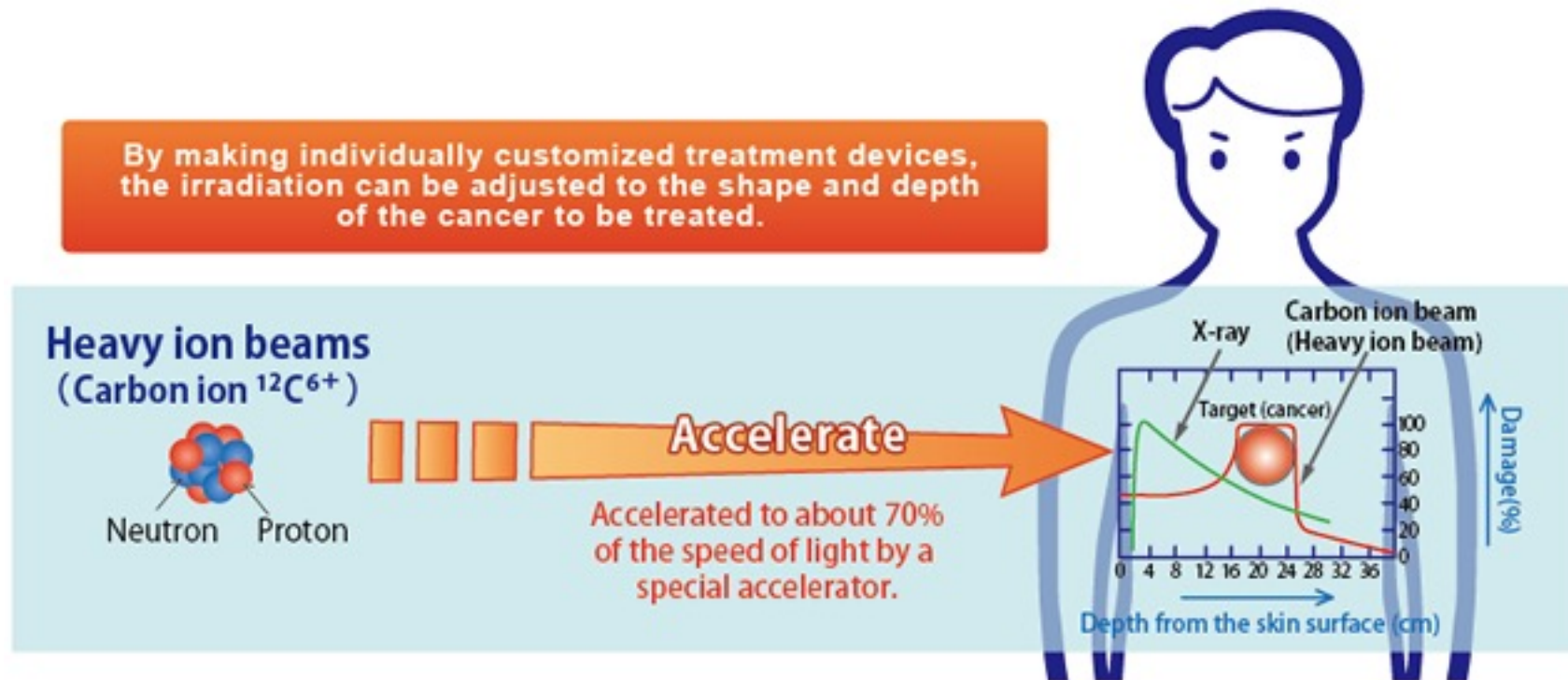
$^{16}\text{C}(p, n)^{16}\text{N}, ^{16}\text{C}@100\text{MeV/u}$
**S. Lipschutz, PhD thesis,
MSU(2018)**

Partial cross sections for application

核反应分截面

“有用”的科学

重离子(^{12}C , ^{20}Ne)治癌

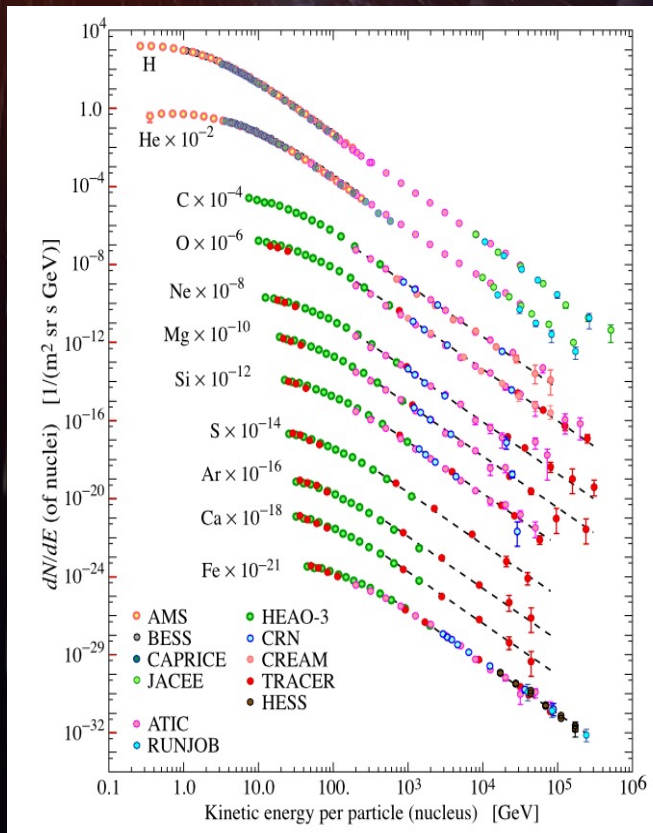


次级反应： $^{12}\text{C}+\text{p}$, ^{12}C , ^{16}O 等

高能宇宙射线: 银河系、太阳

银河宇宙射线是来自太阳系之外的高能量带电粒子流。

太阳射出超声速等离子体带电粒子流

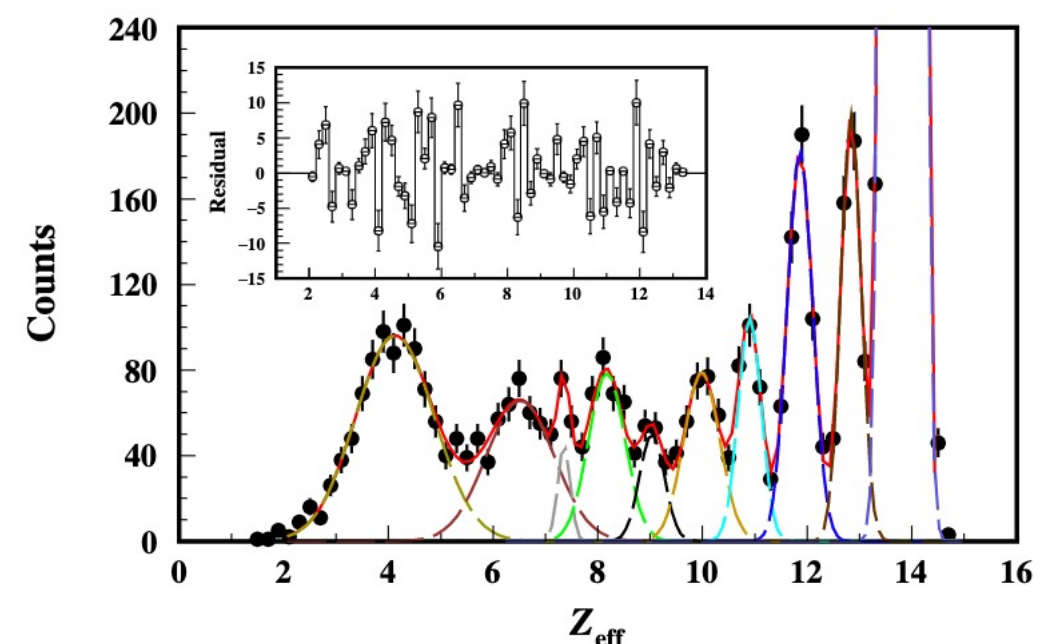
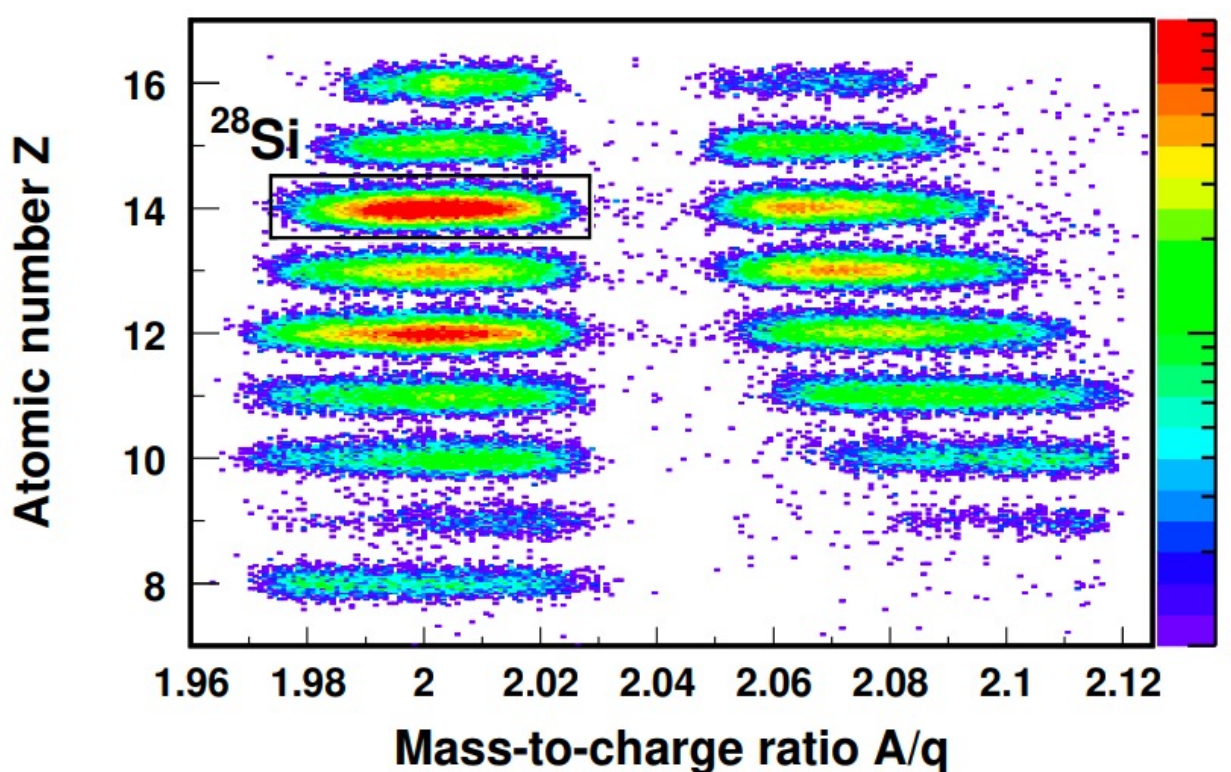


高能粒子的能量为 $10^8\sim 10^{20}$ 电子伏，通量密度为 $2\sim 4$ 个/
(平方厘米·秒)。

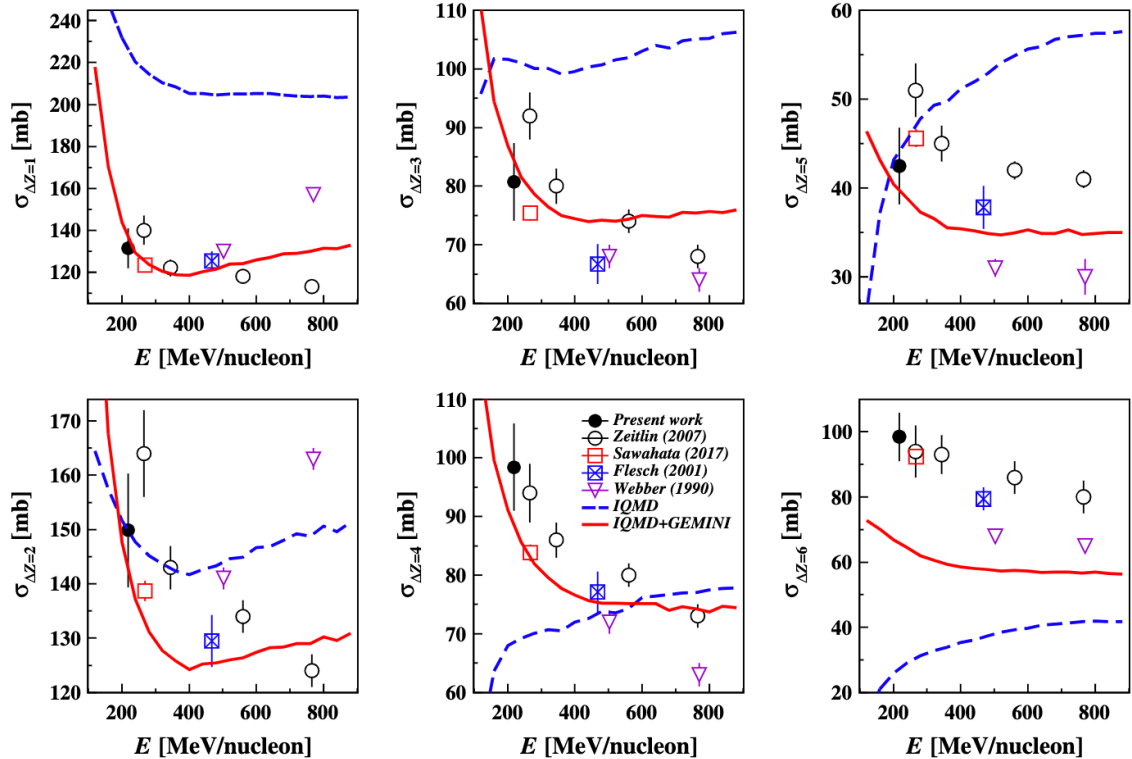
重离子在银河宇宙射线中危害最大，它不仅能穿透航天器的
舱壁，而且击中人体后能造成组织器官的损伤。

Elemental fragmentation cross sections

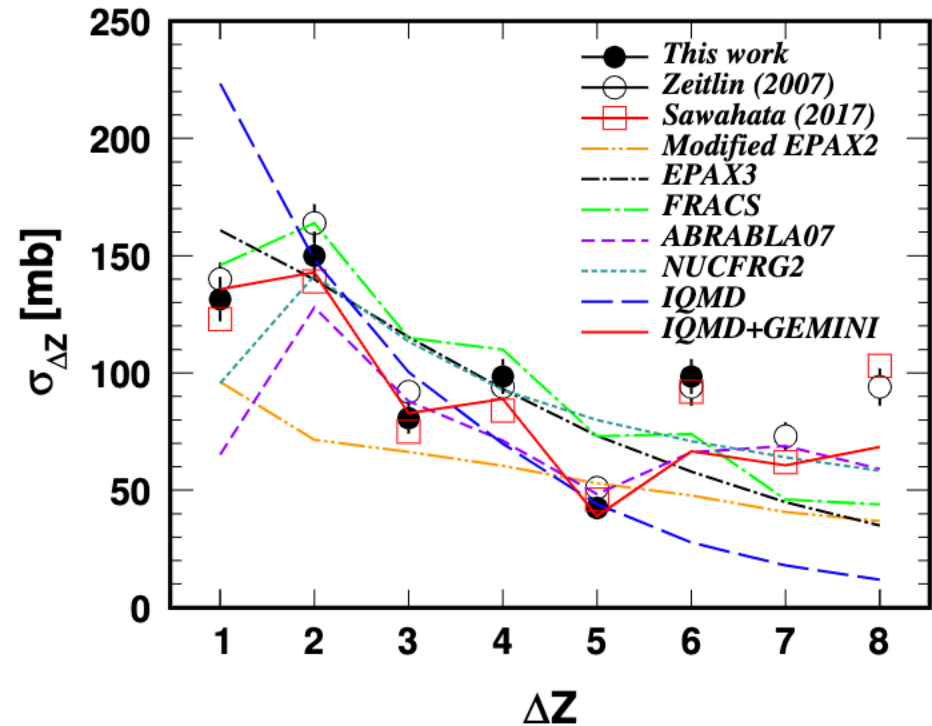
$\sigma_{\Delta Z}=1$: ^{28}Si ($Z=14$) \rightarrow Al ($Z=13$); $\sigma_{\Delta Z}=2$: ^{28}Si ($Z=14$) \rightarrow Mg ($Z=12$)
 $\sigma_{\Delta Z}=3$: ^{28}Si ($Z=14$) \rightarrow Na ($Z=11$).



EFCS系统数据的实验和理论对比



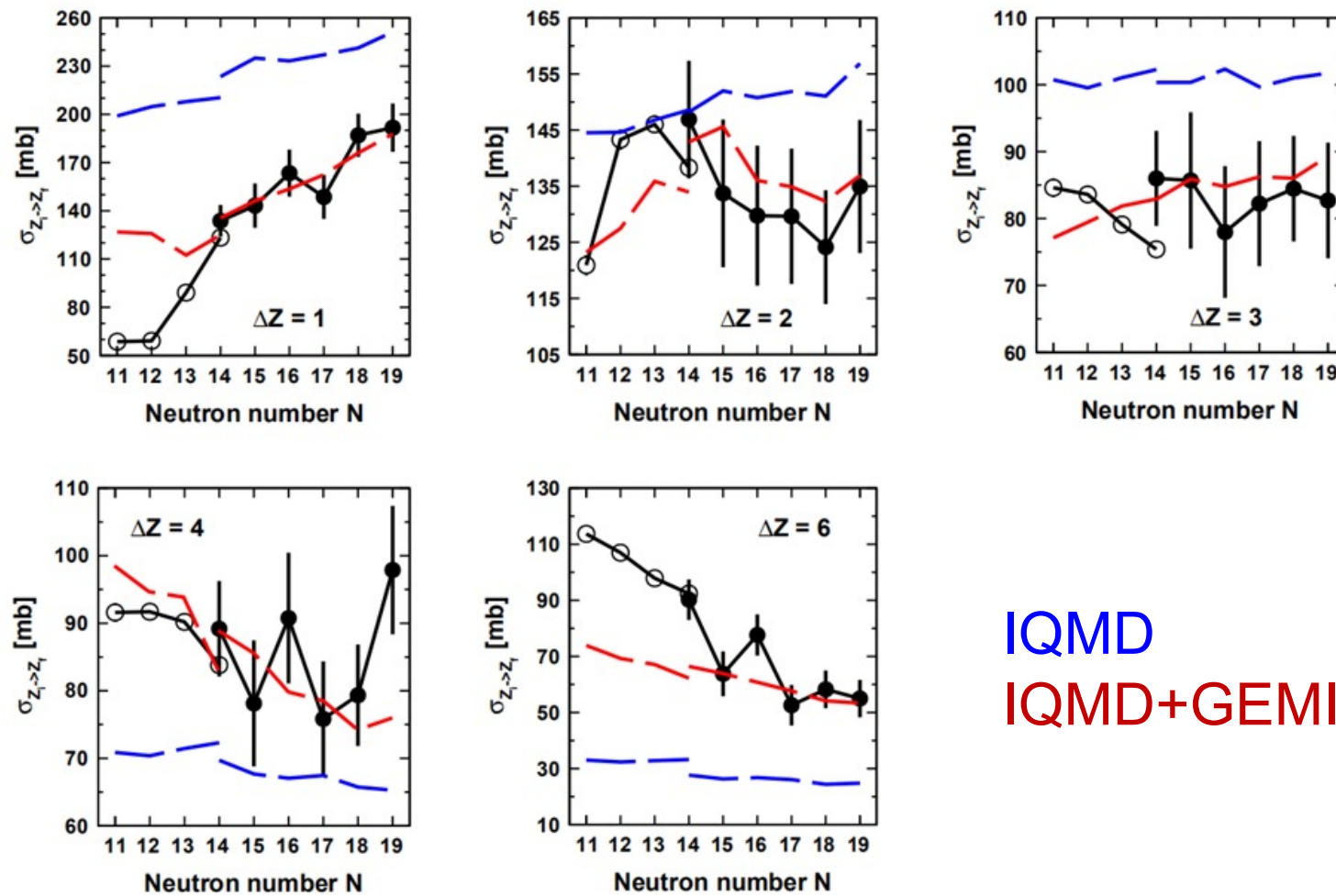
奇偶效应



李光帅 et al.

理论计算，苏军，梅波

EFCS for $^{25-33}\text{Si}$, and also Mg,Al,P,S,Cl isotopes

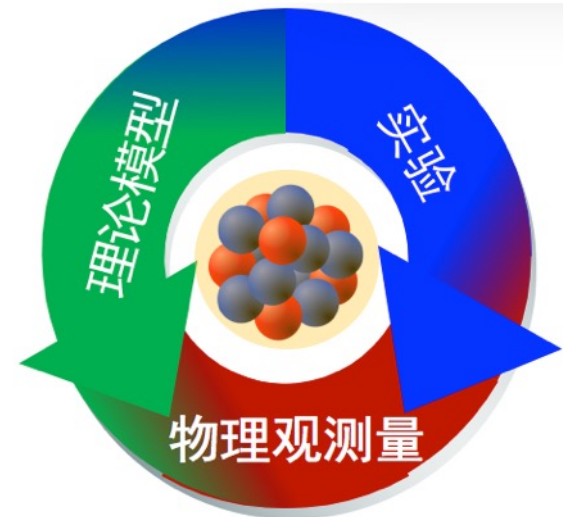


可能提供最大的
分截面数据库

IQMD
IQMD+GEMINI

总结

- 天体物理能区的核反应理论
- 相对论能区的核反应理论



Experiments can be performed with high precision, however, theoretical interpretation are urgently called for.